STELLARATOR WENDELSTEIN W VII

Information Presented at the
8th Symposium on Fusion Technology
The Netherlands

W VII - Team

IPP 2/224 June 1974

MAX-PLANCK-INSTITUT FÜR PLASMAPHYSIK

GARCHING BEI MÜNCHEN

MAX-PLANCK-INSTITUT FÜR PLASMAPHYSIK

GARCHING BEI MÜNCHEN

STELLARATOR WENDELSTEIN W VII

Information Presented at the
8th Symposium on Fusion Technology
The Netherlands

W VII - Team

IPP 2/224 June 1974

Die nachstehende Arbeit wurde im Rahmen des Vertrages zwischen dem Max-Planck-Institut für Plasmaphysik und der Europäischen Atomgemeinschaft über die Zusammenarbeit auf dem Gebiete der Plasmaphysik durchgeführt.

Abstract

This report covers the material presented by the Garching WENDELSTEIN W VII group at the 8th Symposium on Fusion Technology, Nordwijkerhout, The Netherlands, 17-21 June, 1974, namely the papers Nos. 7, 11, 12, 26.

Paper No. 7 entitled "Technical Concept and Status of the W VII Stellarator"was given as a 30 minutes oral presentation by G. Duesing and summarizes the following papers:

7a On the Technical Concept of the W VII Stellarator

7b Status of WENDELSTEIN VII (WVII)

7c Cooling Systems of the W VII Stellarator

7d Vacuum System of the W VII B Stellarator

7e Design and Manufacturing of the Toroidal Field Coils of W VII

7f Ohmic Heating and Vertical Field Coil Systems of W VII

The last three papers of this report had been presented as 10 minutes talks at the S.O.F.T., describing further details of the W VII project:

11 The Effect of Perturbations on the Magnetic Field of the W VII Stellarator

12 Torus with Helix W VII A

26 High-Power DC Neutral Particle Injection for W VII

Paper No. 7

TECHNICAL CONCEPT AND STATUS OF THE W VII STELLARATOR

Lecture given at the 8th Symposium on Fusion Technology, The Netherlands, June 1974

G. Duesing
Max-Planck-Institut für Plasmaphysik, D-8046 Garching, W.Germany

The WENDELSTEIN VII facility is a stellarator being constructed in Garching. It has first been presented at the 7th S.O.F.T., Grenoble, in October '72, with its main technical and physical parameters as well as with its scientific aims.

This lecture on WENDELSTEIN VII, which I will just call W VII in the following, is the summarizing presentation of the papers 7 a to 7 f at this symposium (Fig.1). These papers appear as such in the conference proceedings. I'll first give a general description of the machine with its main components, then speak about two major design problems, namely the introduction of the magnetic loads on the toroidal field coils into the support structure and the magnetic loads acting upon the helical windings. After that I'll try to give you some high-lights about the ohmic heating transformer and vertical field coils system, the cooling system, the vacuum system and the manufacturing of the toroidal field coils, and finally I'll give you the status of the project.

The two most important components of W VII (Fig. 2) are the toroidal vacuum vessel with the helical conductors and the toroidal field coils. The helix is directly wound upon the vacuum vessel. It consists of four packages of conductors, which permit a pure l=2 as well as a l=2 and l=4 mode of operation. The toroidal field coils can be slid upon the torus by means of a removable torus segment, which has a width of 18^{o} of azimuthal angle. We have chosen a high number of 40 coils to keep the toroidal field ripple below 1 %. The value of the toroidal field is 4 T on the toroidal axis.

The power supply for helical windings and toroidal field is a flywheel generator which supplies a power of 150 MW during a maximum pulse length of 10 seconds. It needs 6 minutes after a pulse to be reaccelerated to its original speed. The generator, after rectification, supplies a DC current of 40 kA, which flows through a circuit that, all in series, contains the toroidal field coils and the single conductors in the helical conductor packages. There is the paper No. 19 at the conference about this generator, which has been constructed by Siemens.

You see on Fig. 2, which gives the correct proportions, that the design is not especially favourable for the installation of pumping and diagnostics ports. As is shown in Fig. 3, we have done all we could by putting

port-holes wherever free space is left between the toroidal field coils on the one hand and the helical windings on the other. The total number of ports is 90, the diameter normally varies between 90 and 160 millimeters, in extreme positions it is only 30 millimeters.

Fig. 4 gives a cutaway view of the main components of the machine. What is left out, are the support structure, the portholes and all peripheral parts. To give you the dimensions: the major torus diameter is 4 m, the toroidal field coils have an outer diameter of 2.1 m, and the outer diameter of the two largest coils is 7.2 m.

For ohmic heating of the plasma, W VII is equipped with an air-core transformer. The magnetic flux its primary can produce has been fixed to 2.9 Vs in order to get a plasma current of 500 kA. The primary coils are arranged outside the toroidal field coils. There is a central cylindrical coil, which is the actual flux producing coil, and twice three compensation coils, here on top and the same at the bottom - you just see the outermost one. The compensating coils keep the magnetic field in the plasma region below 5 G.

A geometrically similar system are the vertical field coils. There is a central cylindric coil inside the central transformer coil and twice two additional coils on top and

bottom. Since the plasma current will possibly have long pulse lengths of the order of a second, W VII needs a vertical field for the positioning of the plasma, i.e. for improving the equilibrium configuration already existing. Both the transformer and the vertical field coils are being manufactured by Lintott in England.

Furthermore, Fig. 4 shows one of the two beam lines for neutral particle injection. I'll not go into any details here, as our neutral injection will be described in the paper No. 26 at this conference. You see the geometry of a possible solution : We haven't touched the helical windings, but there is an inclination of the beam line, and there are special toroidal field coils where the beam line goes through.

Fig. 5 is a section of the machine with now the support structure added. There is a stainless steel reinforced concrete foundation set upon the basement floor of the hall. The torus with the helical windings is supported by five pillars like this one. The other components of the machine are not mechanically connected with the torus. Most of them and especially the toroidal field coils are supported by a separate structure, which consists of this central supporting cylinder and two large supporting disks connected with the cylinder at top and bottom.

The experimental floor is at ground floor level, the torus mid-plane is 1.5 m above this floor.

I'm now going to describe, how the loads on the toroidal field coils are introduced into the support structure. In Fig. 6 you see the support structure again: Here the cylinder, which is 2.2. m high, has a wall thickness of 12 cm and a weight of 16 t, and here the two disks fastened to it, which have an outer diameter of more than 6 m, a height of about 25 cm, and a weight of 15 and 17 tons, respectively. This dimensioning was fixed by the given tolerances: The maximum admissible tilt of the toroidal field coils is 1 milliradian and the maximum admissible radial compression of the central cylinder is 1 mm.

The cylinder is fabricated in two halves. Fig. 7 shows one of the halves and the assembled cylinder. Each disk consists of 10 segments. In Fig. 8 you see one of these segments after casting. There are several large openings in each segment for the torus ports, the cooling water tubes, etc.. All these parts have been cast by the Deutsche Edelstahlwerke (DEW) from a non-magnetic steel the German standard of which is DIN 1.4311. They have been machined by Krupp, Bochum.

In Fig. 9 you see the acting magnetic forces and torques. The weights are omitted as being small compared with the magnetic forces.

The centripetal force of 160 t per coil, which is the resultant of the interaction of the coil currents with the toroidal field, is led into the supporting cylinder by these feet.

On each coil a torque of 19 tm is acting. This torque is due to the interaction of the coil currents with the vertical field, which typically has a value of 0.1 T.

By structural elements, which are not given in the figure, this tilting moment is led via the coil feet on top and bottom into the supporting disks and into the cylinder, where it now is a vertical torque, which tries to twist the structure as is shown in Fig. 10. This torque has the considerable value of 710 tm.

The main design problem with these loads were the two vertical slots in the supporting cylinder, which have to be insulated against the loop voltage induced by the transformer. At these slots, the torque results in considerable opposite vertical forces on the section surfaces. That is why we have inserted insulated shear bolts in the slots as indicated here (lower part of Fig. 10). We have put 18 shear bolts into one slot and Fig. 11 shows such a bolt. It is fitted into double-cone sleeves, which on their part are pressed into an insulating bushing.

In Fig. 12 an insulating foil is being inserted. At the right hand the sleeves are already mounted.

I now want to speak about the loads on helix and torus. The total magnetic force acting upon a helical conductor package points essentially into the direction of the minor torus radius, either outwards or inwards, as shown in Fig. 13 , it is screwed around the torus together with the conductors and has a mean value of 2.5 t per cm conductor length in our original case of a current of 1 000 kA per package.

Thus this force, which is roughly ten times higher than the corresponding force in the largest stellarators built up to now, either presses a helical conductor against the vacuum vessel - and this on its total length - or pulls it away from it.

The results are an elliptical deformation of the torus cross-section (lower part of Fig. 13), which is screwed around the toroidal axis, too, and longitudinal stresses in the conductors. This conductor, e.g.,is being pulled away from the torus. It is now wound around the torus on a larger radius than before and thus it is elongated and suffers a longitudinal tensile stress. In the same way, the conductors being pressed against the torus suffer longitudinal compressive stresses. To give you a number: If the structure around the helix allows a radial shift of a conductor of 1 mm, this stress amounts typically to 7 $kp/mm^2 \approx 7\ KN/cm^2$. This presents a

difficulty for the design of the conductors with their connections, their water supply and discharge holes and their current joints.

Similarly, the deformation of the torus results in helical stresses in the torus wall, which are either compressive or tensile. This is especially obstructive to an easy design of the connection of the torus with its removable segment, which in addition to being vacuum-tight and electrically insulating now has to cope with azimuthal stresses as shown in Fig. 14. These stresses try to deform the section surfaces and make the connections gape. A typical value is 120 t for the force in Fig. 14 integrated over 90°, in the case of a radial deformation of 1 mm.

In order to find a safe design for the supporting of all these stresses, we have investigated various compound structures of the torus, the helical windings and bandages around them. The different manufacturing processes have been studied and above all the strength of the structures has been carefully analysed by numerical calculations.

Finally, we have seen that for each of the designs there were stresses arising either in the steel structure or in the conductors which were at the limit of the strength of the materials.

Consequently, we have now slightly reduced two physical parameters of the machine, namely both the toroidal field and the vacuum vessel aperture by 10 %, which gets the aperture down to 66 cm in diameter. By means of these changes and by a reduction of the helical current to 720 kA per package, we have considerably reduced the acting forces without changing the original regime of the rotational transform of 0.4 to 0.5, and now we seem to have got to a design with the resulting stresses sufficiently away from the yield strength of the materials used.

Nevertheless, the manufacturing of this component will be difficult and will take a long time. Therefore we are constructing a smaller torus with helical windings, which we call W VII A, in the meantime. This torus will be ready at the same time as the other components of the machine. I'll give you our time-schedule at the end of my talk.

Now I want to say a few words about the transformer and vertical field coils system. Fig. 15 shows on top schematically the energy supply and in the middle the time behaviour of the transformer current, the plasma current and the vertical field current.

Before the shot, a flywheel generator supplies the transformer current, which fills the transformer with magnetic flux. When starting the pulse, the HV breaker S_1 is opened and the current is forced into the large resistor R. By this fast flux change, a plasma current of 430 kA or slightly more is induced. The induced loop voltage is 200 V.

On the HV DC breaker high demands are made, as it has to interrupt a current of 35 kA against a maximum admissible voltage of 30 kV. The well-known principle in such cases with a switching frequency of a few minutes is to use an AC breaker and to commute the current from it into a parallel resistor by means of the discharge of a capacitor bank in order to get a current-zero in the breaker. For W VII, a mercury vapor AC switch is being developed for that purpose by Hughes Air Craft, California.

For the vertical field current, the inductive energy stored in the transformer presents the power supply. During the rise of the current, the vertical field circuit is electrically coupled to the transformer circuit. Later on, the level of the vertical field current, and i.e. the proportionality to the plasma current, is controlled by a second generator.

In order to keep the plasma current constant, the decrease of the transformer current into the negative regime is continued by reversing the current and controlling the flywheel generator. Not later than at the time when the maximum admissible transformer current is reached, the plasma current starts to break down.

Fig. 16 which shows the water supply tubes around the foundation of our machine is just to indicate that I will now be speaking about the cooling systems. Let us have a look at the two most powerfull ones: The cooling of the toroidal field coils, where a power of 65 MW is dissipated, and of the helical windings with 40 MW dissipated during the ten seconds of pulse duration.

In the toroidal field coils, the coil heat capacity is sufficiently large to store the total released energy. Thus the design has been that, practically without cooling, the conductors are heated adiabatically during the pulse. The temperature rise in the conductors is 22 C at the end of the pulse. A relatively low water flow is sufficient to cool the coils down during the 6 min break between two pulses.

By way of contrast, the heat capacity of the helix is not large enough for adiabatic heating, and the conductors have to be effectively cooled during the pulse. Thus the system will be provided, depending on the final design, with 1000 or 1500 cooling ducts in the conductors of 3 m length each, which will all be fed in parallel, and the total water flow required for the helix is 1500 m^3/h. The maximum temperature rise in a conductor will be smaller than 40 C.

The next topic of my talk is the vacuum system. For W VII, the given parameters are

- 35 m^2 of non-bakeable inner vacuum vessel wall and
- 60 portholes for pumping, which altogether represent 3 % of the vacuum vessel surface.

The requirements on the system are:

- Handling of high hydrogen loads during the experiments
- Fast pumping of contaminants during discharge cleaning
- Ultra high vacuum between the experiments
- No interference with the diagnostics.

The pumping system that best appears to fulfil these requirements, is the compound system shown in Fig. 17.
It mainly consists of 10 turbomolecular pumps, 150 volume getter pumps and 30 Electro-Ion pumps. The Electro- Ion pumps will only be used to maintain the UHV between the experiments. They should give a final pressure of 10^{-8} torr.

The main pumping system is being represented by the volume getter pumps, the big scale application of which is a novelty. They are fabricated by SAES in Milano.
Their total effective pumping speed is 160 000 l/s for hydrogen or 50 000 l/s for oxygen.

Each pump consists of a cartridge as shown in Fig.18. It is 13 cm high and 10 cm in diameter. The getter substance is a specially treated zirconium-aluminum alloy.

The working temperature of the pump is 400 C. At this temperature the total hydrogen capacity of the system is 10^5 torr l at a pressure of 10^{-6} torr. The hydrogen gettering is reversible.

The pumping of active gases other than hydrogen with these pumps is irreversible, but the system can absorb 3 x 10^5 torr l until being used up. This is equivalent to 10^5 monolayers of the total torus surface. With some precautions, e.g. venting of the torus with rare gases only,this capacity should be sufficient for several years of operation.

What these getters do not pump, are rare gases. This,on principle,is a disadvantage, but for discharge cleaning, which usually is done with Argon, it is favourable again.

To finish the technical description let me show you a few pictures on the toroidal field coils, which are being manufactured by BBC Mannheim.

Fig. 19 . The copper bars are butt-brazed and then wound on this turn-table. Each coil has 25 turns in two pancakes. In the Fig. the second pancake of a coil is being wound.

During winding the copper bar is pressed towards the axis of the table by a pair of rollers.

Fig. 20 shows a single conductor. The conductor cross-section is shaped such that one turn is mechanically interlocked with the next by a slot and key system. Here you see the slot side of the conductor. Furthermore, you see the turn-to-turn insulation, which consists of fiber glass foils preimpregnated with epoxy resin.

In Fig. 21 you see two finished coils in their non-magnetic frames mounted for a force test. There is a frame at the circumference of the coil only. The outer diameter of a coil is 2.1 m, the weight is 3.4 t.

I'll now speak about the status of W VII. Fig.22 gives the time schedule. All major components, as the TF coils, the fly-wheel generator, the transformer and vertical field coils, the cooling system and the supporting structure will be delivered in the fall of this year at the latest. Unfortunately, this is not true for the large torus with the helix. This is down here. For this component, we had placed two development contracts with the industry last year, in order to have the detailed manufacturing concept

defined. Due to the difficulties I have been speaking about, the results were not really satisfactory, and it is only now, after the changes we have made, that we hope to be soon in a position to call for tenders for the manufacturing of the large torus W VII B.

In the meantime, as I have said earlier in my talk, we have been constructing another torus with helical windings, which will be ready this fall as the other main components are. This torus W VII A will have an aperture of 35 cm in diameter and helical currents of 160 kA per package. There will be a special paper given on the A torus at this conference: It is the paper No. 12.

Thus the first experiments with this torus are expected to start in the middle of next year. They should enable us to study an ohmically heated stellarator plasma and its confinement properties in the range up to an ion temperature of 1 keV and up to a toroidal field of 4 T.

This first stage of experiments will also be a good opportunity to learn more about the requirements on various technical components as the programming of the vertical field or the control of the helical currents by external means.

The duration of the scientific programme to be carried out with the A torus will be determined by the delivery of the final torus and is expected to be at least two years.

General description

Loads on the TF coils Loads on the helical windings M.Blaumoser, G.Duesing, G.Grieger, R.Jaenicke, J.Junker, J.Kolos, P.Meyer, B.Streibl, G.H.Wolf	Paper 7 a
Transformer and VF coil systems R.Jaenicke, R.C.Kunze, H.Lohnert, G.Müller	Paper 7f
Cooling A.Elsner	Paper 7 c
Vacuum H.Hägelsperger, W.Heiland, W.Poschenrieder and R.Scherzer	Paper 7 d
TF coils manufacturing K.Freudenberger, H.Lohnert,	Paper 7 e
Status M.Blaumoser, G.Duesing, G.Grieger, J.Junker and G.H.Wolf	Paper 7 b

Fig. 1

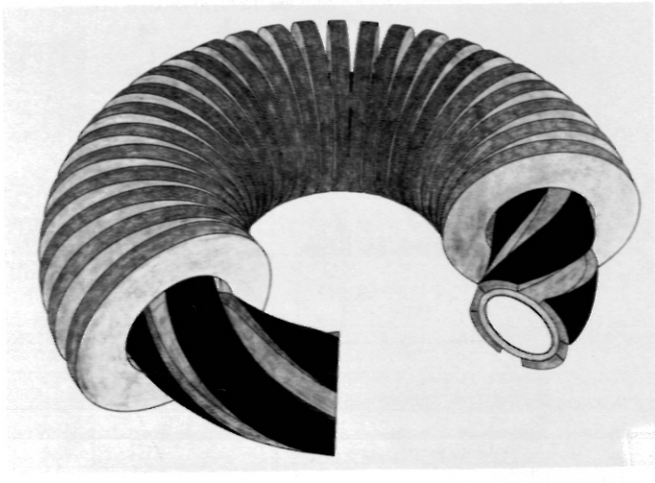

Fig. 2

Fig. 3

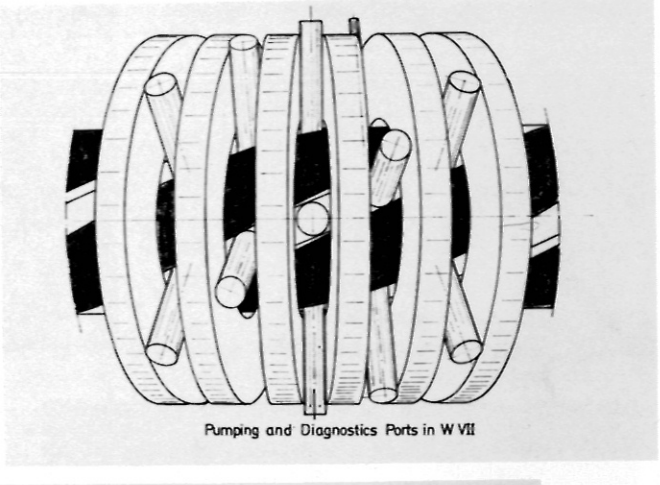

Fig. 4

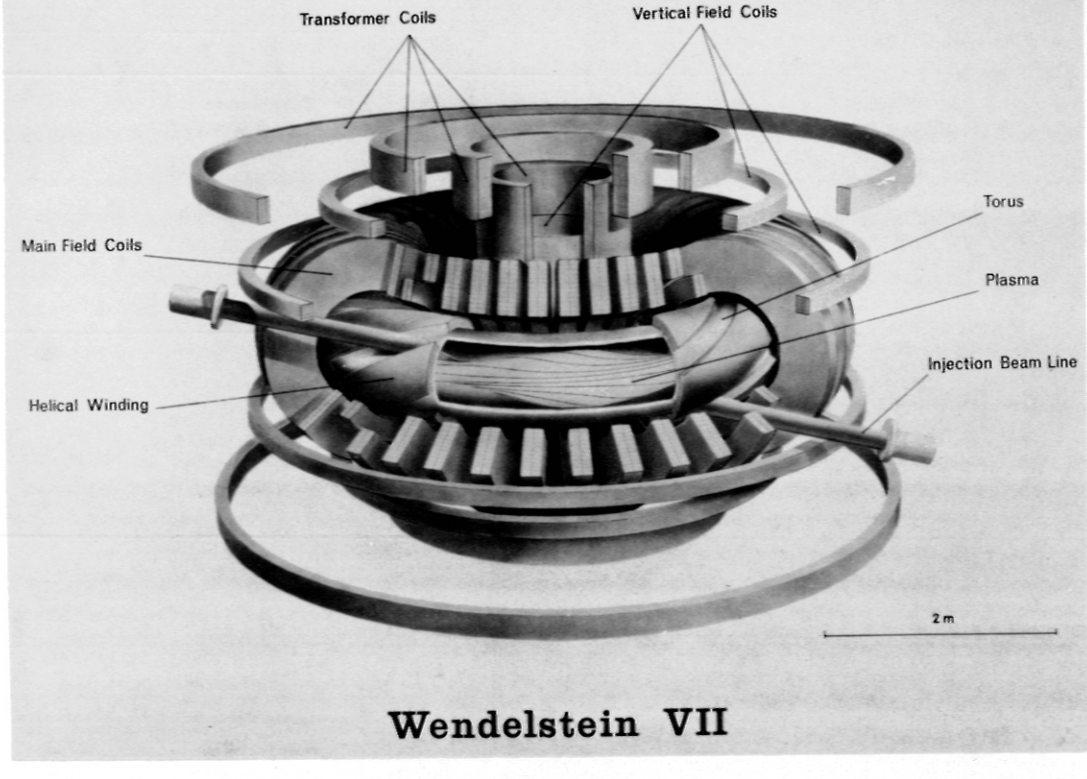

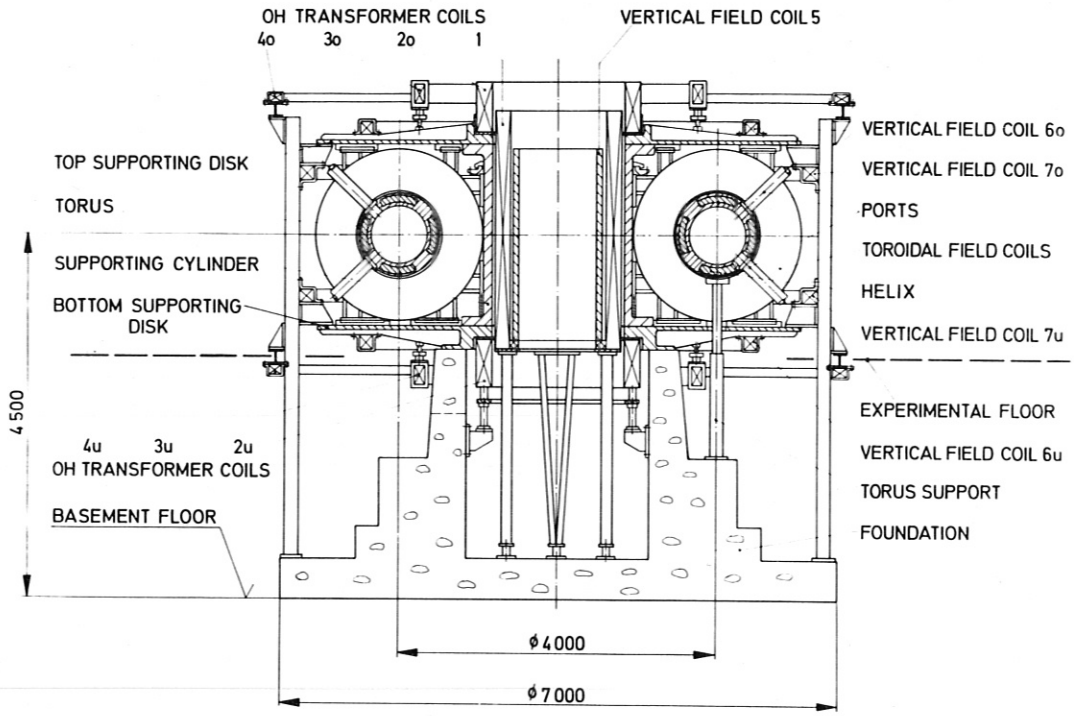

Fig. 5

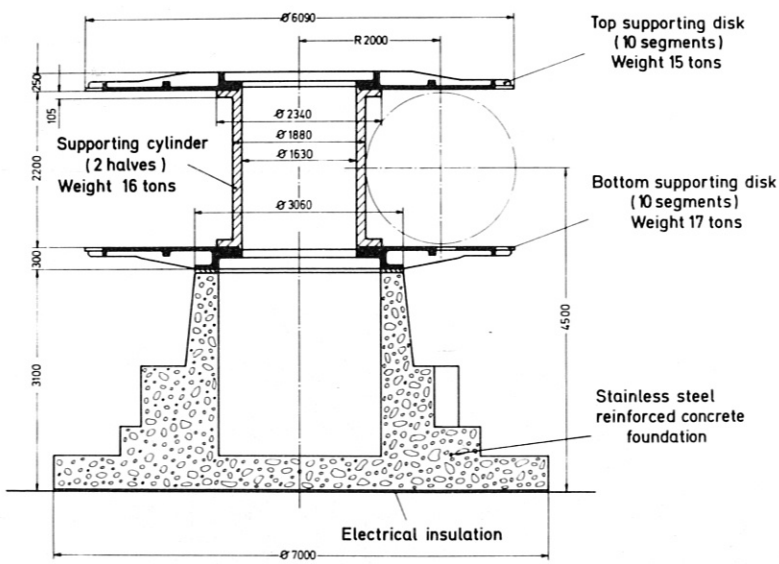

W VII Support Structure

Fig. 6

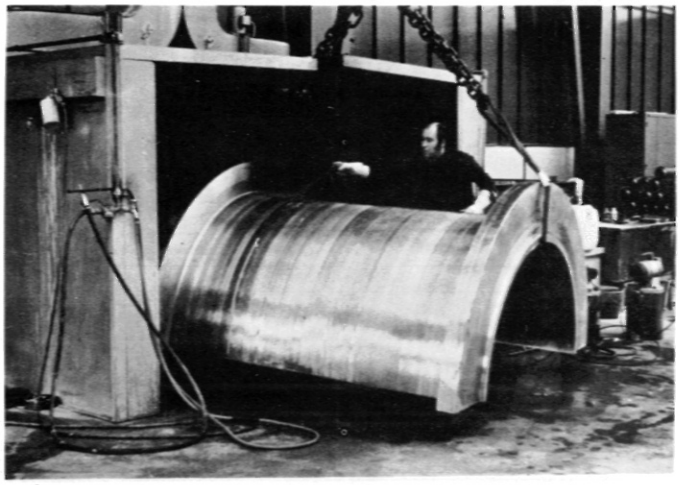

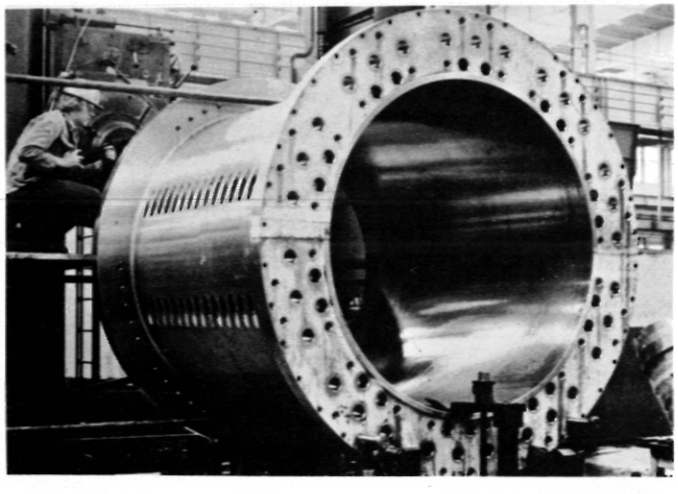

Fig. 7

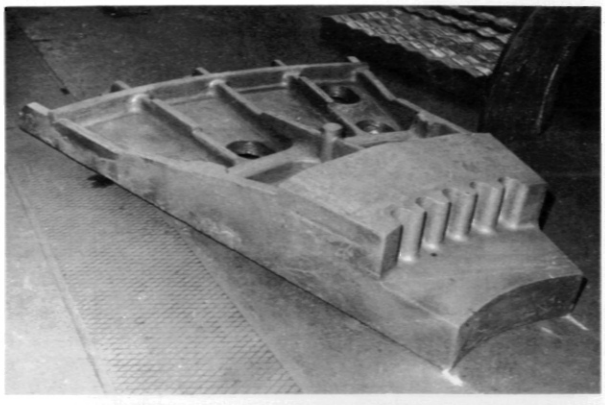

Fig. 8

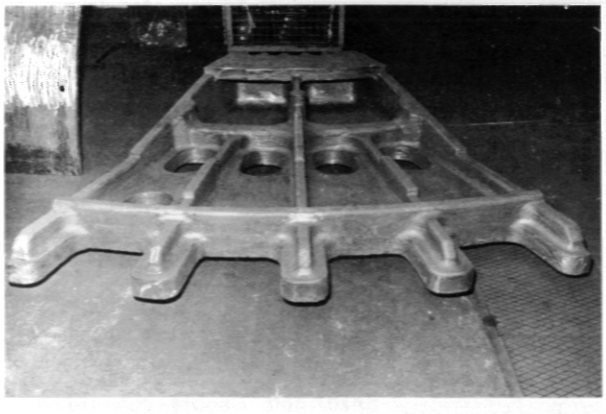

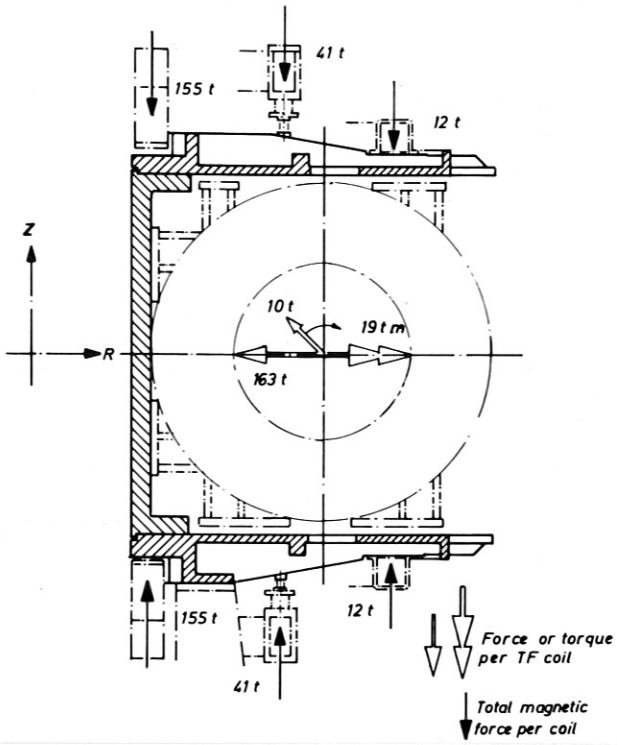

Magnetic Loads on the Support Structure

Fig. 9

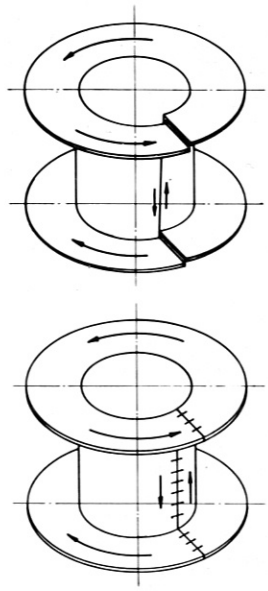

Fig. 10

Fig. 12

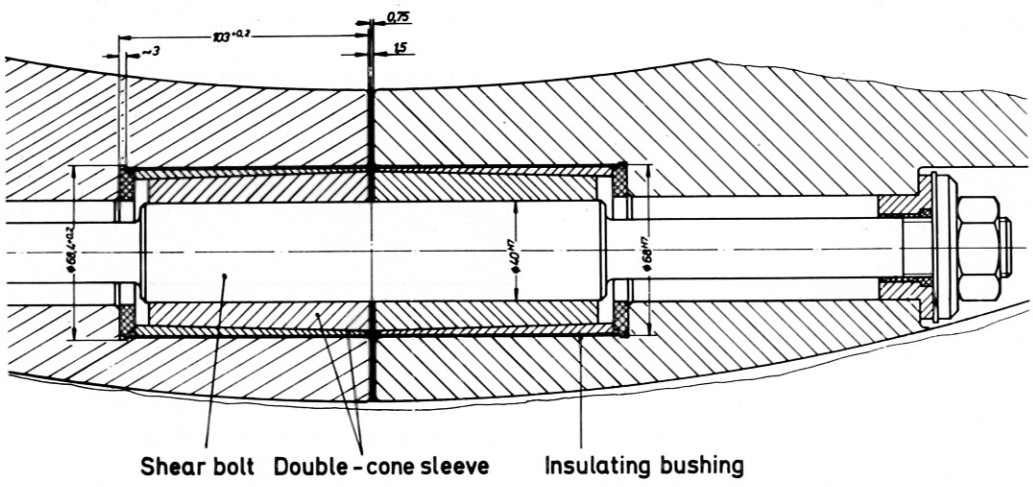

Fig. 11

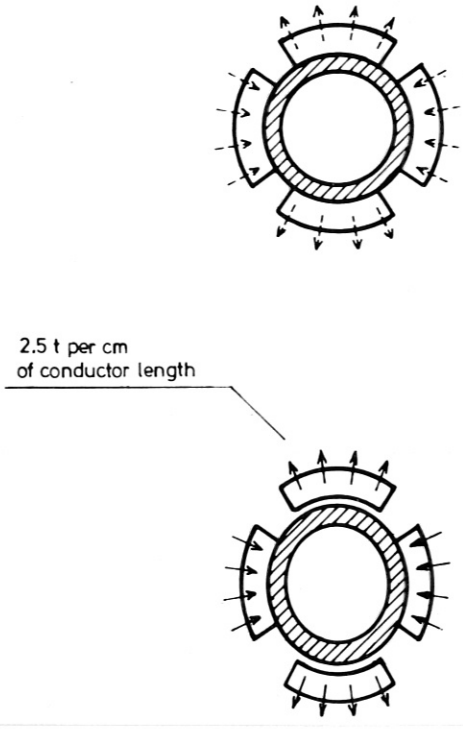

Fig. 13

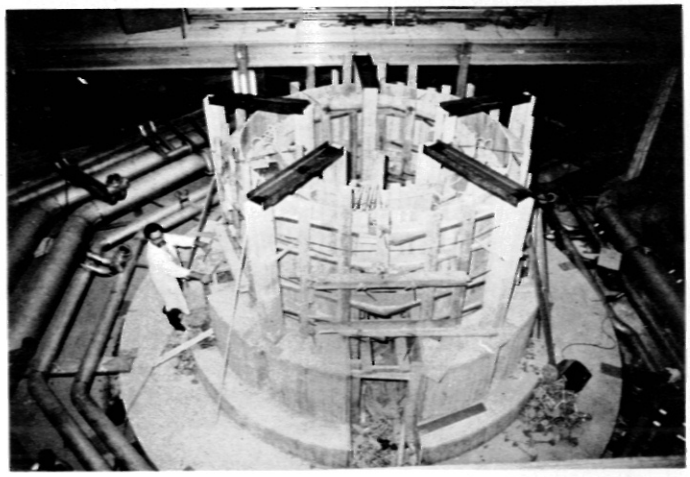

Fig. 16

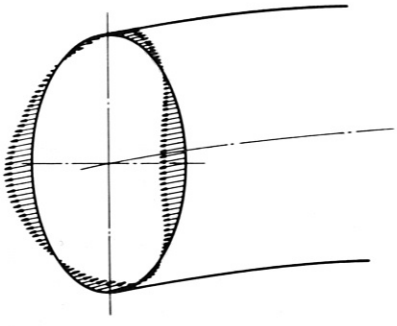

Fig. 14

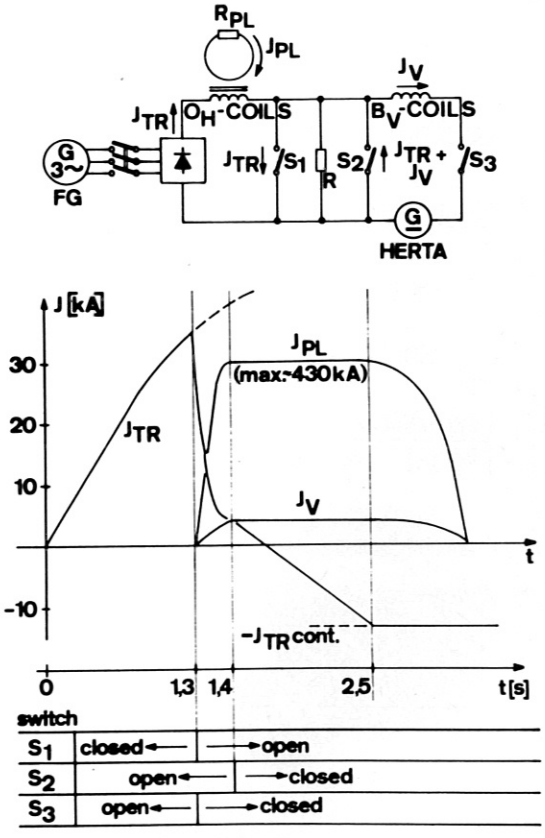

Fig. 15

W 7 Compound Pumping System

TYPE OF PUMP	NUMBER	NOMINAL SPEED EACH, l/s	EFFECTIVE SPEED, TOTAL, l/s
ROTARY FOREPUMPS	2	28	(56)
ROOTS PUMPS	2	280	(560)
TURBOMOLECULAR PUMPS	10	1500	10 000, (H_2)
SAES SORB-AC C 500 (VOLUME GETTER PUMPS)	150	2000 (H_2) 800 (CO,O_2) 500 (N_2)	160 000 (H_2) 50 000 (CO,O_2) 30 000 (N_2)
ELECTRO-ION PUMP	30	1600 (CO,N_2,O_2) 22 (Ar) 2.2 (He)	30 000 (CO,N_2,O_2) 660 (Ar) 60 (He)

Fig. 17

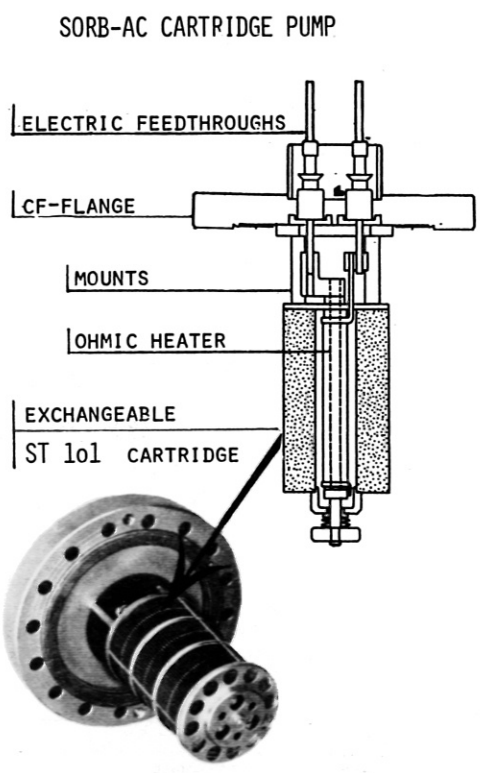

Fig. 18

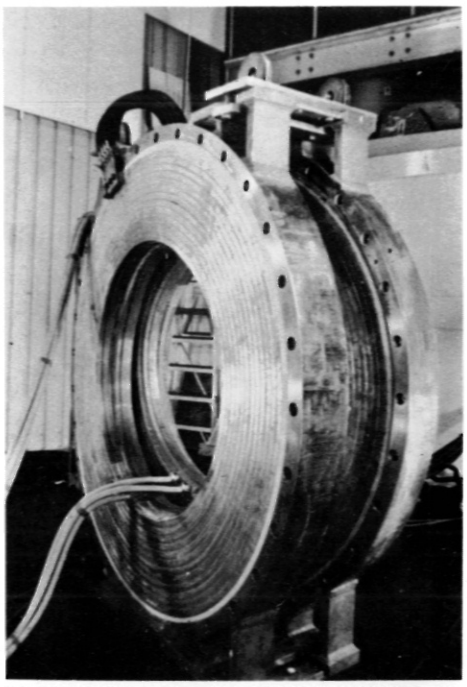

Fig. 21

Fig. 20

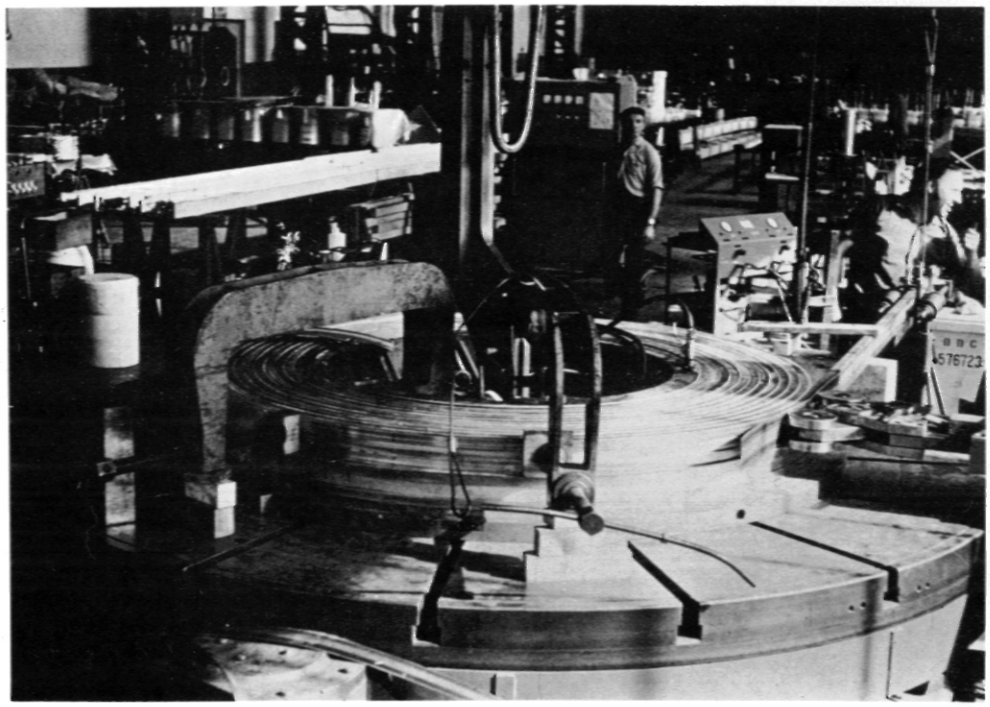

Fig. 19

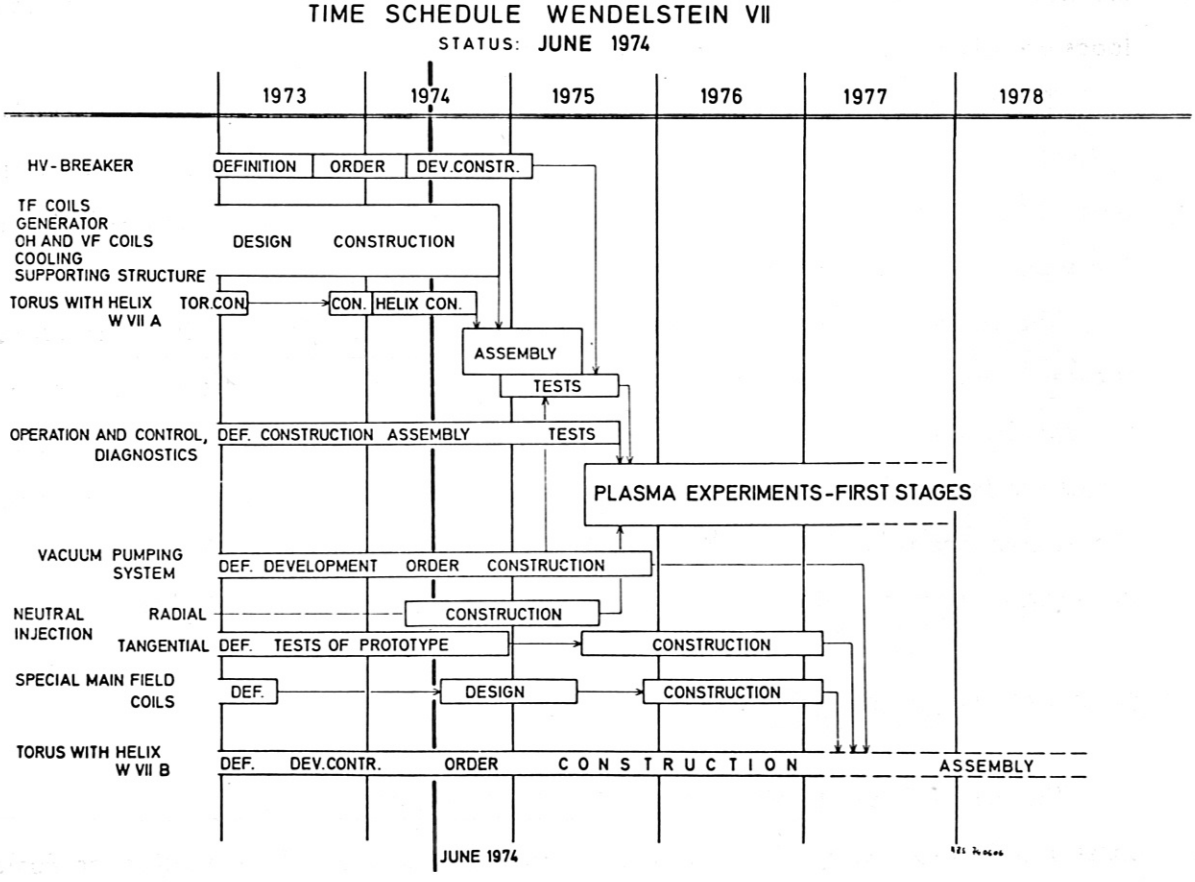
TIME SCHEDULE WENDELSTEIN VII
STATUS: JUNE 1974
1973
1974
1975
1976
1977
1978
HV-BREAKER
DEFINITION
ORDER
DEV.CONSTR.
TF COILS
GENERATOR
OH AND VF COILS
COOLING
SUPPORTING STRUCTURE
DESIGN
CONSTRUCTION
TORUS WITH HELIX
W VII A
TOR.CON
CON.
HELIX CON.
ASSEMBLY
TESTS
OPERATION AND CONTROL, DIAGNOSTICS
DEF. CONSTRUCTION ASSEMBLY TESTS
PLASMA EXPERIMENTS-FIRST STAGES
VACUUM PUMPING SYSTEM
DEF. DEVELOPMENT ORDER CONSTRUCTION
NEUTRAL INJECTION
RADIAL
CONSTRUCTION
TANGENTIAL
DEF. TESTS OF PROTOTYPE
CONSTRUCTION
SPECIAL MAIN FIELD COILS
DEF.
DESIGN
CONSTRUCTION
TORUS WITH HELIX
W VII B
DEF. DEV.CONTR. ORDER CONSTRUCTION
ASSEMBLY
JUNE 1974

Fig. 22

Paper No. 7 a

ON THE TECHNICAL CONCEPT OF THE W VII STELLARATOR

by

M.Blaumoser, G.Duesing, G.Grieger, R.Jaenicke, J.Junker, J.Kolos, P.Meyer, B.Streibl, G.H.Wolf, Max-Planck-Institut für Plasmaphysik, D-8046 Garching, W.Germany, EURATOM- Association.

ABSTRACT

A description of the machine is given, emphasizing the interaction between the main technical components with respect to the acting forces as well as to the assembling of the machine. This serves as an introduction to particular papers on W VII components in these proceedings.

The magnetic loads on the toroidal field coils and those on the helical windings are treated in more detail. In both cases, the technical solutions to cope with the loads are discussed.

The torque on the toroidal field coils is introduced into a central supporting cylinder via two supporting disks on top and bottom of the coils. The cylinder being twisted by this torque suffers considerable shear stresses on its vertical insulating gaps. The support structure is fabricated of cast non-magnetic steel.

The magnetic load on the helical conductors results mainly in longitudinal stresses in the conductors and corresponding helical tensile stresses as well as bending moments in the vacuum vessel. Since in the case of the W VII b torus the acting forces are ten times higher than in the largest stellarators built up to now, the strength of this component has been a major design problem, especially at the removable torus segment and at the conductor connections and water supply holes.

GENERAL DESCRIPTION

The WENDELSTEIN VII (W VII) facility is a stellarator being constructed in Garching. It has first been presented at the 7th Symposium on Fusion Technology, Grenoble, in October 1972 with its main technical and physical parameters as well as with its scientific aims[1].

The first section of this paper gives a general technical description of the machine with its main components and is intended to serve as an introduction to a series of papers on special components of W VII contained in these proceedings[2-8].

Torus, helical windings and toroidal field coils

Fig.1 is a cutaway view of the machine, where the support structure, the portholes and all peripheral parts are left out. The toroidal vacuum vessel (torus) has a major diameter of 4 m. Directly wound upon it are the helical windings (helix). They consist of four packages of conductors, which permit a pure $l = 2$ as well as a $l = 2$ and $l = 4$ mode of operation.

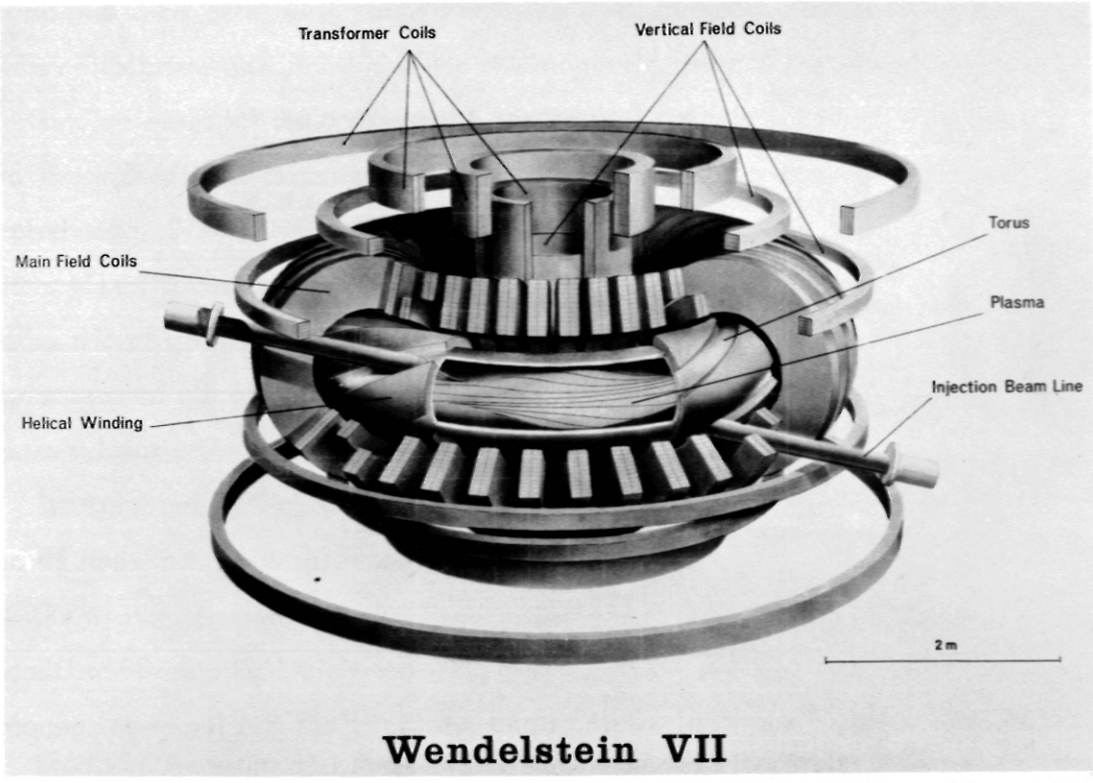

Fig.1. Central components of W VII

A high number of forty toroidal field (TF) coils (main field coils) has been chosen to keep the TF ripple below the ripple of the magnetic mirrors produced by the helical field. The TF ripple will be below 1 % and thus by a factor of 2 to 5 smaller than the helical ripple. The value of the field is 4 T on the toroidal axis. The outer diameter of a TF coil is 2.1 m, the weight is 3.4 t. The coils are slid upon the torus by means of a removable torus segment, which has a width of 18° of azimuthal angle. For the mounting of the connection of the helical conductors across the sections at this torus segment, the TF coils have to be moved aside and have to be readjusted afterwards. This is a mounting difficulty due to the high number of coils, which, however, would be similar with a torus made of two separate halves. The TF coils are being manufactured by BBC Mannheim.

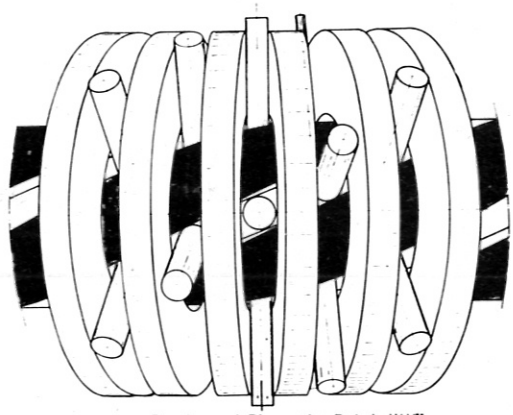

Pumping and Diagnostics Ports in W VII

Fig.2

Due to TF coils and helical windings, the installation of torus ports for pumping and diagnostics is heavily restricted. As shown in Fig.2, port-holes have been put wherever free space is left between the TF coils on the one hand and the helical windings on the other. The total number of ports is 90, the aperture normally varies between 90 and 160 millimeters, but in extreme positions it is only 30 millimeters.

The power supply for helical windings and toroidal field is a fly wheel generator[6] constructed by Siemens, which supplies a power of 150 MW during a maximum pulse length of 10 seconds. It needs 6 minutes after a pulse to be reaccelerated to its original speed. The generator supplies a DC current of 40 kA after rectification, which flows through a series connection of the TF coils and the single conductors in the helical conductor packages.

Furthermore, Fig.1 shows one of the two beam lines for neutral particle injection[8] and the geometry of a possible solution: The helical windings have not been modified, but there is an inclination of the beam line, and special toroidal field coils are provided where the beam line goes through.

Transformer and vertical field coils

For ohmic heating[5] of the plasma, W VII is equipped with an air-core transformer. The magnetic flux its primary can produce has been fixed to 2.9 Vs, which is estimated to be sufficient for achieving a plasma current of 500 kA. For pure tokamak operation this value would correspond to a safety factor of $q = 2$. The primary coils (Fig.1) are arranged outside the toroidal field coils. There is a central cylindrical coil, which is the actual flux producing coil, and twice three compensation coils on top and bottom. The compensating coils keep the magnetic field in the plasma region below 5×10^{-4} T. The outer diameter of the two largest coils is 7.2 m.

Since W VII has been designed to control long plasma current pulses of the order of a second in case they can be reached, a vertical field is needed for the positioning of the plasma, i.e. for improving the equilibrium configuration already existing. The vertical field coils[5] are geometrically similar to the transformer coils. They consist of a cylindric coil inside the central transformer coil and two additional coils both on top and bottom (Fig.1).

Both the transformer and the vertical field coils are being manufactured by Lintott, England.

Support structure

Fig.3 is a section of the machine with now the support structure added. A stainless steel reinforced concrete foundation is set upon the basement floor of the hall. The torus with the helical windings is supported by five pillars. The other components of the machine are not mechanically connected with the torus in order to permit an independent adjustment and to avoid an interaction of the different deformations of the torus and the TF coils during a pulse.

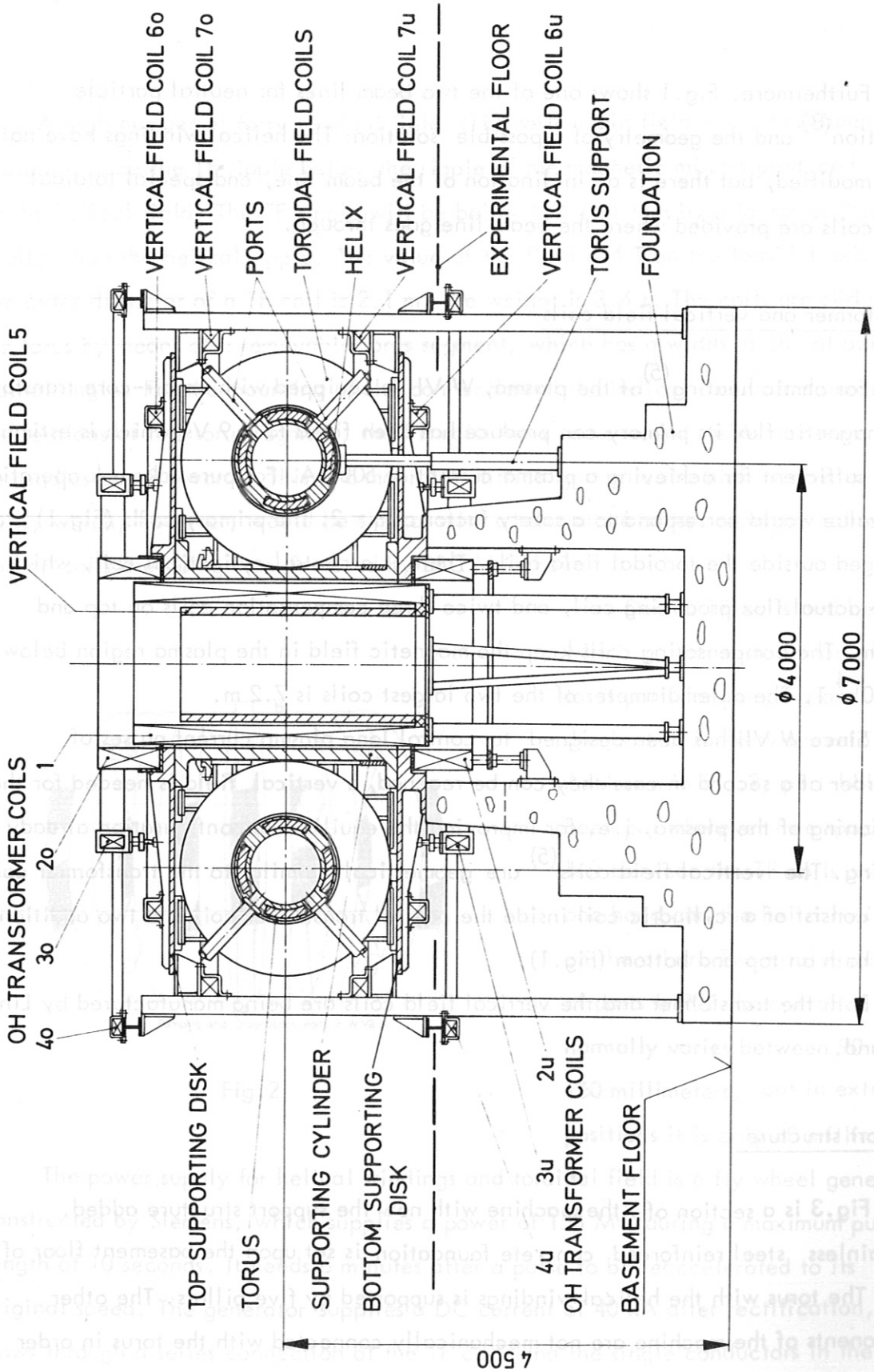

Fig.3.W VII main components and support structure

The TF coils and most of the other components are supported by a separate structure, which consists of a central supporting cylinder and two large supporting disks connected with the cylinder at top and bottom. The cylinder is 2.2 m high, has a wall thickness of 12.5 cm and a weight of 16 t. The disks have an outer diameter of 6.1 m, a height of about 25 cm, and a weight of 15 t and 17 t, respectively. This dimensioning was fixed by the given tolerances: The maximum admissible tilt of the toroidal field coils is 1 milliradian and the maximum admissible compression of the central cylinder is a radial shift of 1 mm.

The cylinder is fabricated in two halves, each disk consisting of 10 segments. Each of these has several large openings for the torus ports, the cooling water tubes, etc. These parts, produced by the Deutsche Edelstahlwerke, are castings made from a non-magnetic steel according to the German standard DIN 1.4311. This is a nitrogen stabilized low carbon steel with a relative magnetic permeability of $\mu = 1.01$ and possessing a yield strength(when cast)of $\sigma_{0.2\,\%} = 20$ kg/mm^2 and a tensile strength (when cast) of $\sigma_B = 45$ kg/mm^2. Certain heavily stressed pieces in this support structure like connecting bolts are made of the stainless steels DIN 1.3952 and DIN 1.3991, which after a special treatment have a yield strength up to 70 and a tensile strength up to 90 kg/mm^2. The final machining of the support structure is being done by Krupp Bochum.

LOADS ON THE TOROIDAL FIELD COILS

This section describes how the loads on the TF coils are transmitted to the supporting structure. Fig.4 shows the acting magnetic forces and torques. The weights, being small compared with the magnetic forces, are omitted.

The centripetal force of 160 t per coil, which results from the interaction of the coil currents with the toroidal field, is transmitted to the supporting cylinder by two coil feet.

The torque of 19 tm acting on each coil is due to the interaction of the coil currents with the vertical field, which typically has a value of 0.1 T. By means of wedges between the coil feet, which are not given in the figure, this tilting moment

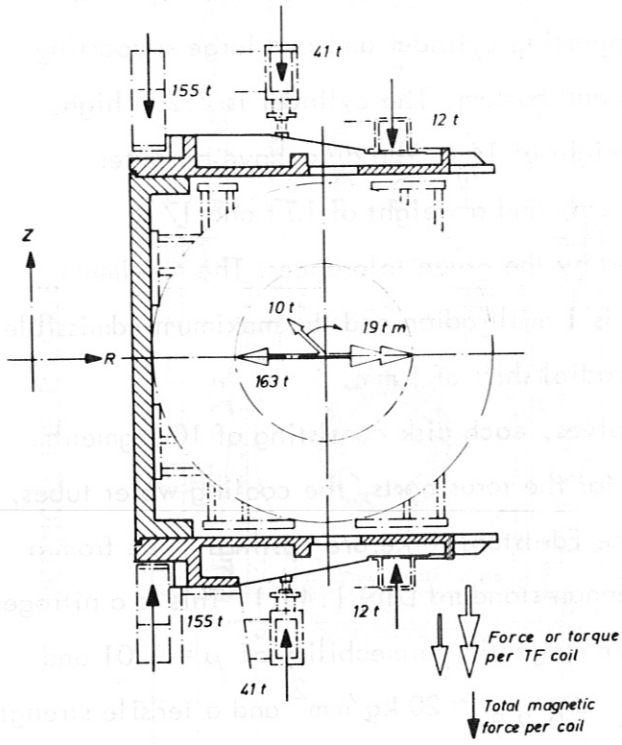

Magnetic Loads on the Support Structure

Fig.4

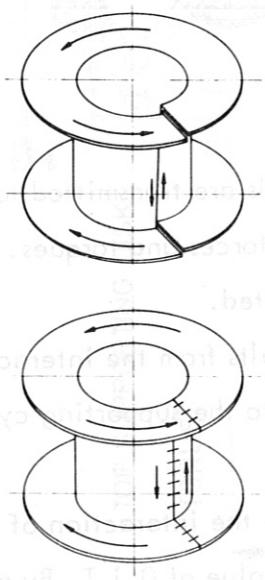

Fig.5. Torque on the support structure

is transmitted via the coil feet on top and bottom to the supporting disks and to the cylinder, where it becomes a vertical torque which tries to twist the structure as is shown in Fig.5. This torque has the considerable value of 710 tm.

The main design problem with these loads were the two vertical slots in the supporting cylinder, which have to be insulated against the loop voltage of 200 V induced by the transformer and against a much higher loop voltage due to disruptive instabilities. At these slots, the torque results in considerable opposite vertical forces on the section surfaces. Therefore insulated shear bolts have been inserted in the slots as indicated in the lower part of Fig.5. Each bolt is fitted into double-cone sleeves, which on their part are pressed into an insulating bushing.

The reason to choose this spool-like support structure of central cylinder and disks was the following: The central cylinder is needed to support the centripetal forces in any

case; since due to their high number, the coils cannot be easily wedged against these forces: The wedge angle is small and the coils have to be moved against each other for the mounting of the removable torus segment. On the other hand, it was desirable to have free access to the many torus ports provided and hence to avoid an exterior structure with e.g. diagonal beams supporting the acting torque.

Additional forces arise in the case of the failure of TF coils: If a single coil is short-circuited, the neighboring coils each suffer a force of 290 t perpendicular to the coil mid-plane. This force is not supported by the disks, but mainly by the above mentioned wedges between the coil feet. These wedges are not bolted to the disks: The torque on the coils is transmitted to the disks by static friction only. In the case of failure of a coil, the azimuthal forces surpass these friction forces and are supported by the toroidal arrangement of TF coils and wedges.

LOADS ON HELIX AND TORUS

The total magnetic force acting upon a helical conductor package points essentially into the direction of the minor torus radius, either outwards or inwards, as shown in Fig.6, along the path of the conductors and has a mean value of 2.5 t per cm conductor length in the case of 1 000 kA per package, which is the original design value for the large W VII b torus[9].

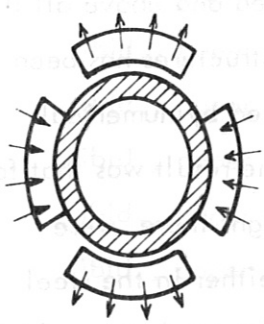

Fig.6. Forces on the helix (Minor torus cross-section)

Thus this force, which is roughly ten times higher than the corresponding force in the largest stellarators built up to now, either presses a helical conductor against the vacuum vessel - and this on its total length - or pulls it away from it.

The results are an elliptical deformation of the torus cross-section (Fig.6), which proceeds helically with the conductors around the toroidal axis, as well as longitudinal

stresses in the conductors. E.g. a conductor that is being pulled away from the torus is wound around it on a larger radius than before and thus it is elongated and suffers a longitudinal tensile stress. In the same way, the conductors being pressed against the torus suffer longitudinal compressive stresses. If the structure around the helix allows a radial shift of a conductor of 1 mm, this stress amounts typically to 7 kg/mm^2. This presents a difficulty for the design of the conductors with their connections, their water supply and discharge holes and their current joints.

Similarly, the deformation of the torus results in helical stresses in the torus wall, which are either compressive or tensile. This is especially obstructive to an easy design of the connection of the torus with its removable segment, which in addition to being vacuum-tight and electrically insulating now has to cope with azimuthal stresses as shown in Fig.7. These stresses try to deform the section surfaces and make the connections gape. A typical value is 120 t for the force in Fig.7 integrated over 90° in poloidal angle from one zero-point of the force to the next, in the case of a radial deformation of 1 mm.

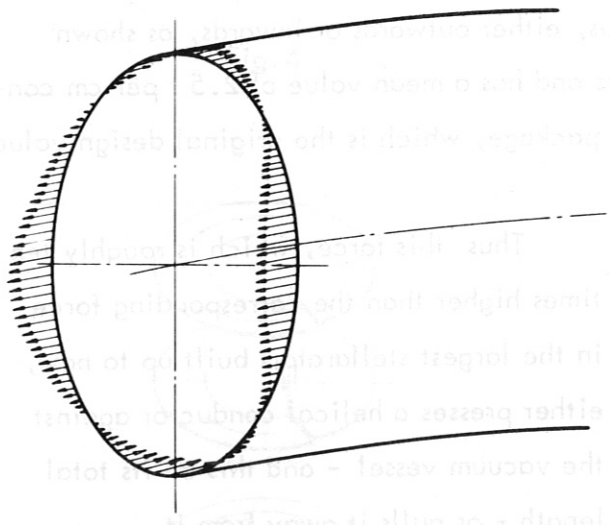

Fig.7. Forces on the torus section surfaces

In order to find a safe design for the supporting of all these stresses, we have investigated various compound structures of the torus, the helical windings and bandages around them. The different manufacturing processes have been studied and above all the strength of the structures has been carefully analysed by numerical calculations. The result was that for each of the designs there were stresses arising either in the steel structure or in the conductors which were at the limit of the strength of the materials.

Therefore we have rediscussed the physical parameters of the machine and have seen that the acting forces can be considerably reduced by the following means: Reduction of the helical currents to 720 kA per package, slight reduction of the torus aperture to 68 cm in diameter, operation of the machine such that the maximum rotational transform of 0.4 to 0.5 is reached only at reduced toroidal field and that vice versa the rotational transform is reduced at the maximum toroidal field of 4 T. With this reduction of the design parameters the resulting stresses should be sufficiently below the yield strength of the materials used.

Nevertheless, the manufacturing of this component will be difficult and time-consuming. Therefore we are constructing a smaller torus with helical windings[7] in the meantime. This torus W VII a will have an aperture of 35 cm in diameter and helical currents of 160 kA per package. It will be ready in the fall of this year[9] together with the other main components.

REFERENCES

1) G.H.WOLF et al., "Status and Technical Concept of the Garching Stellarator WENDELSTEIN VII", Proc. 7th Symp. on Fusion Technology, Grenoble, EURATOM Report Eur.4938 e, p. 239 (1972).

2) Proc. 8th Symposium on Fusion Technology, The Netherlands, (1974), paper 7c: "Cooling Systems of W VII ".

3) ibid. , paper 7 d: "Vacuum System of W VII b"

4) ibid., paper 7 e: "Design and Manufacturing of the TF Coils of W VII "

5) ibid., paper 7f: "Ohmic Heating and Vertical Field Coil Systems of W VII"

6) ibid., paper 19: "Flywheel Power Supply in the IPP Garching"

7) ibid., paper 12: "Torus with Helix W VII a"

8) ibid., paper 26: "DC Neutral Particle Injection for W VII"

9) ibid., paper 7b: "Status of W VII"

Paper No. 7 b

STATUS OF WENDELSTEIN VII (W VII)

by

M.Blaumoser, G.Duesing, G.Grieger, J.Junker, F.Rau, and G.H.Wolf,
Max-Planck-Institut für Plasmaphysik, 8046 Garching, W.Germany,
EURATOM-Association.

ABSTRACT

W VII is under construction. All major components have been ordered and will be delivered in the course of the year 1974, except for the final torus and its pumping system. As planned, operation of W VII will start in 1975, using however, that torus vessel (W VII a, r_i = 17.5 cm) which had been originally foreseen, i.e. before we attempted to start W VII with the larger torus (W VII b, r_i = 35 cm, tangential injection access). The delivery of this larger torus is expected to be delayed by about two years, partly because of the necessity to place development contracts with industry before the manufacture of this component can be started.
The first experiments in W VII will be devoted to the ohmic heating studies in order to allow for an immediate application of the neutral injection programme when the W VII b torus will be available.

According to present knowledge, the total capital costs of the W VII will be about 20 Mio DM (without the main power generator).

The number of professionals engaged in the design and construction of W VII and in the preparation of the operational phase is about 25.

The stellarator W VII is under construction. All major components have been ordered and will be delivered in the course of this year. First experiments are expected to start around mid of 1975, nearly in agreement with our original schedule.

Note, however, that this first stage of W VII will be equipped with the small bore torus W VII a ($r_i \approx 17,5$ cm) as foreseen only in a very early state of planning. By way of contrast, lateron we were aiming at starting the experiments immediately with the large bore ($r_i \approx 35$ cm) torus W VII b, thus following also the recommendations of the EURATOM Advisory Group on Stellarators (September 1971). It was our belief at that time that no serious delay would result by this conceptual change. During the design phase, however, we were faced with problems concerning the concept and the manufacturing procedure for the W VII-b torus, which resulted in two development contracts we had placed with potential manufacturers of this component.

The difficulties are caused by the forces and stresses on the torus which originate from the interaction of the helical currents and the toroidal magnetic field. The larger radius envisaged by us and the further increase of the rotational transform which was made possible after the purchase of the new large electric power generator for the normal conducting field coils, have led to a strenght problem, the consequence of which could be fully evaluated only after obtaining the results of a rather detailed numerical stress analysis which will be reported elsewhere. It showed the necessity for a slight reduction of the original parameters: helical current and vessel bore, and we expect that under these circumstances the construction of the component "Torus with Helix W VII-b" can be started during the course of this year. For this component, the construction time estimated by industry, is about 3 years. Consequently, also the manufacturing of other components required for experimentation with the large bore torus, which will characterize the second stage of the W VII facility, such as the powerful vacuum system and the special main field coils for tangential neutral injection, will be determined by the delivery of the W VII-b torus.

Thus, as stated, W VII will start operation by using the W VII-a torus. It should enable us to study an ohmically heated stellarator plasma and its confinement properties in the range up to an ion temperature of 1 keV (according to the Düchs code) and up to a magnetic field of 4 T. Compared to the ohmic heating experiments presently running in the W II-b stellarator it looks promising to include a parameter regime where the ohmic current is kept small enough to produce a rotational transform which is smaller than that of the helical currents. The characteristic properties of the stellarator magnetic field configuration in the presence of an ohmic heating current may then be separated more clearly than it is possible now. The technical tests of the various components of the machine are planned to be partly combined with the preliminary physics experiments. In the presence of a real plasma we expect to learn more about realistic requirements on the various technical components, e.g. the induced loop voltage from the ohmic heating transformer and the proper switchgear, the programming of the vertical field and its coupling to the transformer coils, and the regulation of the helical currents by external means (to keep the total rotational transform constant). The duration of the scientific programme to be carried out with the first stage of W VII will be determined by the delivery of the final torus, and it is expected to last at least two years.

Fig.1 shows a graph of the time schedule of W VII. There the interlinked system of the major components and their various stages of completion are plotted vs time. The graph is roughly subdivided into two parts characterizing the first stage of W VII (upper part) and the additional components required for the second stage (lower part). For convenience, the time scale begins in 1973, many activities of the whole W VII project being already well under way. The present date is indicated as the bold vertical line labelled June 1974 and the planning is extended until 1977. There is sometimes an overlap between design and construction since e.g. the ordering of material often is made at an early time. The activities (boxes) are connected by thin arrows. In general, these arrows lead to the assembly and tests preceding the plasma experiments of the first stage of W VII. The last group of components describes

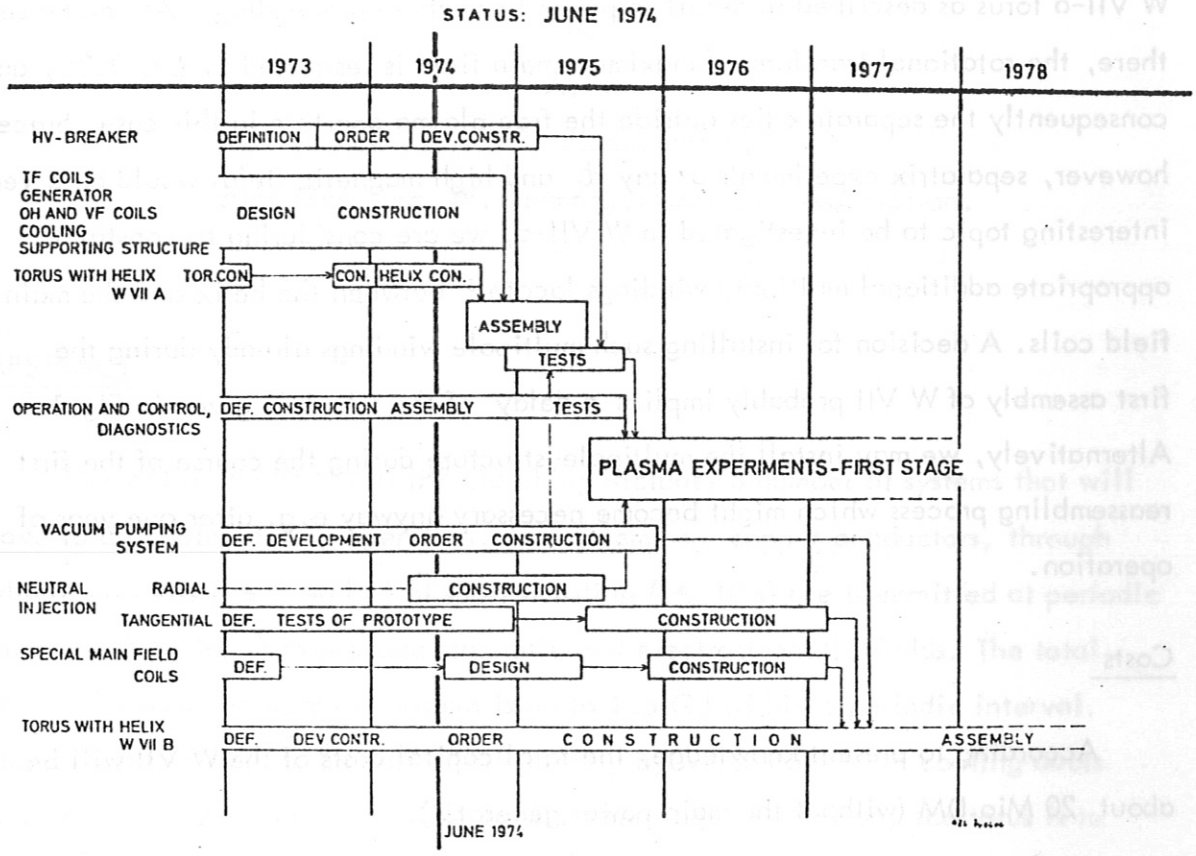

Fig.1. Time schedule WENDELSTEIN VII

the activities directed towards stage two of W VII; i.e. torus with helix W VII B, its elaborate vacuum pumping system, the long duration neutral injection systems, and the necessary special main field coils. The times given on the left hand side of the line labelled June 1974 correspond to acutal dates of events. In certain cases these actual dates deviate towards the unfavorable when comparing them with dates stated previously. This is mainly due to delays during the external manufacture. So we have to state that sometimes even in cases where a penalty was agreed upon in the contract with the manufacturer a certain delay in delivery could not be excluded. Consequently, we have to consider the estimated times of the future activities given in the present planning as being somewhat uncertain, within limits which expand towards the future.

The figures given in the time schedule correspond to a state of equipment of the W VII-a torus as described in detail in paper 12 of these proceedings. As can be seen there, the rotational transform at maximum main field is restricted to $\iota \lesssim 0.25$, and consequently the separatrix lies outside the free plasma aperture in this case. Since, however, separatrix experiments at any ι and high magnetic fields would be a very interesting topic to be investigated in W VII-a, we are considering to construct appropriate additional multipole windings located between the helix and the main field coils. A decision for installing such multipole windings already during the first assembly of W VII probably implies a delay of the schedule given in Fig.1. Alternatively, we may install the multipole-structure during the course of the first reassembling process which might become necessary anyway e.g. after one year of operation.

Costs

According to present knowledge, the total capital costs of the W VII will be about 20 Mio DM (without the main power generator).

Manpower

The number of professionals engaged in the design and construction of W VII and in the preparation of the operational phase is about 25.

Paper No. 7 c

COOLING SYSTEMS OF THE W VII STELLARATOR

by

A. Elsner

Max-Planck-Institut für Plasmaphysik,

8046 Garching, W. Germany, EURATOM Association.

ABSTRACT

The stellarator W VII at IPP Garching includes a number of systems that will have to be cooled during operation. The systems are copper conductors, through which currents ($\leq$ 40 kA) of short duration ($\leq$ 10 s) are transmitted at periodic intervals ($\geq$ 360 s) to produce magnetic and electromagnetic fields. The total heat to be removed from all systems is up to 1.5 GJ within a periodic interval. The conductors have to be cooled sufficiently by water flowing in cooling ducts so as not to exceed the permissible level of heating. In addition, the torus is to be cooled by thermal contact with another cooled system, namely the helical windings.

The first part of this report presents numerical calculations of the time dependent thermal system parameters such as the temperatures of the copper conductors and cooling water. The second part describes the dimensioning calculations for designing the cooling systems of W VII, including the heat exchangers and pumps.

PART I

HEAT GENERATION AND TRANSPORT IN STRAIGHT, WATER-COOLED HOLLOW CONDUCTOR

Model for calculating the conductor and coolant temperatures

Figure 1 shows the model of a straight, water-cooled hollow conductor on which the computer calculations are based. The hollow conductor of length L is composed of N segments of equal length dL (L = N . dL). In general, the cross-sections for the electric current, A_c, and for the water flow, A_w, as well as the surface for heat transfer, A_t, are functions of the segment n ($1 \leq n \leq N$). Temperatures are assumed to be constant within a segment.

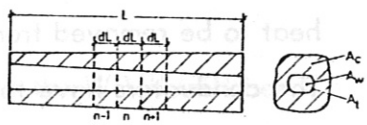

Fig.1 Model of straight, water-cooled hollow conductor

To calculate the time-dependent temperature of each segment, an energy balance is set up for each time step. This energy balance considers the heat transfer from conductor to water, the heat conduction between adjacent segments as well as the generation of ohmic heat in the conductor.

If the initial temperatures of the water T_w (n, 1) and conductor T_c (n, 1) and the water temperature on entry into the first segment, T_w (1, m), are known, it is possible to calculate in succession the time variations of the enthalpy, from which the water and conductor temperatures for all segments n can be determined.

This model is used to calculate the cooling rate of the main field coils, vertical field coils, coils of the trafo, and helix. These components are shown in Fig.1 of paper [3].

Table I contains the data for the main field coils, the vertical field coils, and the helical windings on which the computer calculations are based.

TABLE I

		main field coil	vertical field coil	helix
Length of cooling duct	L [m]	59	122	3
Cross-section for water	A_w [cm^2]	4	0.332	1.9
Cross-section for current	A_c [cm^2]	20.8	3.868	10.6
Electric current	I [kA]	40	6	40
Time of current pulse	t_I [s]	10	5	10
Time of repetition	t_r [s]	360	120	360
Number R_{wc} (equation 1)	R_{wc}	4	0.4	42

MAIN FIELD COILS

Figure 2 shows for a main field coil the temperature of the copper conductor and cooling water at four different test sites along the cooling duct, at distances of 0, 20, 40 and 59 m from the cooling water inlet point. The plot shows that the temperature curves coincide during the current pulse (40 kA, 10 s) and increase linearly with the current pulse length t_I. The temperature of the conductor thus increases by the same amount at every point of the coil winding. Evidently, the temperature increases with both $(I/A_c)^2$ and t_I, but this increase is independent of the water flow rate as long as the time t taken by the water to pass through the cooling duct is greater than the current pulse length t_I:

$$t > t_I .$$

This is shown by curves ΔT and t in Fig. 3, where further results of the computer calculation are given. The various quantities on the ordinate have different scales depending on the quantitiy plotted. The abscissa refers to the water flow rate through one cooling duct.

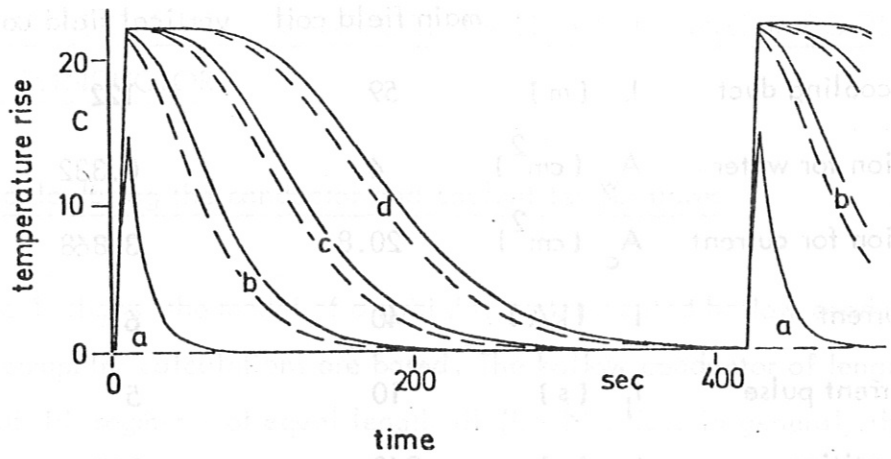

Fig.2. Main field coil temperature during and after current flow. Coil current 40 kA, pulse length 10 sec, water flow rate through one cooling duct 0.6 l/sec. Solid curves: temperature rise of conductor. Dashed curves: temperature rise of cooling water. Curves a: at cooling water inlet, curves b and c: 20 m and 40 m from cooling water inlet, curves d: at cooling water outlet (duct length 59 m).

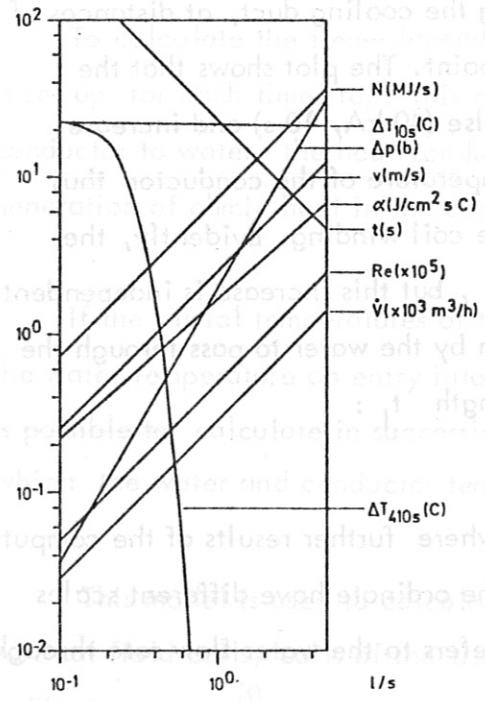

Fig.3. Data for main field coil cooling dependent on water flow rate through one cooling duct (l/s). Coil current 40 kA, pulse length 10 s. N thermal power removed from 40-coil system by cooling water at end of pulse, $\Delta T_{10\ s}$ and $\Delta T_{410\ s}$ temperature rise of coil and water at end of cooling duct and at end of pulse, respectively 410 s after pulse, Δp pressure loss due to viscosity of water in cooling duct, v flow velocity of water in cooling duct, α mean heat transfer coefficient, t time taken by water flow through cooling duct, Re Reynolds number in cooling duct, $\dot{V}$ water flow rate through 40 coils.

Returning to Fig.2 once again we note that the temperature at the water exit starts decreasing after 100 s. Complete cooling of the coil does not occur, however, until a cooling time of approximately 350 s has elapsed. As can be seen, with the water flow rate chosen here (0.6 l/s) the time between two successive current pulses is just sufficient to allow complete cooling after every current pulse. The numerical ratio of the "heat capacities" of the cooling water and copper conductor,

$$R_{wc} = (c_w / c_c) \cdot (\varrho_w / \varrho_c) \cdot (A_w / A_c) \cdot (t_r / t), \qquad (1)$$

can be enlisted as a criterion for determining whether the temperature level of the coil is raised after the first pulse during the shortest repetition time t_r or not. (c_w, c_c, ϱ_w, ϱ_c specific heat and density of water and copper, respectively). According to Table I the value of R_{wc} is 4, and according to Fig.2 complete cooling is just achieved. The critical value for complete cooling is therefore considered to be

$$R_{wc} = R_{crit} = 4, \qquad (2)$$

and this value has to be maintained to prevent the temperature level from rising after the first current pulse.

VERTICAL FIELD COILS

The time taken by the water to pass through the cooling ducts in the vertical field coils is about 30 s and is thus much longer than the intended current pulse length of 5 s:

$$t > t_l.$$

On the short time scale the heating of the coils does not depend on the water flow rate. According to Table I

$$R_{wc} < R_{crit},$$

and so the temperature level can be expected to rise after a number of current pulses have been transmitted through the coils. Therefore, on the longer time scale the temperature will saturate to a value which depends on the flow rate.

As an example Fig. 4 shows the temperature distribution in coil No 6a. Periodically recurring temperature changes appear after the third current pulse. Then the water completely removes the heat generated in the last interval between two successive current pulses.

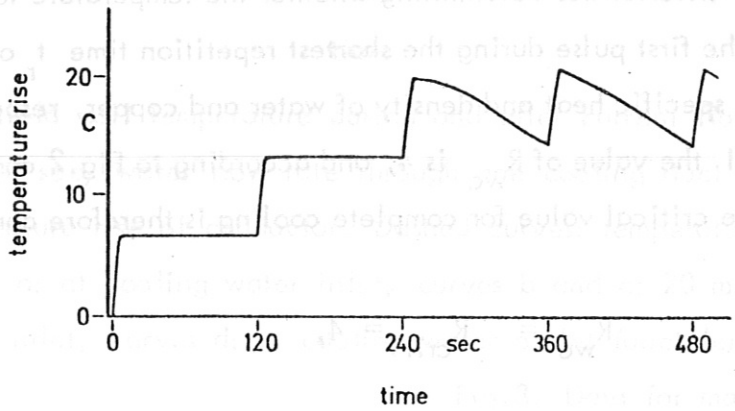

Fig. 4. Temperature of vertical field coil No6. Coil current 6 kA, pulse length 5 sec, water flow rate 0.12 l/sec.

HELIX

The helix and main field coils are electrically connected in series. As the conducting cross-section of the helix is only half as large as that of a main field coil, the heat loss per unit length occurring in the helix is four times that in a main field coil. However, the heating would be less than a factor of 4 if the major part of the heat generated is already removed by water flowing through a number of short ducts (connected in parallel) during the current pulse. Because the transit time of the water in the cooling duct is short compared with the pulse duration,

$$t < t_l,$$

the heating of the helix is essentially dependent on the water flow rate. See Fig. 5 curves ΔT and t depending on the flow rate.

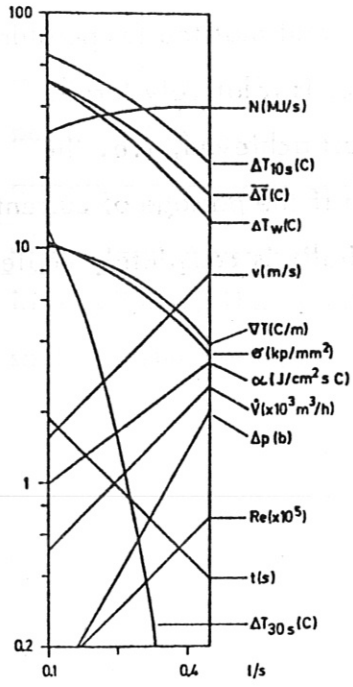

Fig. 5. Data for helix cooling dependent on water flow rate through one cooling duct (length 3 m). Helix current 960 kA, pulse length 10 sec. Symbols N, ΔT, v, α, $\dot{V}$, Δ.p, Re, t as in Fig. 3. $\overline{\Delta T}$ mean temperature rise of helix after one pulse, ΔT_w temperature rise of water at end of pulse, ∇T temperature gradient in conductor after one pulse, σ sum of tensile and compressive stresses due to $\overline{\Delta T}$ at a fixed length of helix conductor.

To maintain the exact position of the helical windings on the torus (i.e. to avoid significant thermal expansion) the temperature change of the helix should not exceed 40 degrees. The water flow rate through the helix ducts that is needed during a current pulse is therefore large. Since the value of R_{wc} at 42 is very much higher than $R_{crit} = 4$,

$$R_{wc} \gg R_{crit},$$

there is good reason for reducing the water flow rate after the current pulse (see Part II).

The result of the computer calculation with a given flow rate of 0.3 kg/s is shown in Fig.6. Compared with Fig. 2 it is noted in the case of the helix that the temperature curves already fan out widely during the current pulse, i.e. that a temperature gradient immediately appears in the conductor, and that the temperature difference between the helix conductor and the cooling water is relatively large. After 10 s (end of current pulse) thermal equilibrium is almost achieved, i.e. the temperature of the conductor and water would increase little if the passage of current were to continue. About 20 s after the end of the pulse the helix is completely cooled.

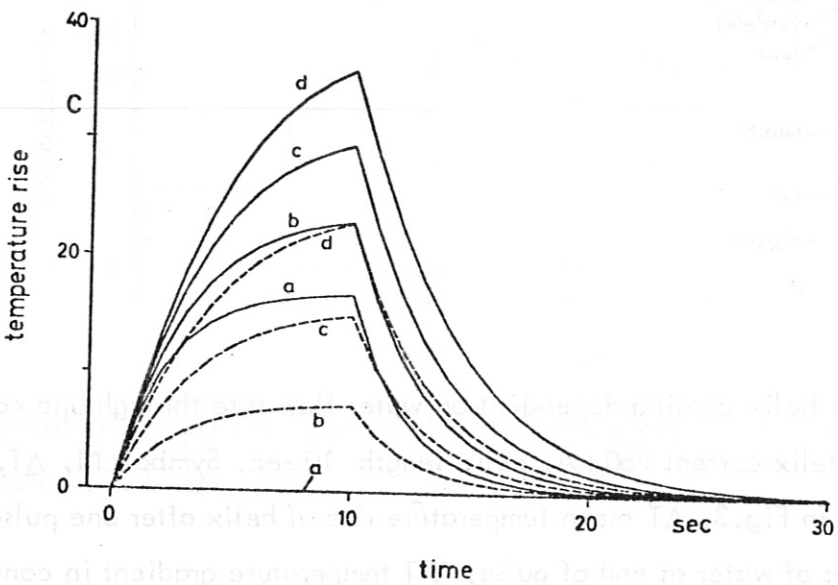

Fig.6.: Helix temperature during and after current flow. Helix current 24 x 40 kA, pulse length 10 sec, water flow rate through helix 1500 m^3/h.
Solid curves: temperature rise of helix. Dashed lines: temperature rise of cooling water. Curves a: at cooling water inlet, b and c: 1 m and 2 m from cooling water inlet, d: at cooling water outlet (duct length 3 m).

ENERGY ABSORPTION AND TRANSPORT IN THE TORUS WALL

Model for calculating the torus wall temperature

Figure 7 shows a cross-sectional view of the torus with the four helical winding packs. The heat generated in the plasma volume during each shot (single experiment or discharge) impinges on the inner wall of the torus and is absorbed. The starting point for the calculation is the fact that the heat transport takes place in the radial direction as a result of the temperature difference between the inner and outer region of the torus wall. The model for the calculation thus considers the thermal conduction in a cylinder. The cylinder is divided into segments of equal length and equal cross-section. The temperature is constant in each segment.

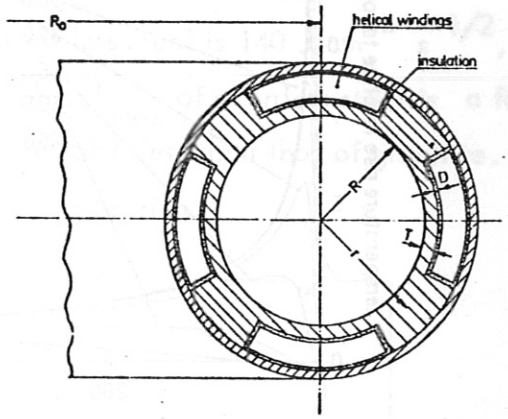

Fig.7. Torus with Helix

The numerical values used for the calculations are listed in Table II:

TABLE II

Inner radius of torus vessel	R	=	36 cm
Inner surface of torus	A	=	28.8 m^2
Volume of torus wall	V	=	2.2 m^3
Thickness of torus wall below helix	T	=	3.5 cm
Thickness of insulator	D	=	0.5 cm
Irradiation power	P	=	1 Mw
Irradiation time	t_P	=	10 s
Repetition time	t_r	=	360 s

TEMPERATURE AT THE INNER WALL

If the radiation energy absorbed in the torus wall diffuses in the radial direction the inner surface of the torus is heated very rapidly, whereas the outer layers of the torus wall are warmed slowly and continuously. The results are shown by Fig. 8.

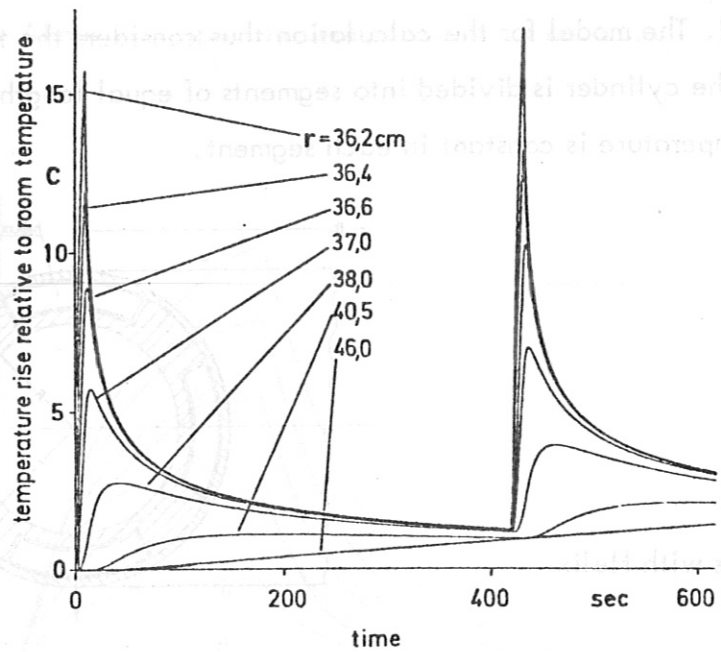

Fig.8. Heating of uncooled stainless-steel torus wall at various radii r. Radiation power 1 MW uniformly distributed on first wall, radiation time 10 sec, repetition frequency 7 min.

Fig. 9 gives the temperature profile within the torus after one shot. The curves indicate that the inner surface of the torus can be heated to intolerably high temperatures when the energy impinged on 1 cm^2 is large, i.e. when the product of irradiation time t and power density p has a large value. The temperature increase ΔT at the surface is approximately given by

$$\Delta T = ß \cdot p \cdot \sqrt{t}, \qquad (3)$$

where the coefficient ß equals $1/\sqrt{k \cdot \varrho \cdot c}$, and k, ϱ, c are the thermal conductivity, density and specific heat of the wall material. Eliminating ΔT in equation (3) and in the well known "stress formula"

$$\Delta T = \sigma / (E \cdot \alpha) \qquad (4)$$

(σ thermal stress, E Young's modulus, α thermal expansion coefficient), we find a relation for the maximum absorbed energy h_{max} dependent on the maximum stress σ_{max} (= tensile strength):

$$h_{max} = p \cdot t = \sigma_{max} \cdot \sqrt{t} \; / \; (E \cdot \alpha \cdot ß). \qquad (5)$$

The value of $\sigma_{max} / (E \cdot \alpha \cdot ß)$ for stainless steel is 140 J cm^{-2} $s^{-1/2}$, for tungsten 440 [1], and for graphite 900 [1]. Thus h_{max} of stainless steel is a factor of 3 less than that of tungsten, and a factor of 6 less than that of graphite. The considerations above do not refer to wall evaporation.

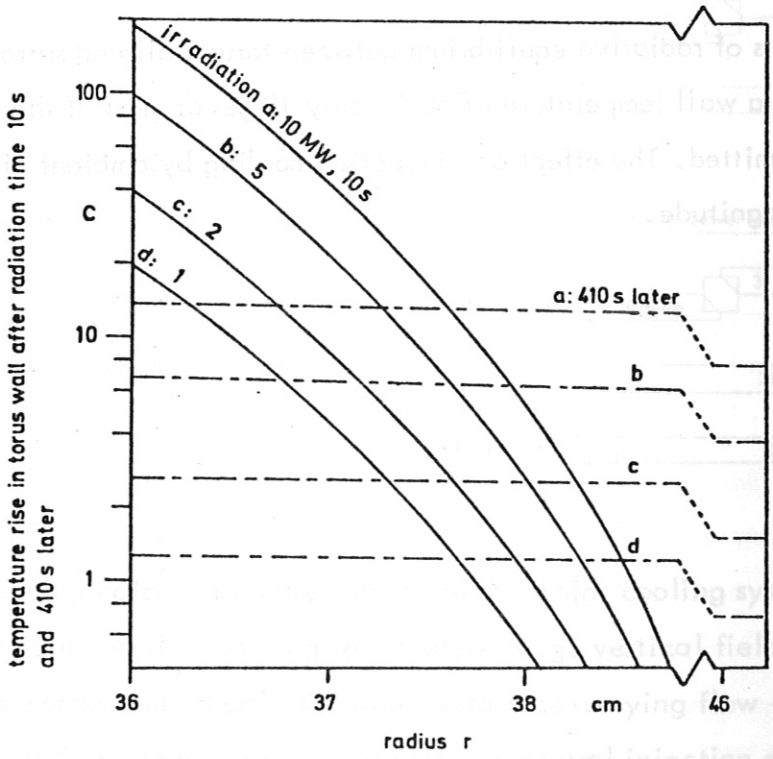

Fig.9. Heating of uncooled stainless-steel torus wall by uniform irridiation of first wall at r = 36 cm

TORUS COOLING BY THE HELICAL WINDINGS

The temperature which the outer surface of the torus would assume in stationary equilibrium is a result of heat conduction to the helical windings, heat radiation and free air convection. From the fact that two-thirds of the torus surface is covered by the helical windings it follows that the torus is mainly cooled by the helical windings. In the thermally stationary state there exists a temperature difference across the insulation layer between the torus wall and helical windings of

$$T_{wall} - T_{helix} = (P/A) \cdot (t_p/t_r) \cdot (D/\lambda)_{insulator}. \qquad (6)$$

The value of the temperature difference of 16 C indicates that the outer wall of the torus will reach a temperature of about 60 C. To heat the torus wall on the average from 20 to 60 C, nearly 30 shots are required. Then the torus is in thermal equilibrium after 3 hours.

Calculations of radiative equilibrium between torus wall and surroundings estimate that at a wall temperature of 60 C only 10 % at most of the absorbed energy will be emitted. The effect of convection cooling by ambient air is of the same order of magnitude.

PART II

DIMENSIONING OF COOLING WATER SYSTEMS

Part II of this report deals with the dimensioning of pumps and heat exchangers in the cooling systems. The systems required for the operation of the stellarator are schematically shown in Fig.10. Some are connected to the ground water supply of the institute, and some to the cooling tower supply.

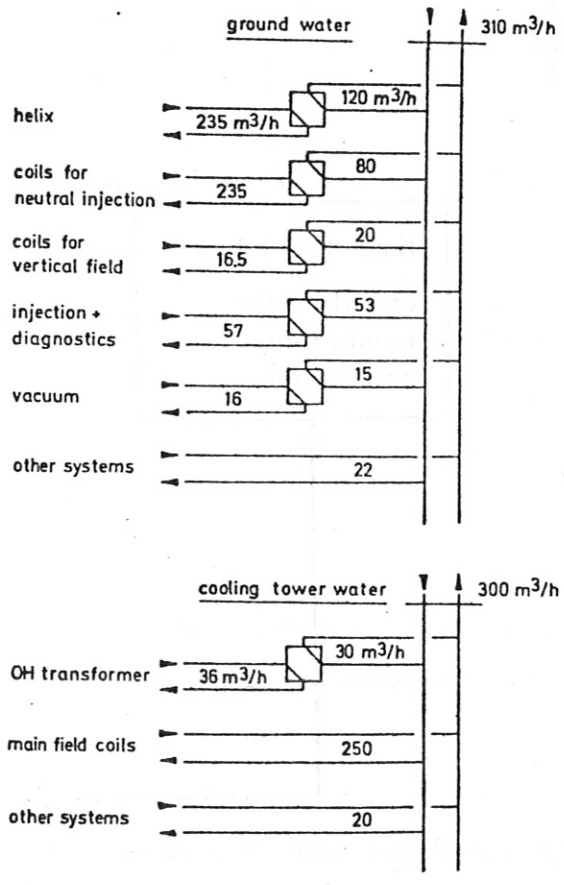

Fig.10. Cooling systems of W VII

The following calculations are related to the major cooling systems,one with constant flow rate and time-varying temperature (e.g. vertical field coils, OH trafo coils, vacuum pumps and others), the other with time-varying flow rate, pressure, and temperature (e.g. helix, main field coils for neutral injection experiments).

Water system with constant flow rate and time-varying temperature

The closed water cycle consists of a system to be cooled (e.g. vertical field coils), a heat exchanger, and pipe lines through which the water is pumped. The dimensions of the pump and heat exchanger are such that the system temperatures are within the required limits. The calculation scheme is reproduced below:

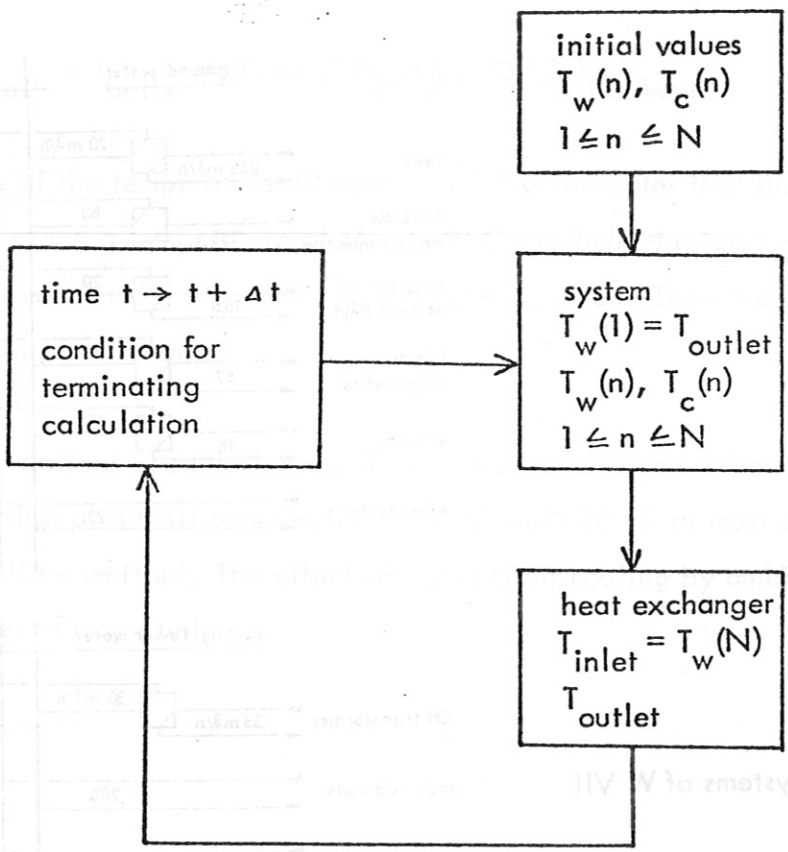

The water flow rate is appropriately chosen and kept constant in time. The water temperature at the inlet of the system is set equal to the temperature with which the water leaves the heat exchanger: $T_w(1) = T_{outlet}$. The water temperatures at the outlet of the system and the inlet of the heat exchanger are also set equal, $T_w(N) = T_{inlet}$. The heat exchanger temperatures are calculated by means of the usual equations[2], the necessary data on the heat exchanger being obtained from manufacturers' catalogues. The time variation of the temperature in Fig.4 is calculated according to this scheme.

Water system with time-varying flow rate

Figure 11 shows the block diagram of a proposed control system for cooling the helical windings. The system consists essentially of two pressurized water containers (pressure $P_1 > P_2$) joined by two branches, one containing a throttle valve followed by the helical windings, the other containing a heat exchanger and a pump. (The primary side of the heat exchanger is connected to the ground water supply.) The pump continuously displaces the cooling water via the heat exchanger from the one container

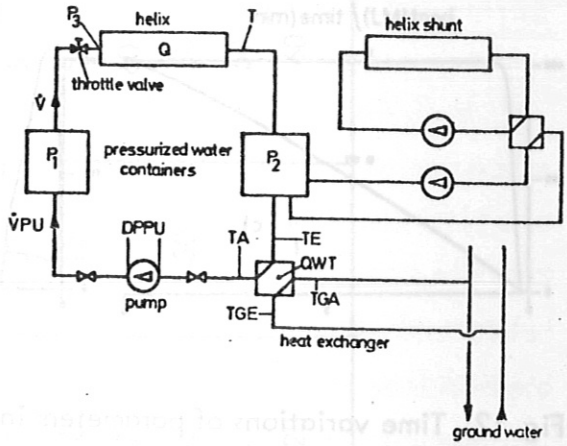

Fig.11. Cooling of helix and helix shunt

(P_2) to the other (P_1). In a short time before, during and after the stellarator discharge (shot) the valve is opened and the water is forced through the helix owing to the difference in gas pressure between the two containers.

The time variations of parameters of interest between two shots are shown in Fig.12 (for explanation of symbols see Fig. 11). The figure gives the water temperatures at the heat exchanger and at the outlet of the helix (Fig.12 a), the pressures in the containers and between the valve and helix, the difference pressure at the pump (Fig.12 b), the heat generated in the helix and transferred to the water, the heat transferred in the heat exchanger to the ground water (Fig.12 c) and, finally, the water flow rates through the helix and pump (Fig.12 d). The dimensions of the pump are such that the water level and hence the pressure in the two containers are restored within 6 min to the initial values. The heat exchanger is designed in such a way that the ohmic heat deposited in the low-pressure container (P_2) is completely transferred within 6 min to the ground water, whereby the water outlet temperature at the heat exchanger ought not to exceed a given value.

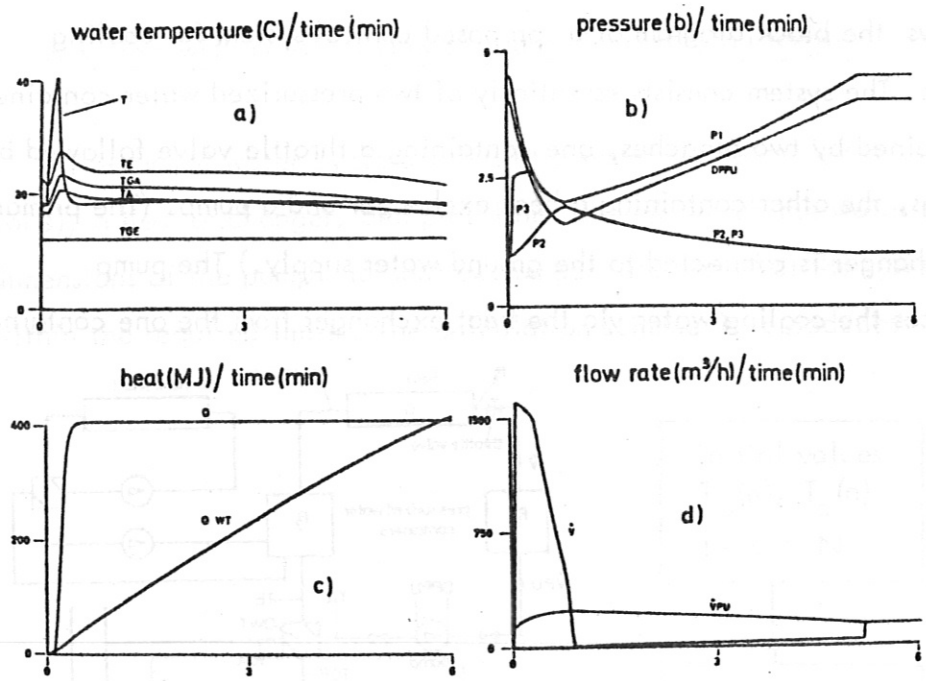

Fig. 12. Time variations of parameters in helix cooling cycle

Table III lists the essential data for cooling. It should be noted that the maximum heat generation within 360 s for each individual system is not achieved simultaneously in all systems (column 3). The maximum heat generated simultaneously in all systems is 1.5 GJ in 360 s.

REFERENCES

1) SCHIVELL, J.F., and GROVE, D.J., "Thermal stress under high-power surface heating", Plasma Physics Laboratory, Princeton University, Princeton, New Jersey 08540 (Nov. 1973).

2) Handbuch der Kältetechnik, Vol. III, p. 197, Editor PLANK, R., Springer Verlag Berlin/Göttingen/Heidelberg (1959).

3) BÄUMLER, J., JUNKER, J., MELKUS, W., PROBST, F., SCHILLING, G., SPETH, E., "High-Power DC neutral particle Injection for W VII", S.O.F.T., 1974.

TABLE III

Water Supply	System to be cooled	Maximum heat generation within 360 s	Water flow rate through system	Water flow rate through heat exchanger	Maximum water temperature	Pump data pressure	Pump data speed	Area for heat transfer in heat exchanger
		MJ	m^3/h	m^3/h	C	b	m^3/h	m^2
ground water	Helix	400	0 - 1500	120	40	4.5	150	200
	Coils for neutral injection	500	0 - 600	80	90	4.5	150	235
	Coils for vertical field	120	16.5	20	65	30	16.5	37
	Injection systems	450	57	53	60	3	55	50
	Vacuum pumps	90	16	15	60	3	15	18
	Other systems	110	22	-	60	-	-	-
cooling tower water	Coils for heating (OH Trafo)	50	36	30	50	7	36	25
	Coils for main field	650	250	-	50	4.5	250	-
	Other systems	30	20	-	60	-	-	-

Paper No. 7 d

VACUUM SYSTEM OF THE W VII B STELLARATOR

by

H. Hägelsperger, W. Heiland, W. Poschenrieder, and R. Scherzer,
Max-Planck-Institut für Plasmaphysik, 8046 Garching, W. Germany,
EURATOM-Association.

ABSTRACT

Main field coils and helical windings of a Stellaratorpermit only limited access to the toroidal vacuum vessel. Utilizing every possible location on the W VII b results in a large number of comparatively small portholes. Still, it should be possible to reach UHV conditions in the non-bakeable vessel. Though pulse cleaning procedures are helpful and necessary means, high pumping speed is mandatory to reach suitable conditions on an acceptable time scale. The requirements in detail are: Absence of hydrocarbons, handling of high gas loads of H_2 during plasma experiments, high pumping speed for contaminants during pulse cleaning, fail safe maintenance of UHV conditions between experiments, and no interference with diagnostics. These conditions are best met by a compound pumping system, comprising turbomolecular pumps, volume getter pumps and non-magnetic ion-sublimation pumps.

INTRODUCTION

On a toroidal plasma experiment, vacuum physicists and engineers are usually faced with numerous and frequently contradicting requirements. The vacuum system should be as unobstrusive as possible, and should not interfere with diagnostics yet have a pumping speed as if all torus walls were black holes. Appealing as it might be, the utilization of gettering walls based upon volume getters, thin film getters, or cryogenic pumping in such close contact with the plasma is not yet feasible. (This subject appears differently in a divertor experiment, which will not be discussed here).

Having resigned to a more modest and conventional pumping system, the most economical approach will be found in the application of a few large portholes connected to big pumps; mainly because conductance goes with the third power of tube diameter. Such a solution, customary on Tokamaks, is not possible on a Stellarator, since access to the torus is very limited by the helical windings and the main field coils. Utilizing about every possible spot leaves us with a maze of portholes. On the W VII b we have 90 such ports ranging from 125 mm to 160 mm in diameter. Of these ports 60 are available for vacuum, corresponding in area to 3.3 % of the total (vacuum) surface of the torus. The "black hole" pumping speed of these ports is 115 000 l/s for air and 430 000 l/s for H_2. Considering the geometric conditions with all the awkward tubulation one will certainly be happy to arrive at an effective pumping speed of 1/3 of above values. With well trapped diffusion pums the system turns out to be everything but unobtrusive, as a matter of fact, the whole experiment would disappear behind a fence of closely stacked pumps. At this point one might be willing to compromise on pumping speed. This would be a poor compromise for a number of reasons.

THE CAUSE FOR HIGH PUMPING SPEED

The stainless steel vessel of W VII b cannot be degassed by baking at any stage. Hence, the only means for obtaining "clean" surfaces are mechanical and chemical - aside from pulse cleaning procedures. Under such conditions, removal of physisorbed species will be very sluggish, e.g. reaching an outgassing rate of water vapor below 10^{-6} torr/cm^2 s, will be a matter of many days, initially and after extended air exposure. However, the time required is also inversely proportional to the effective pumping speed[1]. Furthermore high pumping speed is not only mandatory for removal of physisorbed gases within a reasonable span of time. It is well realized that even a baked surface is not clean if in contact with a plasma. - As a matter of fact, it has been shown[2] that by a sharp bake physisorbed species become strongly bound by activated chemisorption, which can be of disadvantage here. - Without going into any further details of the intricate interaction between an oxydized stainless steel

surface and a hydrogen plasma, one may state that in any case pulse cleaning will be a necessity. Here, the problem of pumping speed becomes still more aggravated. Under pulse cleaning conditions a degree of surface coverage is reached where we are far away from Knudsen-flow for all desorbed species in the torus. Thus, a contaminant has a chance to be pumped out only if it directly goes into the pumping port right after dislodgement from the surface. Thus, pulse cleaning is very inefficient and frequently takes weeks, and a factor of two in pumping speed represents an enormous saving in time.

Until now we have talked about pumping speed for contaminant gases. For the plasma experiment itself, the pumping speed for H_2 is an important parameter as well. For a crude approximation we may assume that the plasma is surrounded by a neutral gas blanket, the pressure of which is given by the particle flux out of the plasma, and by the effective pumping speed. Recycling back into the plasma is then simply a linear function of this pressure. Thus, pumping speed appears as a critical parameter in the particle and energy balance of the plasma, e.g. with neutral injection[3].

SELECTION OF PUMPING SYSTEM

The pumping system which seems best to fulfill these requirements for the W VII b was found in a compound system comprising 10 turbomolecular pumps of nominal 150 l/s pumping speed each; 150 SAES SORB-AC volume getter pumps, type C 500[4], with a nominal pumping speed each of 2000 l/s for H_2, 800 l/s for CO, O_2, and 350 l/s for N_2; and 10 to 30 Electro-Ion pumps (Granville Phillips) with a nominal speed each of 1600 l/s for CO, O_2 and N_2, 22 l/s for Ar and 2.2 l/s for He. The Electro-Ion pumps will only be used for UHV maintenance in between experimental phases, and should give a pressure finally below 10^{-8} torr with the turbomolecular pumps valved off. The turbomulecar pumps were chosen for their relative oil free vacuum and for their very efficient pumping at pressures of several 10^{-3} torr, e.g. during regenaration of the SORB-AC pumps.

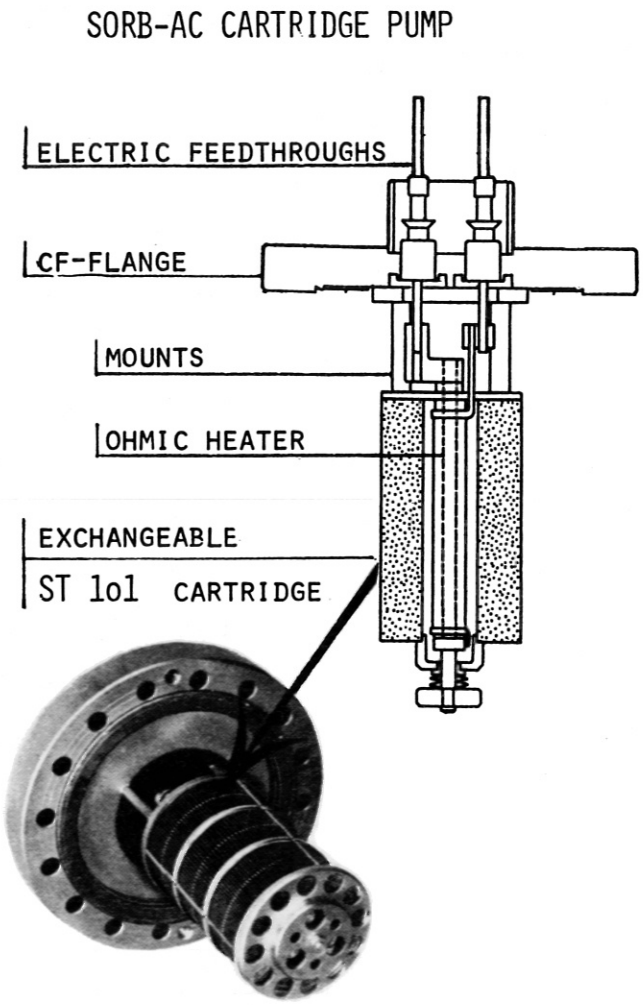

Fig.1. View and cross section of a nude Cartridge pump

The main pumping system is represented by volume getter pumps, the large scale application of which is a novelty and requires some more explanation: Each getter pump consists of a cylindric cartridge, 10 cm in diameter and 13 cm high. It is heated by an axial heater (Fig.1). Each cartridge contains about 600 g of active getter substance ST 101 which is specially treated Zr-Al alloy. At a working temperature of 400°C (N = 280 Watts) 1 g ST 101 will hold 1 torrl H_2 at an equilibrium pressure of $1 \cdot 10^{-6}$ torr (Fig.2).

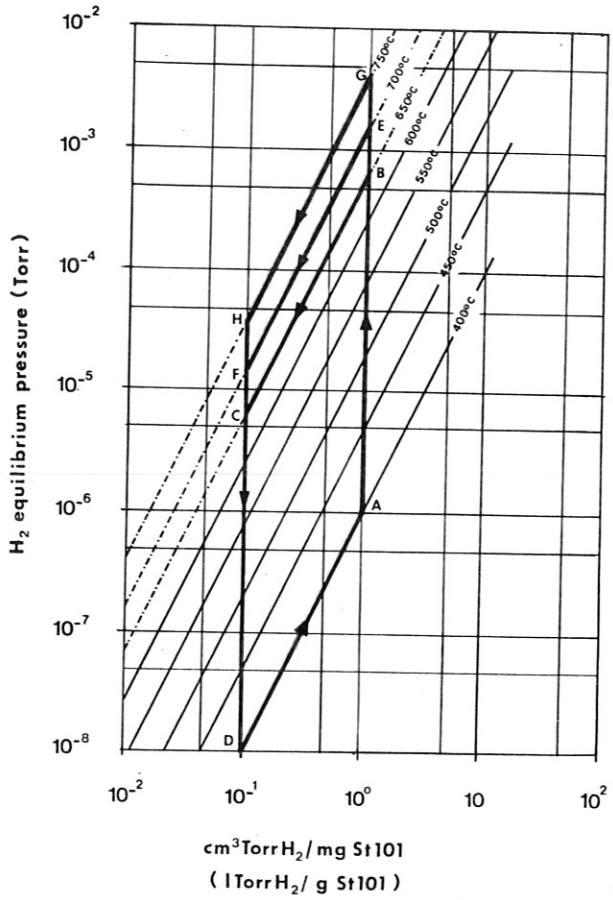

Hence, the total useable H_2-capacity of our system will be 10^5 torrl. If we assume a throughput of 10 torrl H_2 for each "shot" on the basis of a discharge duration of ten confinement times, we arrive at an almost infinite number of shots. Moreover, pumping of hydrogen is completely reversible and by a temperature rise to 700°C most of the sorbed H_2 can be released and pumped away by the mechanical pumps in only 10 minutes.

Fig.2. Equilibrium plot of ST 101 for sorption of H_2.

Pumping of active gases, however, is irreversible, but each cartridge can absorb above 200 torrl of active gases until used up. This corresponds to a total capacity of $3 \cdot 10^5$ torrl, equivalent to 20 Mol O_2, or about 10 torrl/cm^2 of torus surface (10^5 Monolayers). With certain precautions taken, e.g. venting of the torus with a rare gas, this capacity will suffice for several years.

The superior performance characteristics of the ST 101 is also shown in the fact that pumping speed is fully preserved to at least $8 \cdot 10^{-4}$ torr at 400°C. The full speed is also maintained at partial saturation with active gases.

Getter pumps do not pump rare gases. This appears as a drawback but actually is an advantage for pulse cleaning purposes using rare gases, or for experiments with a compound plasma where recycling of the components is being distinguished or controlled.

Because of their handy geometry, these pumps can be mounted very close to the torus. There is also no danger of gas release upon interaction with hot plasma particles as in the case with thin film getters or cryogenic pumps because sorption here occurs in the volume. Hence, no baffles are needed and optimum utilization of pumping speed is possible. Figure 3 shows the arrangement.

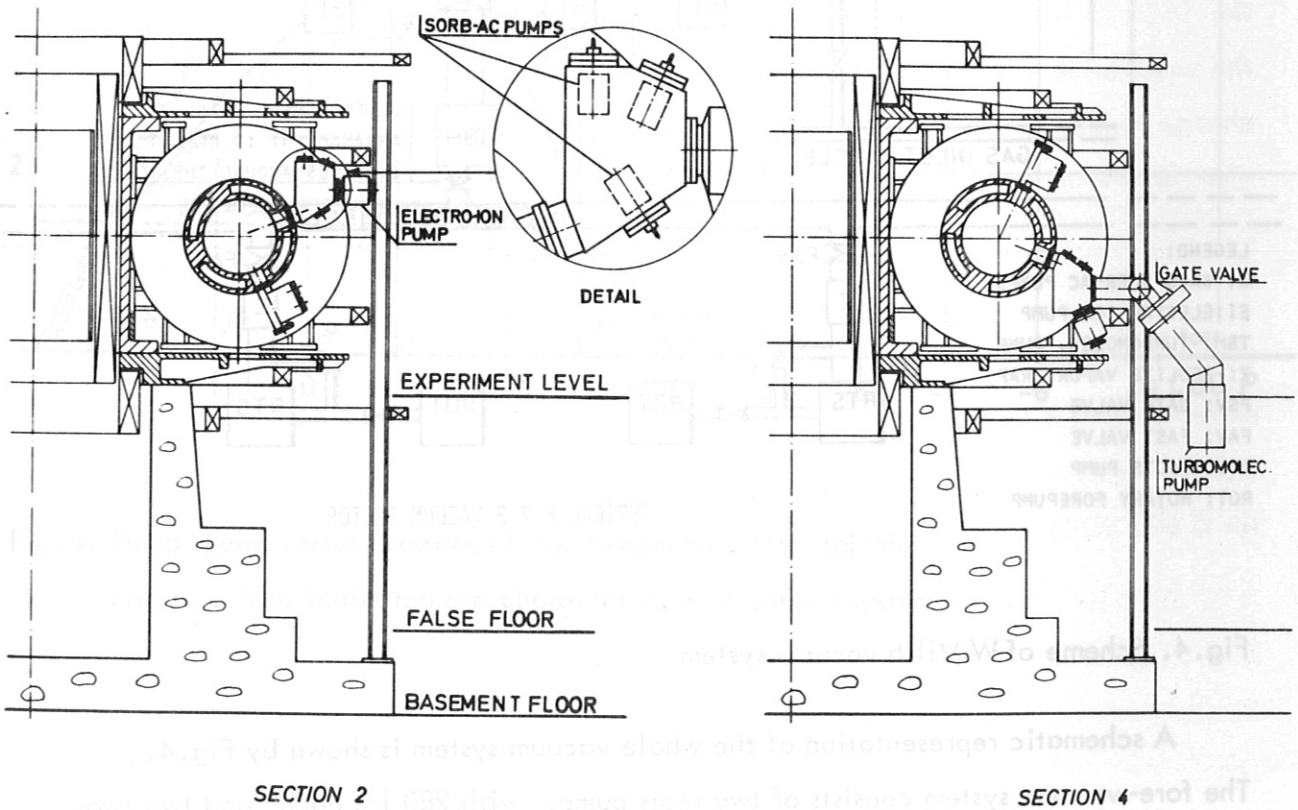

Fig.3. Arrangement of pumps

The volume getter pumps are all contained in the space between the main field coils. Only the Electro-Ion pumps stick out somewhat. The bulkiest part are the tubulations to the turbomulecular pumps, each of which is connected to two portholes. For reasons associated with the magnetic fields, the turbumolecular pumps have to be placed at at distance of 2.5 m from the torus vessel. A 30 cm diameter tubulation is needed for reasonable conductance.

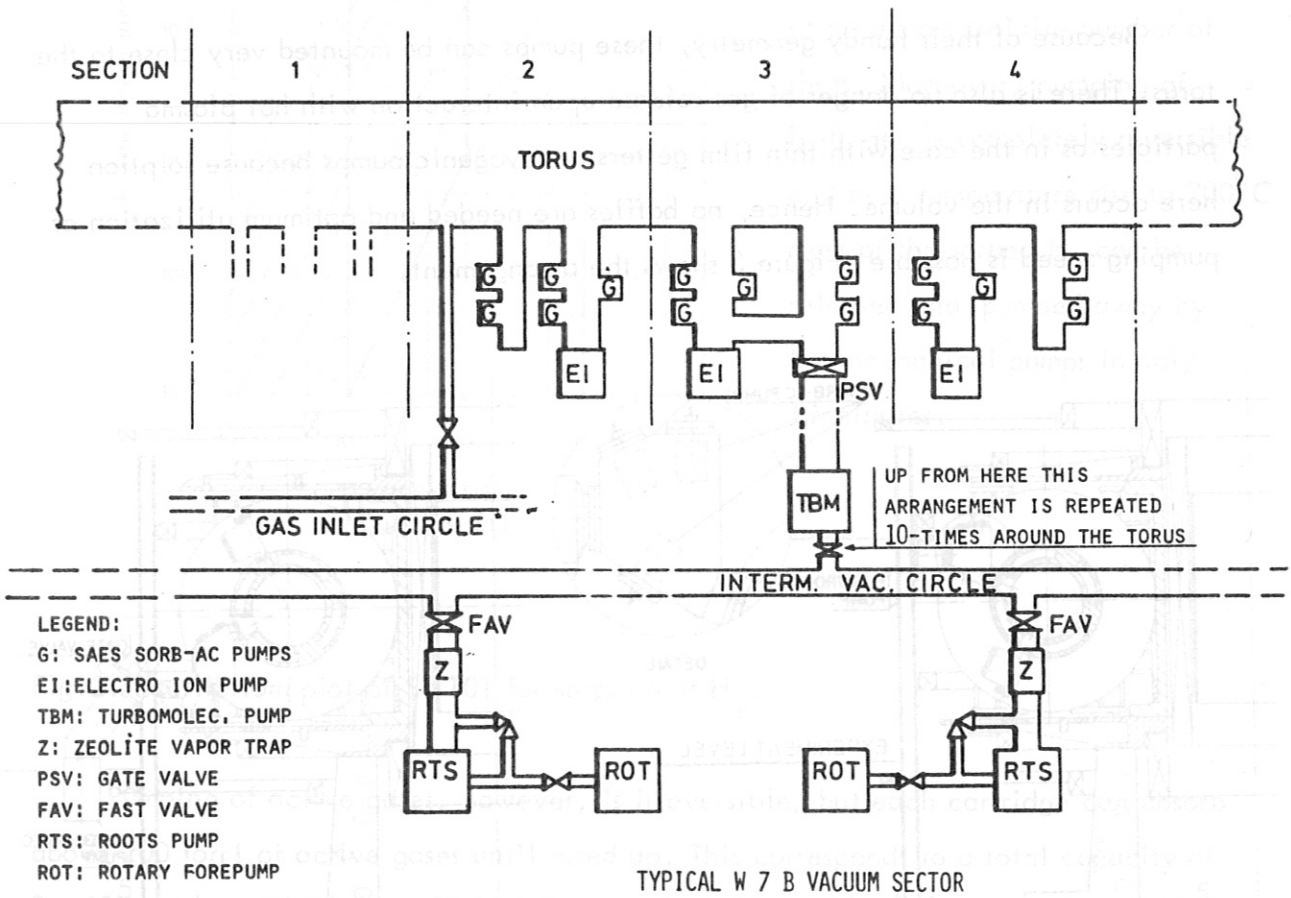

Fig.4. Scheme of W VII b vacuum system

A schematic representation of the whole vacuum system is shown by Fig.4. The fore-vacuum system consists of two roots pumps with 280 l/s each, and two two-stage rotary pumps with 28 l/s each. Zeolite traps serve for the retainment of oil

vapors in the intermediary vacuum line. Figure 5 shows a graph of the calculated effective pumping speeds of the complete system at the various pressure ranges.

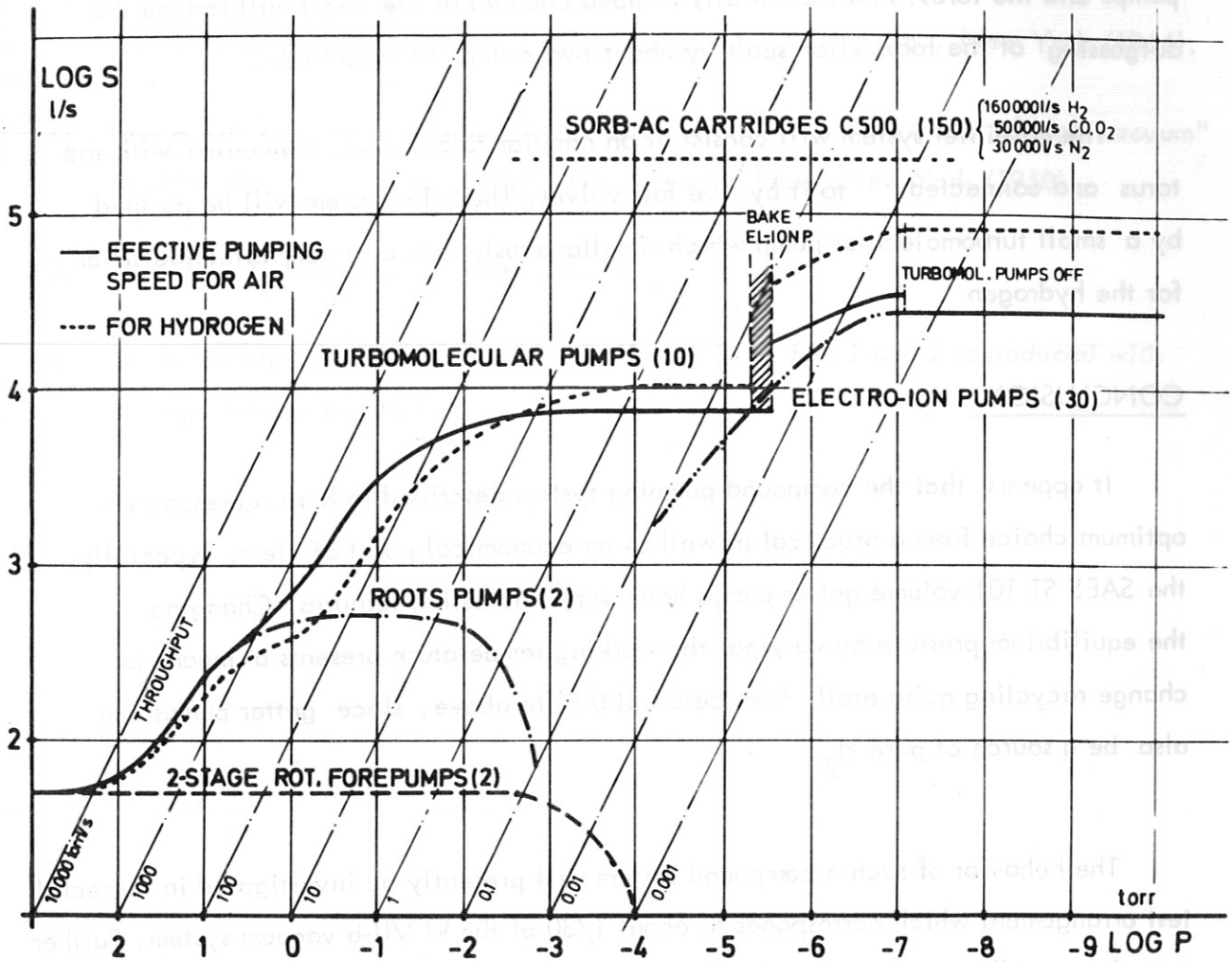

Fig.5. Pump speed versus pressure of the compound system for air and H_2. Also indicated are characteristics of partial system.

With exception of the seals at the torus insert(so called "intermediate piece") only metal to metal seals will be used. Also, the valves to the turbomulecular pumps will be metal sealed. No valves are used between the getter pumps, the Electro-Ion pumps and the torus. A differentially pumped channel at the insert will reduce the outgassing of the torus viton seals by about two orders of magnitude.

The gas-inlet system will consist of an annular turbulation, concentric with the torus and connected to it by five fast valves. The inlet system will be pumped by a small turbomolecular pump which simultaneously acts as a very effective filter for the hydrogen .

CONCLUSION

It appears that the compound pumping system described in here represents an optimum choice from a practical as well as an economical point of view. Es.pecially the SAES ST 101 volume getter pumps have very interesting features. Changing the equilibrium pressure by varying the working temperature presents a means to change recycling quite easily from below 100 % to above, since getter pumps can also be a source of pure H_2.

The behavior of such a compound system will presently be investigated in a special test arrangement which corresponds to about 1/30 of the W VII-b vacuum system. Further experience will be gathered on the first stage of W VII using the W VII-a torus which will be furnished with a combination of turbomolecular pumps (3 x 500 l/s) and a set of six C 500 SORB-AC getter pumps.

REFERENCES

1) KRAUS, T., "A new theory on adsorption and desorption of vapors", Trans. 10 th Nat.Vac.Symp., 1963, 77, The Mac Millan Co., New York (1964).

2) HAYASHI, C., "Role of adsorption in production and measurement of high vacuum" 4th Nat.Vac.Symp. Trans. 1957, 19, Pergamon Press, New York (1958).

3) HUGILL, J. Unpublished note (1972).

4) SAES-Getters, 20151 Milano, Via Gallerate 215. Fig.1 and 2 reproduced with kind permission of SAES.

Paper No. 7 e

DESIGN AND MANUFACTURING OF THE TOROIDAL FIELD COILS OF W VII

by

K. Freudenberger, H. Lohnert

Max-Planck-Institut für Plasmaphysik, 8046 Garching,

W. Germany, EURATOM-Association.

ABSTRACT

The toroidal magnetic field of W VII is produced by 40 normal conducting water cooled coils; 20 of these wound in left handed direction and 20 wound in right handed direction. They will be arranged alternately in toroidal geometry and are electrically series connected. They operate up to a current of 40 kA yielding $B_o = 4$ T.
Two prototype coils and a series of 46 coils have been ordered with BBC, Mannheim. After mechanical and electrical tests of the prototype coils the manufacturing of the series has started by the end of November last year. According the present time schedule, the 40 th coil will be delivered by the end of August 1974.
The main coil parameters are:

large diameter	2110 mm	number of the turns	25
small diameter	1100 mm	copper weight	2.3 tons
width	183 mm	total weight	3.4 tons
		copper conductor	SE-Cu F 25

The peak electric power consumption per coil is 1.8 MW. The cooling parameters for pulsed operation at an average power of 50 kW are temperature rise of 25 C per pulse at a water flow of $0.5\ m^3 \times h^{-1}$. The cooling channel in the copper conductor is designed for D.C. operation.

Each coil has its own stainless steel frame, which has two purposes: i) to transfer the magnetic forces from the coil into the W VII supporting structure and ii), to provide for the individual adjustment of each coil. The insulation material is fiberglass with epoxy resin, cured at 160 C during 14 hours.
The coils are wound in horizontal position, a torque of 12 m tons at 4 rps is produced by a hydraulic motor. The conductors to be connected by brazing (SILFOS, melting point 710 C) are held by hydraulic clamps in a special brazing device.

INTRODUCTION

A toroidal magnetic field of 4 T is to be produced by a certain number of coils, arranged to a torus with a diameter of 400 cm. The coils are to be normal conducting and water cooled.

DESIGNING ASPECTS

When designing the coils, the following conditions were to be considered:

1. The power supply: a flywheel generator having a useful energy of 1.45 GJ, a maximum current of 45 kA, and a voltage of 3300 V.

2. A flat-top time of 10 s at full field, while about one third of the available energy is needed for the helical windings to produce an iota of 0.5,

3. a ripple as low as possible,

4. matching between the number of the toroidal field coils and the number of the helical field periods.

The W VII has a helical winding of the type of $l = 2$, with five periods. Between the four helix parcels there is a certain space for portholes. It seems to be convenient to have the same space between two toroidal field coils. Considering all these points of view it can be shown that it is a good compromise to have a number of 40 coils. The arrangement of these 40 coils is shown in Fig.1. These coils are series connected in two halves - 20 left handed and 20 right handed. Between these two halves the helical winding is connected. Arranging left handed and right handed coils alternatingly, gives the advantage of partial compensation of the currents in the conductors which connect the coils and in the passage turns in the coils.

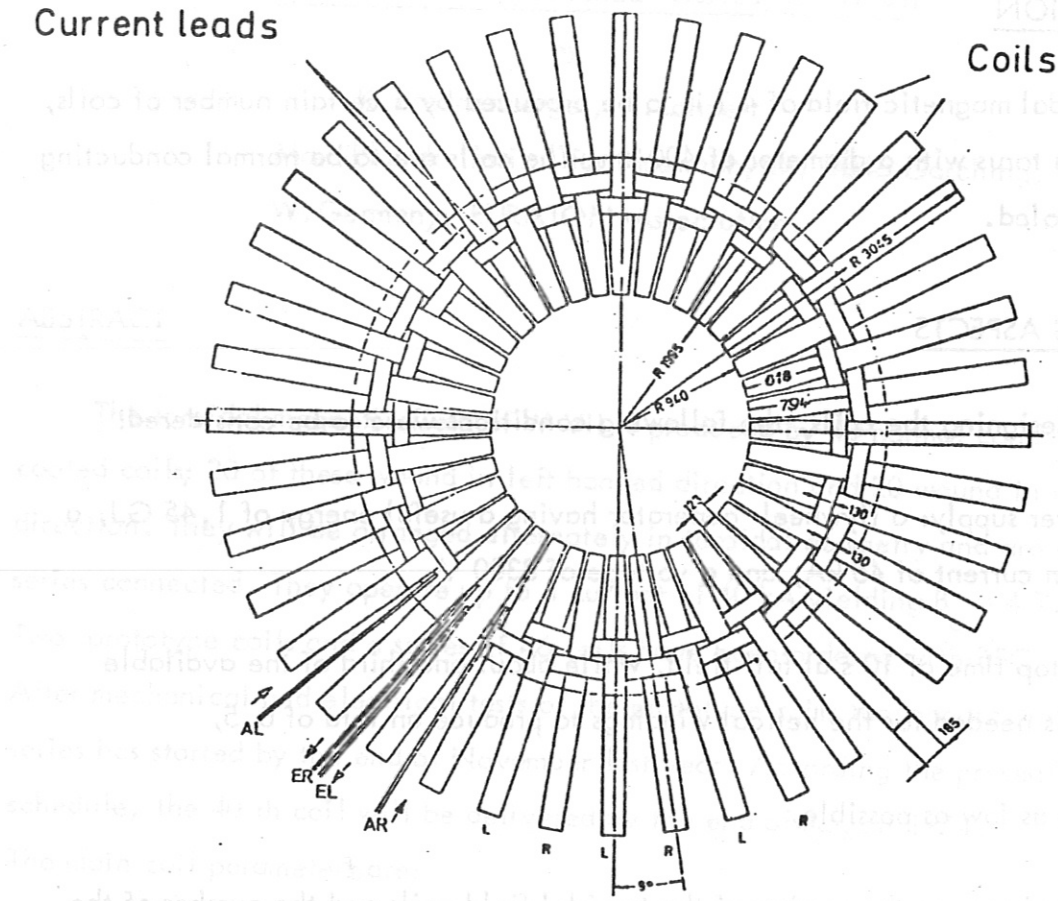

Fig. 1

MAGNETIC FORCES

Because of the toroidal arrangement of the coils there is in each of them an unequally distributed magnetic pressure with values of 85 to 150 kp x cm^{-2}, which on the one hand causes a centripetal force of 190 tons per coil and on the other hand deforms each coil - because of the chosen kind of supporting -in form of a "D". This deformation effects a bending stress of 450 kg x cm^{-2}. The deformation itself is within 0.2 mm. The current in the coil with the vertical field produces a torque of 10 m x tons on each coil. Finally, there are forces on each coil resulting from the currents in the coil and in the helical windings. These forces are small and can be neglected. In case of a failure of one of the coils - for instance a short circuit in the coil or across the terminals - there are axial forces up to 290 tons on those on both sides of the one which has failed. The coils themselves are not able to withstand these

forces and because it is not possible to discharge the stored magnetic energy in the magnetic field in a sufficiently short time, it is necessary to support the coils among one another by means of wedges. This must also be done if one or some coils are to be shunted for magnetic mirror experiments.

Main parameters:

large diameter	2210 mm
small diameter	1100 mm
width	183 mm
number of turns	25
current per turn	40 kA
power consumption	1.8 MW
Cu-weight	2.3 tons
total weight	3.4 tons

Cu-conductor:

cross section	2060 mm^2
current density	20 A x mm^{-2}

Two coils mounted into the testing jig are shown in Fig. 2. Each coil consists of two pancakes with 12 turns each, which are connected at the small diameter by a passage turn. This passage is done continually around 270° in axial direction and around two times 45° in radial direction. This is done to minimize the disturbing field.

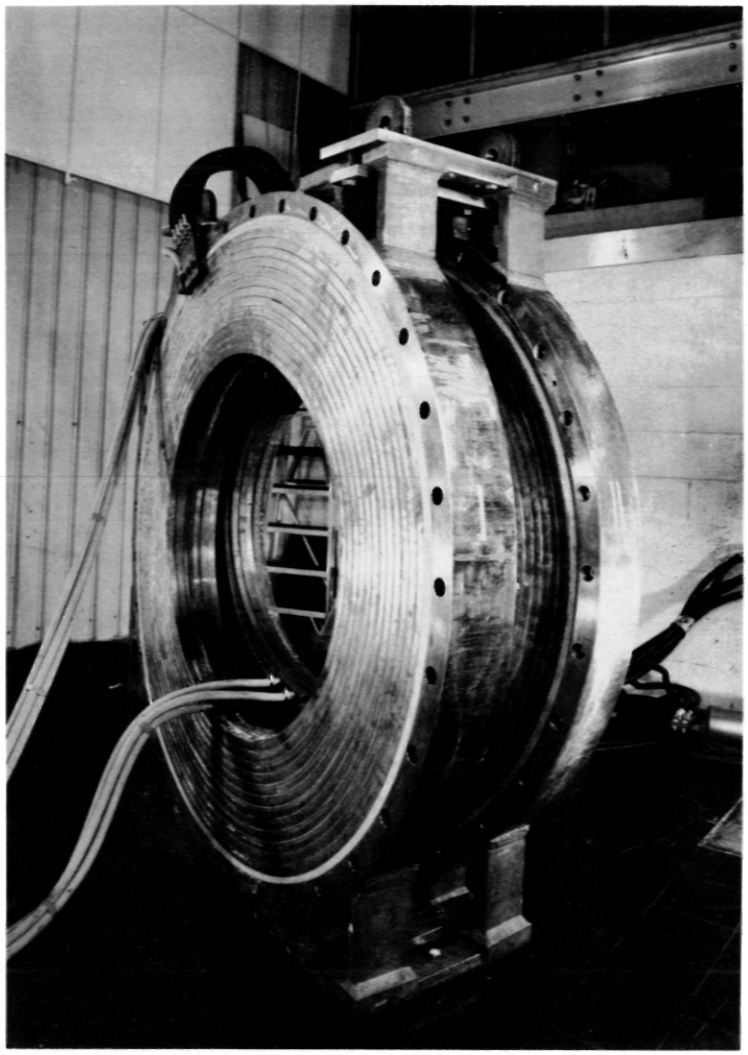

Fig.2.

With regard to the high acuracy of the toroidal field, which is desired, each coil is mounted into a stainless steel frame, whose supporting surfaces are machined relatively to the coil with a tolerance of $\pm$ 0.1 mm, to have the possibility to adjust each coil as exactly as necessary within the assembly of the 40 coils.

COPPER CONDUCTOR

Because of the high axial forces a coil was designed, which is able to carry all forces - resulting from normal operation - itself. In case of a failure the coil must be protected by a minimum of supporting elements, for having space enough for portholes as large as possible. This was the reason for the relative complicated slot and key profile because it makes a solid coil, mainly in axial direction. When winding the coils, some further advantages could be recognized, for instance the slide in slot and key. The cross section of the copper conductor is shown in Fig.3.

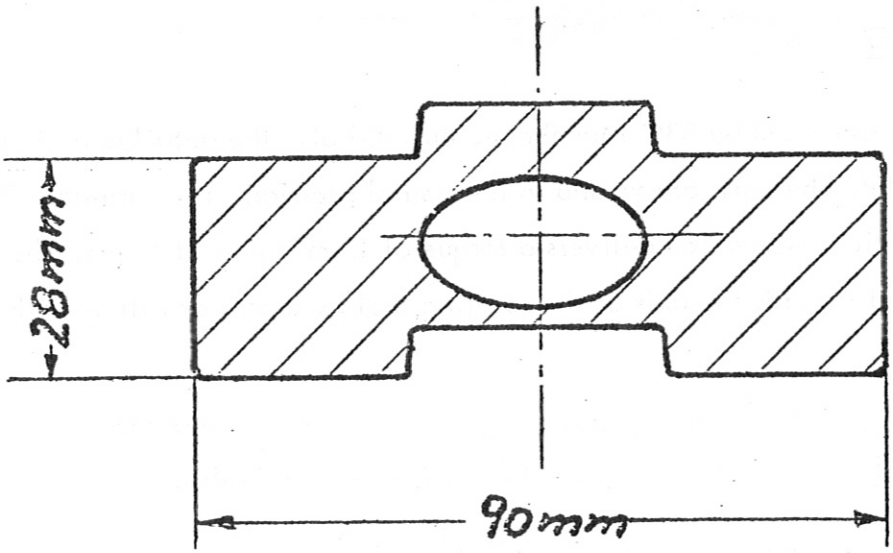

Fig.3

WATER COOLING

The elliptical cooling path with a cross section of 4 cm^2 is dimensioned for DC-operation. The parameters are: 35 atm, 50 $m^3 \times h^{-1}$ per coil, at a temperature rise of 60 C. At pulsed operation of the W VII - 10 sec each 6 minutes - the average power consumption of a coil is 50 kW, the adiabatic temperature rise over one pulse is 25 C and the cooling parameters for this operation are:

2 atm, 0.5 $m^3 \times h^{-1}$ per coil. The two pancakes of a coil are separately cooled. The inlets are at the large diameter, the outlets at the small one so that no mechanical tensions resulting on different temperatures can occur. The temperature in the coil rises to the small diameter. By this the coil gains some additional stability.

CURRENT CONNECTION

The current terminals are on both sides of the coil at the large diameter combined with the water feeds for having an intensive cooling at this point. The connection itself is made by three screws DIN M 16. Special antimagnetic spring discs keep the contact pressure constant.

MANUFACTURING

The coils are produced by BBC-Mannheim. BBC did also the detailed design in corporation with IPP. The coils are wound in horizontal position. The turntable is driven by a hydraulic motor which delivers a torque of 12 m x tons at 4 rpm. The conductor is pressed towards the axis of the rotating tool by a pair of rollers with a force of 20 tons.

BRAZING DEVICE

Each coil is made of 16 copper bars with a length of approximately 7,5 m which are to be butt-brazed together. This is done in a special device, designed and constructed by BBC (Fig.4). The pieces to be brazed are springy held together by hydraulic champs. The brazing material is SILFOS foil with a thickness of 0.2 mm, having a melting point of 710 C. The brazing section is inductively heated with a power of 30 kW at 10 kHz. A brazing process takes about 6 minutes. On both sides of the joint a zone of 10 cm is annealed. Each joint is helium leak-tested immediately after being brazed and wound.

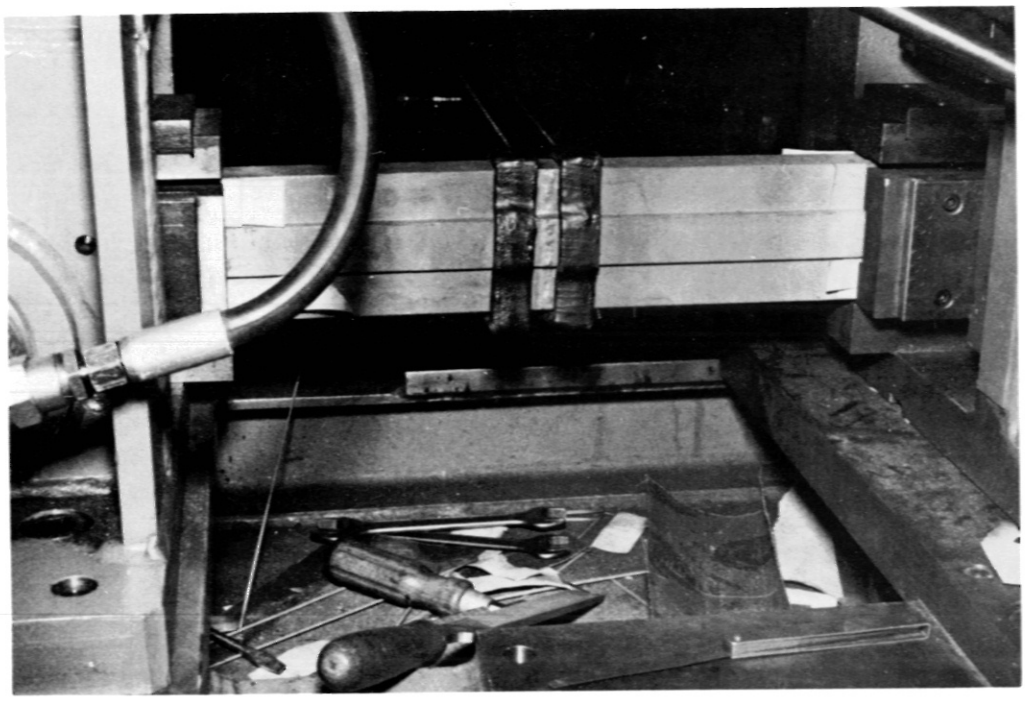

Fig.4.

INSULATION

All used insulating material is glass-epoxy. The conductor itself is bare. There are layers 2 mm thick between the single turns. The turn to turn voltage is 1.6 V. The insulation is tested inductively with 50 V_{pp} at 1 kHz per turn for one minute before mounting the coil into its frame. The insulation between the coil and the frame is made by means of impregnated spun glass. It is wound on a vertical winding machine up to such a thickness which allows to machine the coil circular referred to the center of the coil. The thickness of this insulation after machining is 20 mm at minimum. The maximum operating voltage between a coil and its frame, which is grounded, is 3300 V. The insulation is tested with 7.5 kV for one minute.

CASE

The case is welded of stainless steel DIN 1.4301 with a maximum value of permeability of 1.03, also at the welding seams. The purposes of the case are two: i), to transfer all forces from the coil into the W VII-frame, ii), to give the possibility of an exact adjustment of each coil within the complete assembly. Therefore the supporting surfaces of the case are finally machined with a tolerance of $\pm$ 0.1 mm relatively to the coil itself.

ACCEPTANCE

The following tests are made at the manufacturer :

1. An insulation test coil to case with 7.5 kV of 1kHz for one minute.
2. A water flow test with 6 atmospheres.
3. A water leak test with 50 atmospheres for 5 minutes.
4. A control of the mechanical measures including the axial and radial position of the single turns within the coil. For this purpose a scraper is made into the copper conductor when winding the coils.

In the IPP two coils are tested with regard to their axial strength. The two coils are mounted vertically into a testing device. The distance and the angle between the two coils are the same as in the W VII-frame. The deformation depending on the current is measured and according to this results the supporting elements between the coils are dimensioned.

STATUS

At August 14 th 1972, two prototypes and 46 coils have been ordered with BBC - Mannheim. The prototypes were delivered in August 1973. After a lot of tests with them and some additional agreements with BBC the manufacturing of the series

was started in September 1973. At the end of May 1974 the first four coils have been completed. The latest time schedule announces the 40. coil to be delivered by the end of September 1974.

Paper No. 7 f

OHMIC HEATING AND VERTICAL FIELD COIL SYSTEMS OF W VII

by

R. Jaenicke, R.C. Kunze, H. Lohnert, G. Müller
Max-Planck-Institut fuer Plasmaphysik
D-8046 Garching, W.-Germany, EURATOM Association

ABSTRACT

For ohmic heating (OH) experiments the W VII stellarator is equipped with an air-core transformer which can produce a magnetic flux of about 2.9 Vs. The magnetic fields in the plasma region are kept below 5 G. The fast flux variation required for heating the plasma is produced by forcing the current in the coils into a large parallel resistor by opening a HVDC breaker.

Since the plasma current has long pulse lengths of the order of one second, the W VII needs a vertical magnetic field for equilibrium. This field is produced with coils mounted outside the toroidal field coils. Power is supplied by the OH coils operating as in inductive energy storage system. The field distribution and field amplitude of the vertical field can be varied by varying the number of turns in the individual coils.

INTRODUCTION

Since the last conference at Grenoble in 1972 the ohmic heating and vertical field coil systems for the W VII stellarator have been further developed and designed in detail. All of the major components are now in the development or production stage. Manufacturer: Lintott Ltd. Horsham/Great Britain.

Both systems use air-core coils which are separated from one another and which are all mounted outside the toroidal field coils. The coils within each system are connected in series. The two coil systems are coupled by their mutual inductance but they can also electrically be connected to facilitate the powering of the vertical field coils.

All of the numerical data presented in the following generally apply to the W VII or W VII B.

POWER SUPPLY

The power supply and electrical circuitry of the coils are shown in Fig. 1, a typical time variation of the current being given in Fig. 2. A flywheel generator FG produces the current in the OH coils, which attains its rated value after about 1.3 s. The HVDC breaker S_1 is opened to produce a fast magnetic flux variation in the coils and induce a current in the plasma. At the same time the switch S_3 is closed so that the decrease of the high voltage at the resistor R also leady to a fast current rise in the vertical field coils.

By closing the switch S_2 the B_V coils are again electrically disconnected from the OH coils, and the current I_V is now controlled by the DC generator, "Herta". Further heating of the plasma, e.g. for keeping the current I_{PL} constant, can be achieved by letting the current I_{TR} decrease further until it finally passes through zero and attains its maximum permissible negative DC value. As the current I_{TR} thereby changes sign, either the rectifier system of the generator FG has to be fitted with antiparallel current valves or an additional mechanical switch is needed.

OH COILS

The OH coils consist of a large cylindrical coil and three pairs of compensating coils. The latter ensure that the magnetic field in the region of the plasma remains small. A numerical calculation yielded a value of $\gtrsim 3.5$ G (see Fig. 3). In order to ensure that the coils do in fact afford such good field compensation, they have to produce a defined current distribution with rather narrow manufacturing tolerances (between $\lesssim 1$ mm and $\lesssim 5$ mm). To prevent major changes of the current distribution due to the skin effect, the inner coils are wound from conductors with small cross-section (approx. 20 x 30 mm^2), these being parallel connected in batches of six.

A series of data is presented in Table I

TABLE I

Data of the OH coils

Number of turns	n_1=112, n_2=16, n_3=6, n_4= 3
Inductance	L_{Tr} = 12,7 mH
Resistance (coil + leads)	$R_{Tr} \approx$ 10 mΩ
Charging time constant	$\tau \approx$ 1,3 sek
Rated current	J_{Trmax} = 35 kA
Magnetic flux	ϕ = 2,89 Vs
Max. flux variation	$\Delta\phi \approx$ 3,9 Vs
Max. permissible voltage	V_{max}= 30 kV
Voltage thereby induced in plasma (without vertical field)	V_{ind} = 195 V

B_v COILS

As the plasma current in W VII should have pulse lengths of the order of one second, this current requires a vertical magnetic field for equilibrium. The equilibrium condition thereby has to require that the current in the B_v coils I_V be largely proportional to the plasma current I_{PL}. For this purpose a peak power of approx. 30 MW is needed during the rise time of I_V.

The required proportionality can at least be approximately achieved by using the circuit shown in Figs. 1 and 2, similar versions having already been proposed for the Frascati tokamak [1]. The OH coils thereby act as an inductive energy storage system. The proportionality constant I_V/I_{TR} can be adapted to the requirements by varying the number of turns of the inner B_V coil 5. This changes the mutual inductance, e.g. between the OH and B_V coils, while the vertical field remains largely unchanged.

All the other B_V coils also have a variable number of turns so that the field distribution and magnitude of the vertical

field can be varied from run to run. In order to achieve a given field amplitude in the experiment, it is necessary to know the ohmic losses in the plasma during the heating phase. Global allowance can then be made for these losses when fixing the number of turns for the B_V coils, i.e. one has to know the part of the flux variation $\Delta\Phi_{TR}$ which is used up for the ohmic losses in the plasma and hence does not induce a plasma current.

A series of data for a typical case is presented in Table II.

TABLE II

Data of the B_V coils

Number of turns	$n_5 = 0 \ldots \pm 232$, $n_6 = 16 \ldots 36$, $n_7 = 20 \ldots 4$
Typical values	
Ohmic losses in plasma	$0{,}2\ \Delta\Phi_{Tr}$
Number of turns	$n_5 = 184$, $n_6 = 34$, $n_7 = 38$
Inductance	$L_V = 0{,}13$ H
Resistance	$R_V = 0{,}18\ \Omega$
Current at I_{PL}=580 kA($t \approx 0.5$)	$J_V = 3{,}6$ kA
Magnitude of vertical field	approx. 1 kG

The vertical field coils also produce a magnetic flux variation which makes a significant contribution to the plasma current (approx. 20 to 30 %). Making the rather realistic assumption of 0.35 $\Delta\Phi_{TR}$ for the ohmic losses in the plasma, one thus obtains with $I_{TR,max}$ = 35 kA the following value for the maximum plasma current:

$$I_{PL,max} \approx 430 \text{ kA}$$

During the quasi-stationary phase of the plasma current The B_V coils are powered by a DC generator, "Herta" (see Figs. 1 and 2). This generator also allows slow regulation of the current

I_v in order to preserve the proportionality to I_{PL}. This is particularly important during the decrease of the plasma current, if an experiment with another heating method and without plasma current is to be conducted afterwards, in order to prevent the plasma equilibrium form being destroyed during the transition phase. If the regulating speed of the DC generator is not adequate for the purpose, it can be increased by means of a variable (e.g. switched)series resistor.

HVDC BREAKER

The requirements imposed on the switch S_1 (Fig. 1) are particularly high since it has to interrupt a current of 35 kA against a voltage of 30 kV. All the types of present-day switchgear suitable for a high switching rate (a few minutes) are based on the principle of current commutation, i.e. a capacitor bank is used to commutate the current from a high-power AC switch into a parallel resistor (R in Fig. 1) in order to achieve an artificial zero passage of the current in the actual switch. The following are suitable examples of AC switches:

a) mechanical high-power switches

b) thyristors

c) mercury vapour switches.

For W VII Hughes Aircraft Corporation is developing a switch on the principle c) [2] which may be regarded as a suitably modified ignitron. As it does not employ any mechanical contacts, it promises a long lifetime and a high degree of reliability. Also advantageous is the short deionization time since this allows the required commutation bank to be kept relatively small.

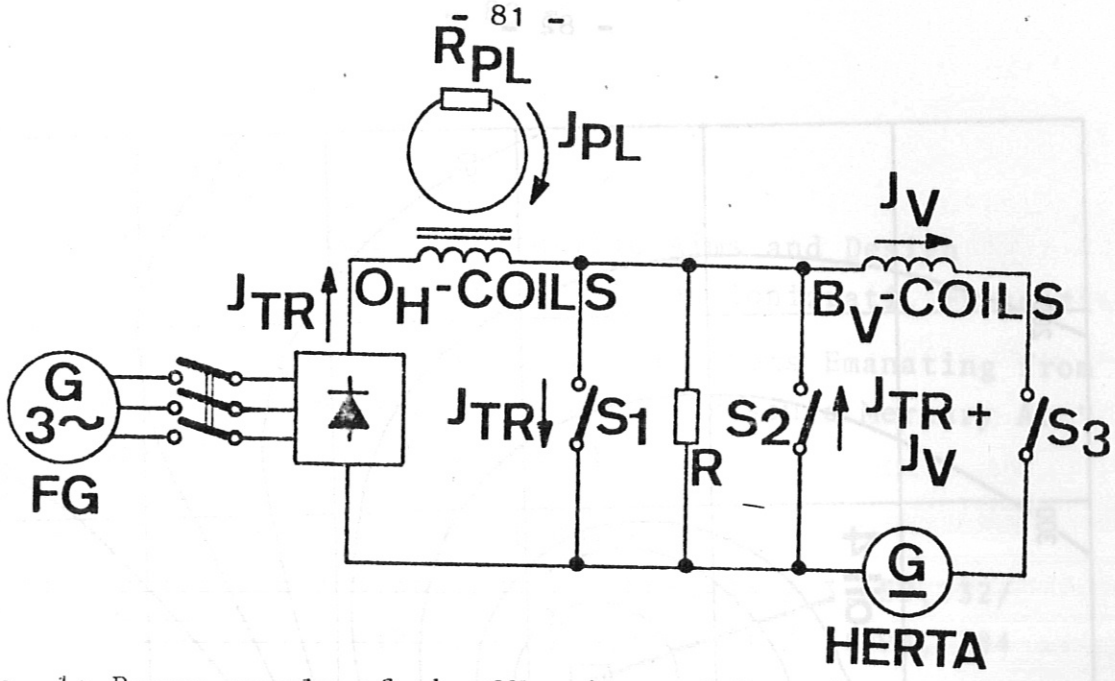

Fig. 1: Power supply of the OH coils and B_V coils

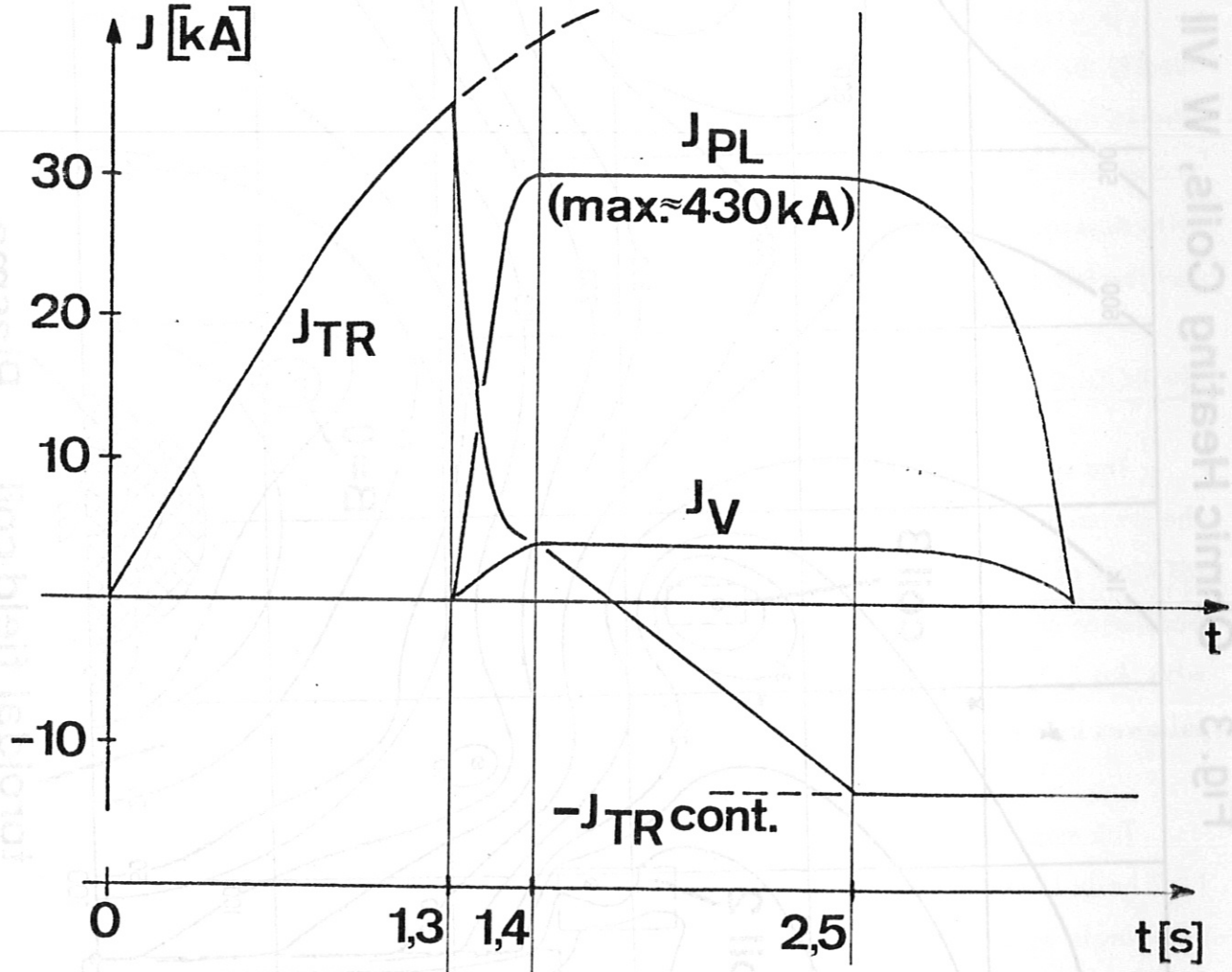

switch		
S_1	closed ←	→ open
S_2	open ←	→ closed
S_3	open ←	→ closed

Fig. 2: Typical time table of currents and of switches

Fig. 3 Ohmic Heating Coils, W VII

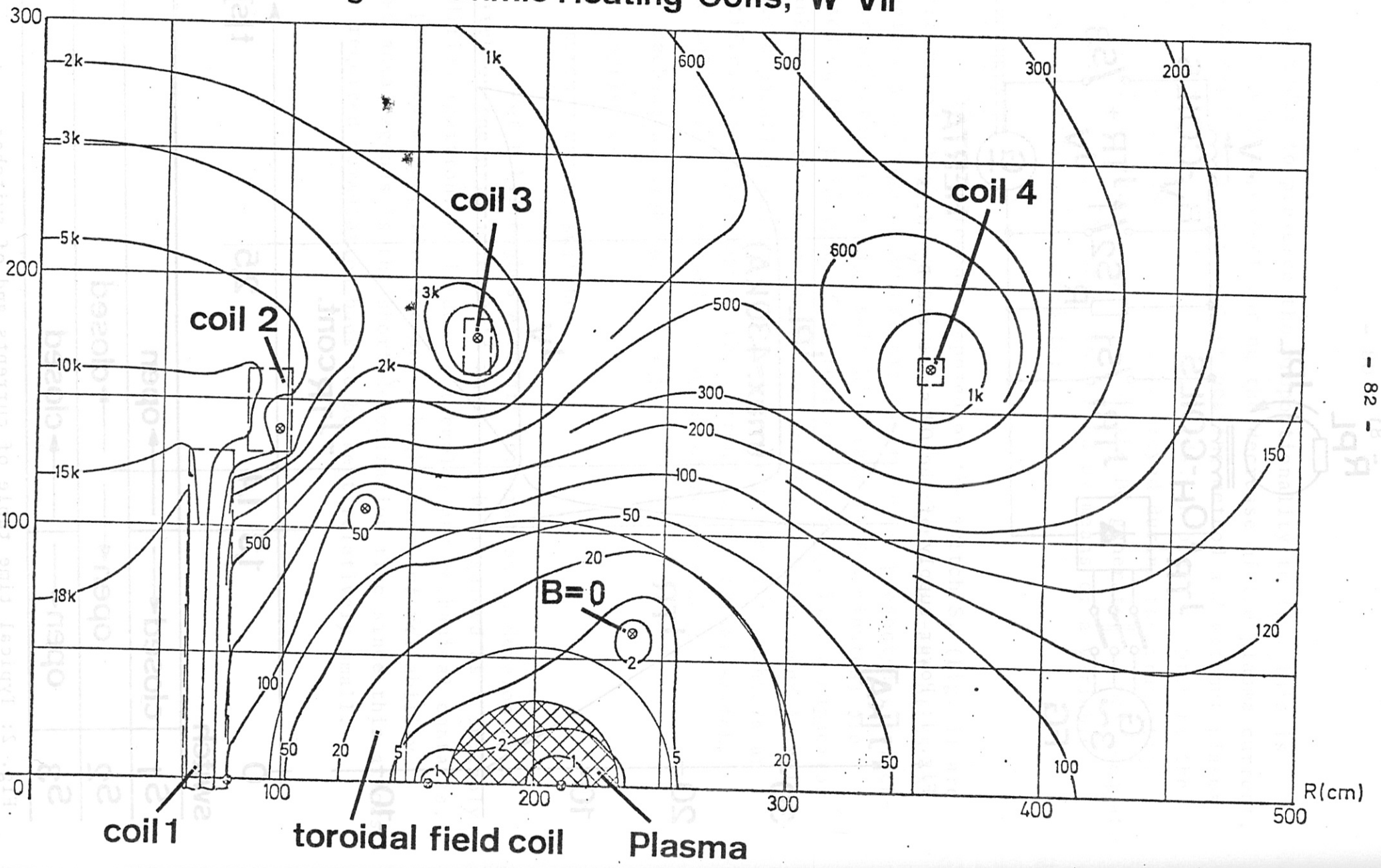

REFERENCES

1) THE FRASCATI TOKAMAK, Scientific Aims and Design Information, Report, Laboratori Gas Ionizzati, Frascati

2) ECKHARDT, G., "Velocity of Neutral Atoms Emanating from the Cathode of a Steady-State Low Pressure Mercury Arc", J. Appl. Phys. 44, 1146 (1973)

US patents on Liquid Metal Plasma Valve
Nr. 3,475,636 / 3,662,205 / 3,668,453 / 3,659,132/
3,586,904 / 3,538,375 / 3,579,001 / 3,696, 384

Paper No. 11

THE EFFECT OF PERTURBATIONS ON THE MAGNETIC FIELD OF THE W 7 STELLARATOR

by

S.Rehker, H.Wobig

Max-Planck-Institut für Plasmaphysik, D-8046 Garching, W.Germany

EURATOM-Association.

ABSTRACT

Due to the imperfections of the coil system perturbation fields occur, which modify the magnetic field of the W 7 Stellarator appreciably. The structure of islands caused by these perturbations was investigated numerically. The width of the islands scales with the square root of the perturbation field. If the coil system can be build with accuracy of 0.1cm the width of the islands can be reduced to a tolerable level, but the islands cannot be avoided completely.

INTRODUCTION

The structure of the magnetic field of the W 7 Stellarator depends critically on the presence of unwanted perturbation fields. These perturbation fields can arise from all kinds of constructional errors. The simplest effect of these perturbations is the occurence of islands, which are localized to a particular resonant magnetic surface with $\iota = 1/2, 1/3, 1/4 \ldots$ More dangerous is an overlapping of the magnetic islands followed by a complete destruction of the magnetic surfaces.

The major radius of the W 7 Stellarator will be 200 cm, the mean radius of the $l = 2$ helix is 45.5 cm. In the numerical calculations we have represented the helix by 5 single wires. These wires are wound with constant pitch in nearly all calculations. For comparison we have considered a case with variable pitch according to the formula

$$\frac{d\Theta}{d\varphi} = \frac{5}{2} \left(1 - \beta \cos\Theta \right)$$

The main toroidal field is generated by 40 circular coils. The ohmic heating and the vertical field is generated by toroidal circular coils. The whole set up can be seen in Fig.1.

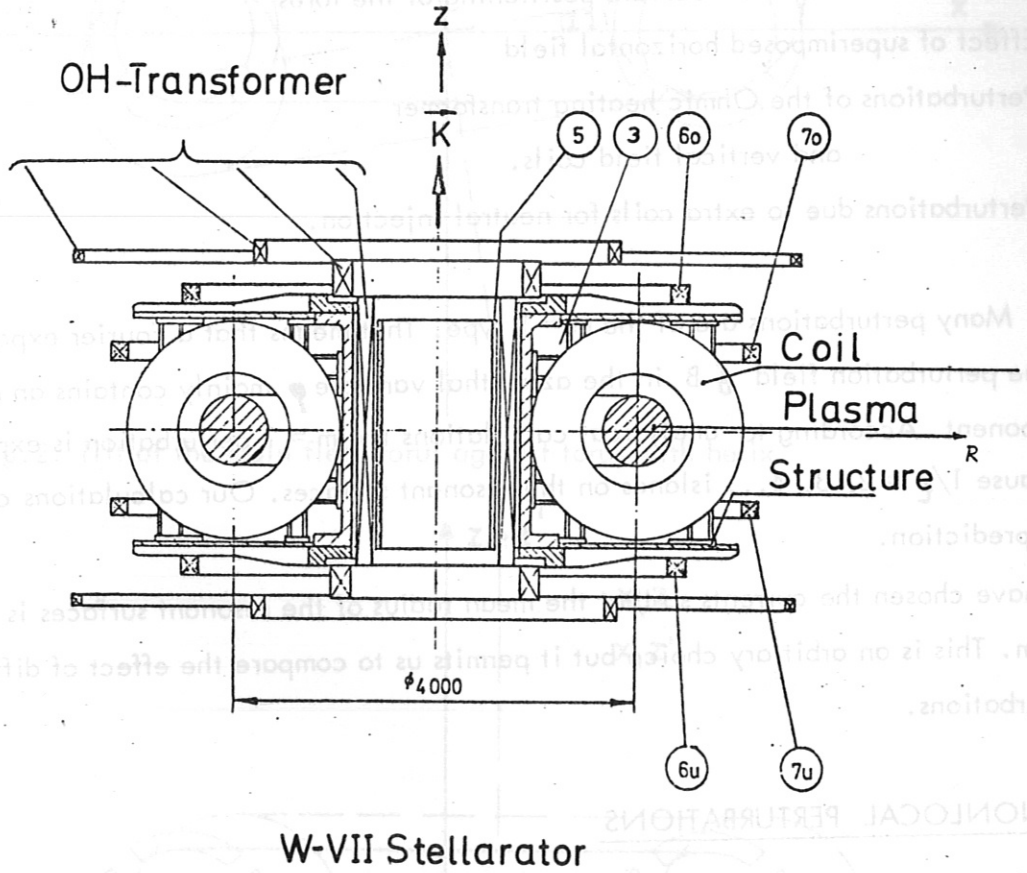

Fig.1. Scheme of the W VII-Stellarator
Helical windings are not shown in this picture

Many deviations from the ideal case are possible.

The list of perturbations investigated by us is

1) Perturbation of the main field coil system
2) " of the helical windings
3) " due to current leads
4) " due to inaccurate positioning of the torus
5) Effect of superimposed horizontal field
6) Perturbations of the Ohmic heating transformer and vertical field coils.
7) Perturbations due to extra coils for neutral injection.

Many perturbations are of the m = 1 type. That means that a Fourier expansion of the perturbation field δB in the azimuthal variable φ mainly contains an m = 1 component. According to analytical calculations the m = 1 perturbation is expected to cause $1/\iota = 2, 3, 4...$ islands on the resonant surfaces. Our calculations confirm this prediction.

We have chosen the currents so that the mean radius of the resonant surfaces is roughly 20 cm. This is an arbitrary choice but it permits us to compare the effect of different perturbations.

II) NONLOCAL PERTURBATIONS

1) Tilting and displacement of the torus

The helical windings of the W VII-stellarator are wound around the vacuum vessel. This torus might be tilted or displaced in the torus which is created by the main field coils. The tilting can be seen in Fig.2, the displacement in Fig.3.

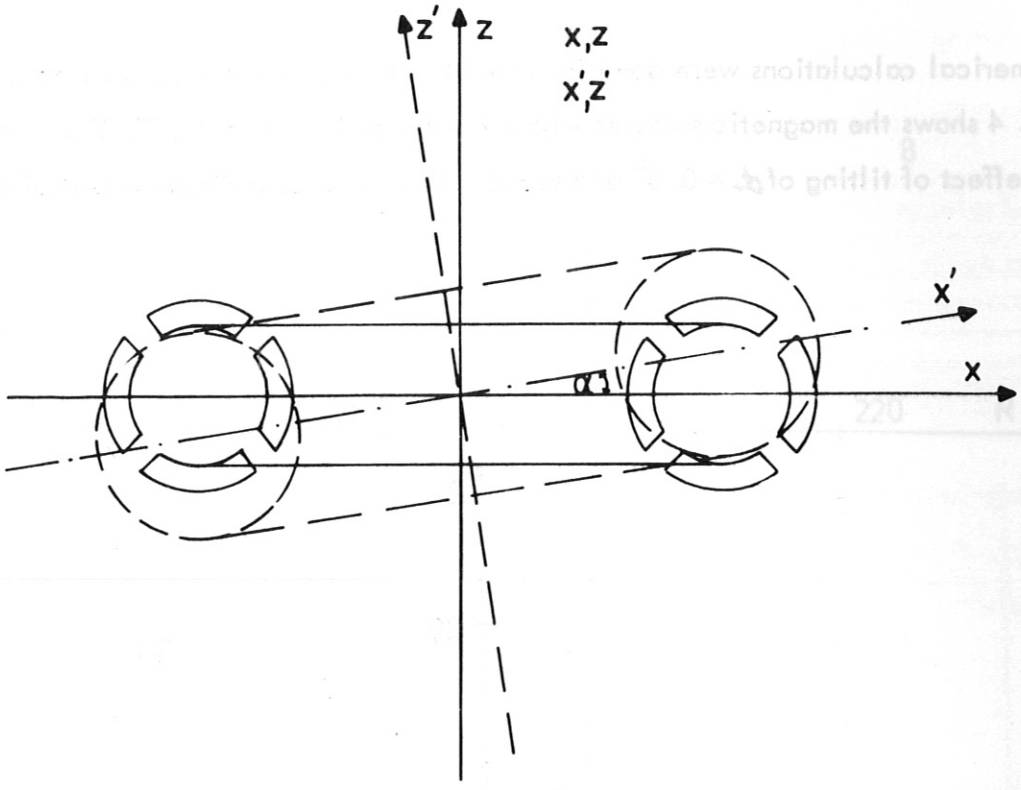

Fig.2. Tilt of the main field torus against torus with helix

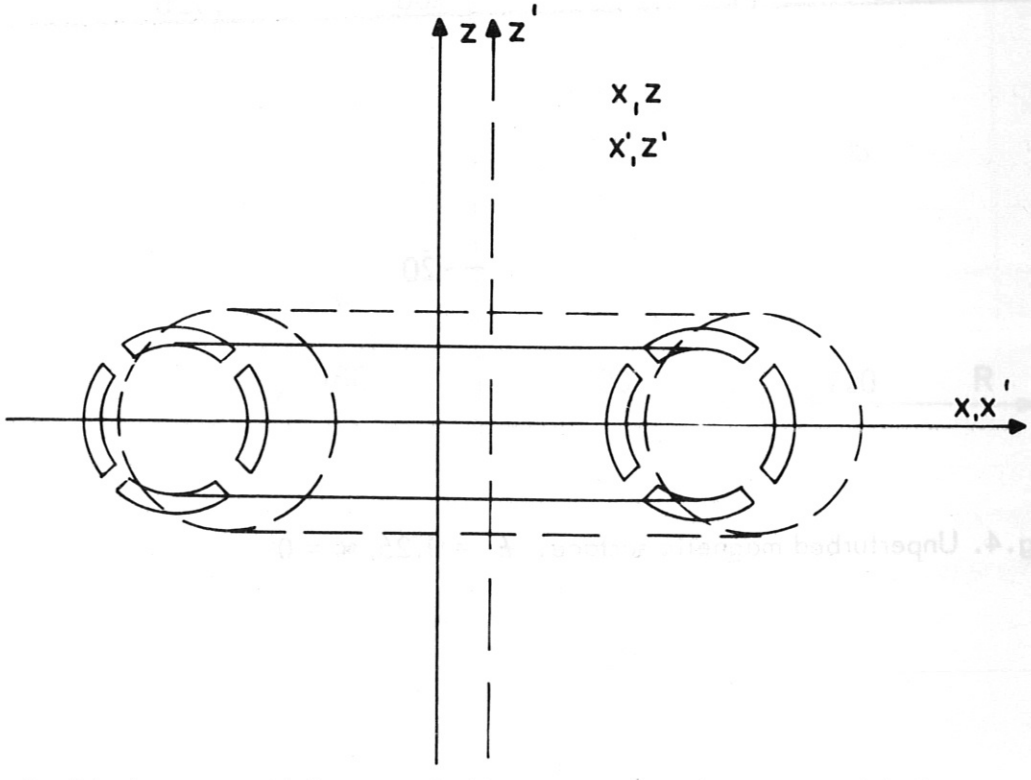

Fig.3. Displacement of the main field torus against the torus with helix

Numerical calculations were done for several values of the rotational transform. Fig. 4 shows the magnetic surfaces without perturbation for $\iota = .25$, Fig. 5 shows the effect of tilting of $\alpha = 0.5^{\circ}$ and Fig. 6 the effect of a displacement of $\Delta_x = 1$ cm.

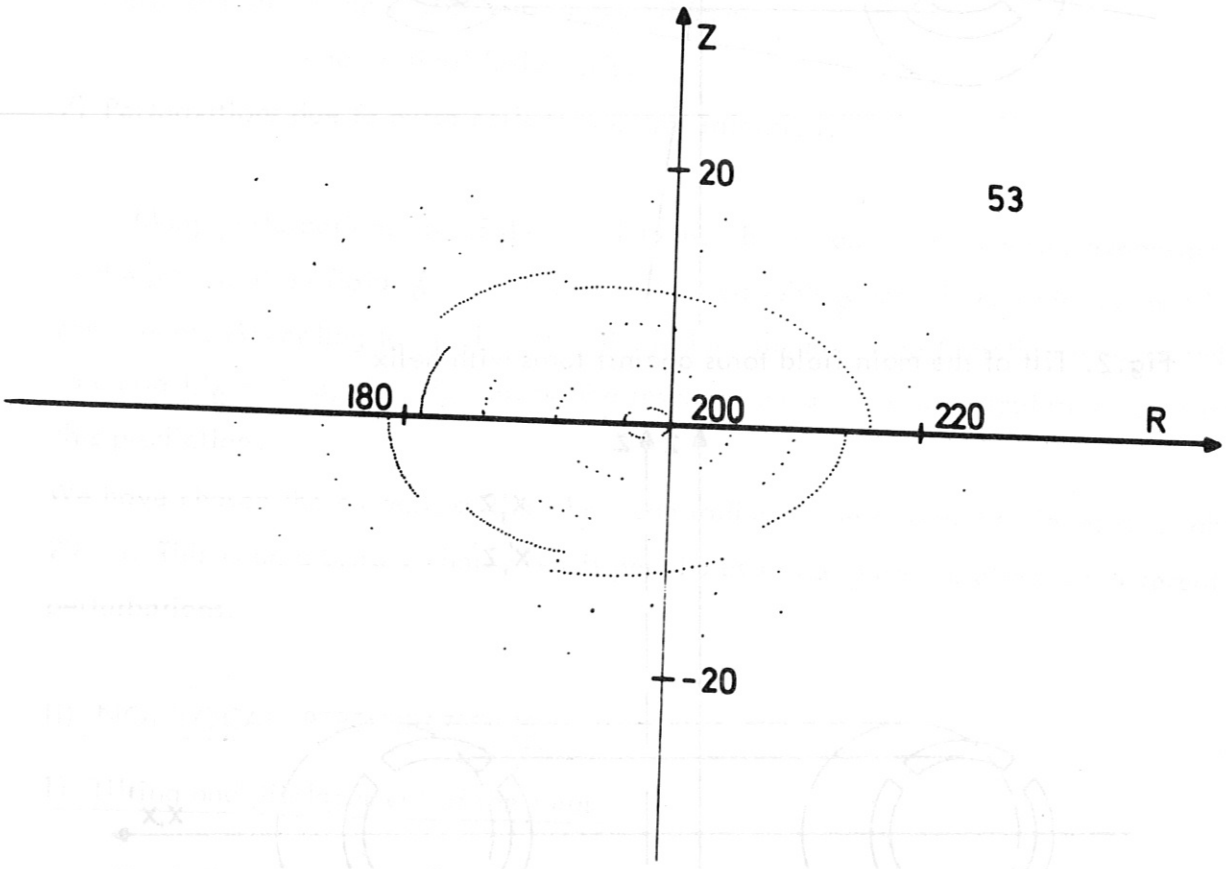

Fig. 4. Unperturbed magnetic surface. $\iota = 0.25$, $\alpha = 0$

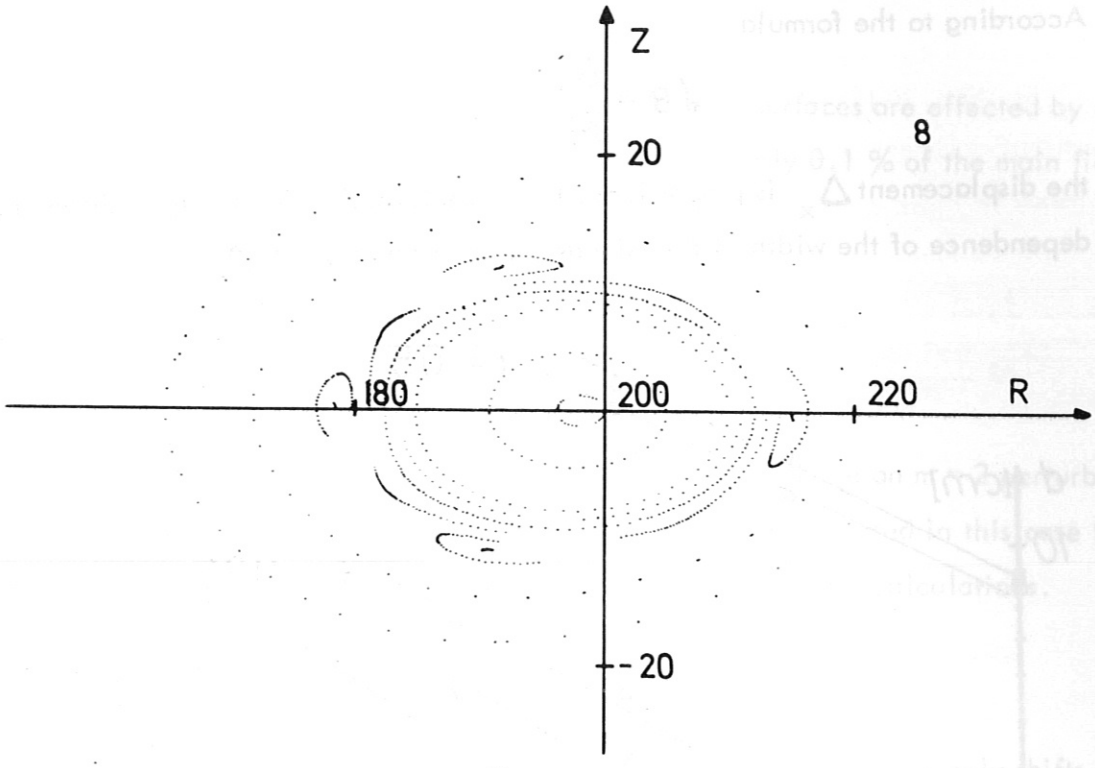

Fig.5. $t = 0.25$, $\alpha = 0.5^{\circ}$

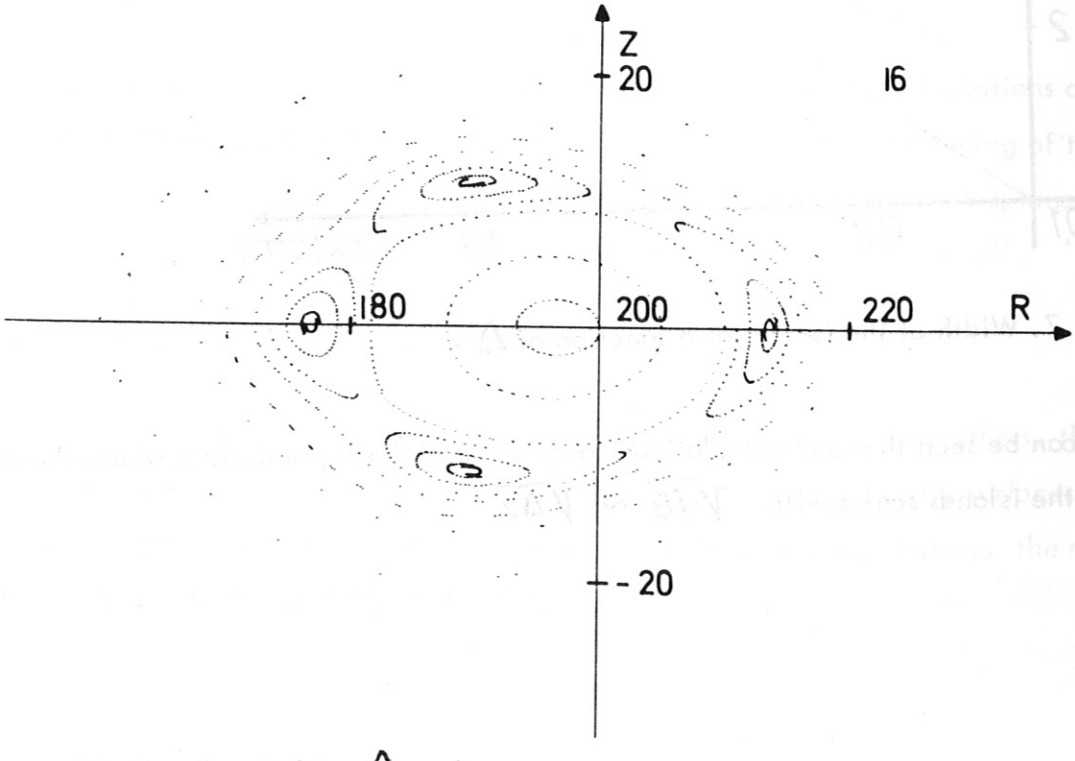

Fig.6. $t = 0.25$, $\Delta_x = 1$ cm

According to the formula

$$\delta B = \frac{\Delta_x}{R} \cdot B_o$$

the displacement Δ_x is proportional to the perturbation field. Fig.7 shows the dependence of the width of the islands d as a function of Δ_x.

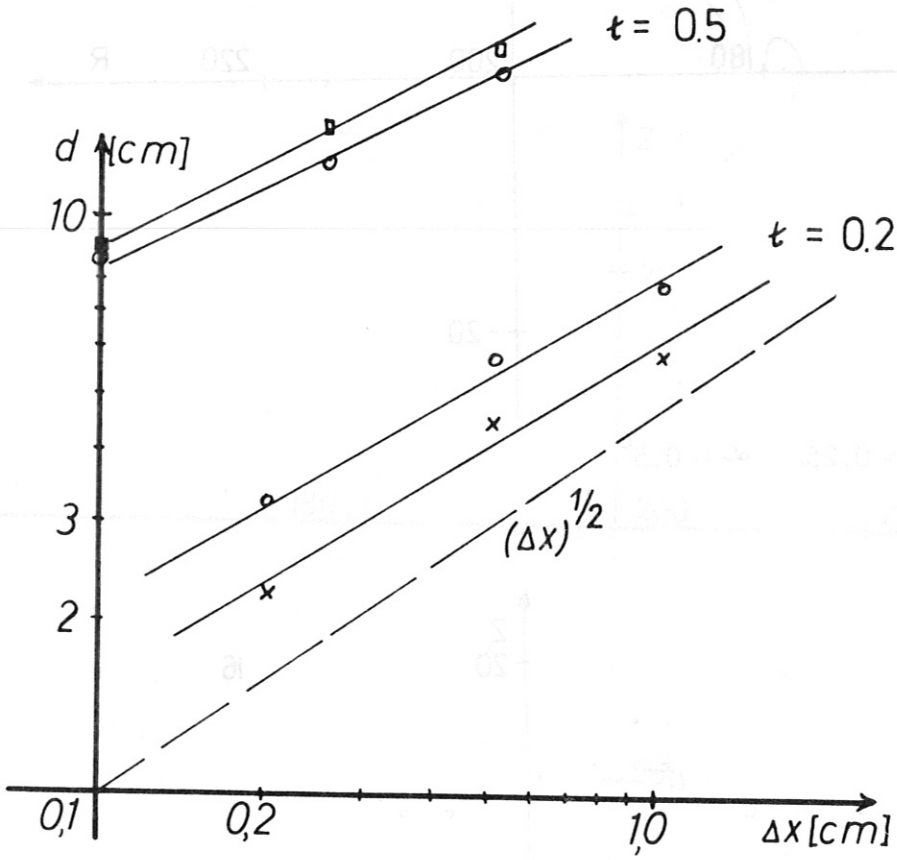

Fig.7. Width of the islands as a function of Δ_x

It can be seen that our calculations confirm theoretical predictions where the width of the islands scales with $\sqrt{\delta B} \sim \sqrt{\Delta x}$

2) Horizontal field

These calculations show how strongly the magnetic surfaces are effected by a horizontal perturbation field. A field of 40 G which is only 0.1 % of the main field can generate islands of 10 cm for $\iota = .5$.

III) PERTURBATION OF THE MAIN FIELD COIL SYSTEM

1) Elliptical deformation of the system

Here the coils are arranged on a ellipse instead on a circle an m = 2 perturbation is expected. A smaller effect on the magnetic surfaces was expected in this case than with an m = 1 perturbation. This was confirmed by our numerical calculations.

2) Systematic tilting of the coils

A systematic tilting of the coils introduced a vertical field. This only shifts the magnetic axis but do not cause any islands.

3) Statistical errors on the coils

Due to inaccurate positioning of the coils around the torus, perturbations of the magnetic field occur. In order to varify these perturbations, the positioning of the coil centers were randomly distributed around the torus. The maximum displacement was $\Delta x = 0.5$ cm. The effect on the magnetic surfaces is negligible small.

4) Modulation of the main field

If the current in one of the main field coils is smaller than in the others, this introduces a perturbation of the m = 1 type. The effect on the magnetic surfaces is very strong, 25 % reduction of the current in one coil completely destroys the magnetic surfaces in the vicinity of $\iota = 0.5$.

5) Modified coils for neutral injection

In order to give access into the torus for neutral beam injection groups of modified coils are foreseen in the main coil system. Fig.8 shows the coils. The currents in these coils do not differ from the other coils.

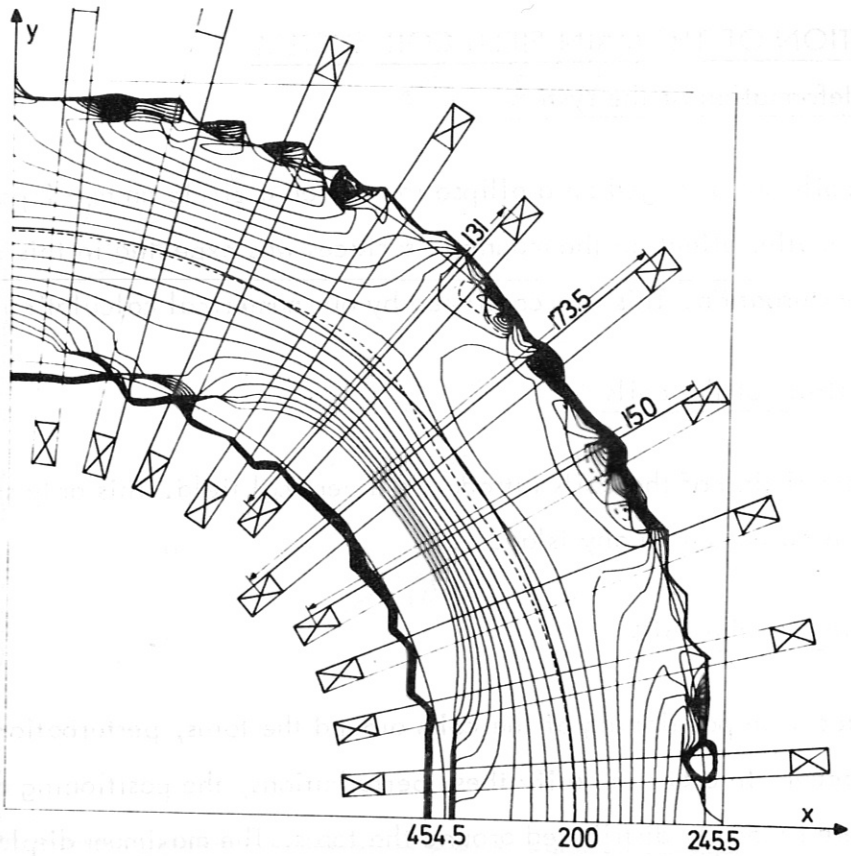

Fig.8. Arrangement of special coils for neutral injection.
The Lines are /B/ = const.-lines

Fig.8 also shows the effect of these coils on the magnetic isobars /B/ = const. Due to these coils magnetic islands occur at $\iota = 0.5$. At $\iota = 0.25$ only very small islands occur. The perturbations from these coils should be tolerable.

6) Current leads to the main field coils

These current leads were simulated by toroidal circular loops. The effect on the magnetic surfaces is negligibly small.

IV) PERTURBATIONS OF THE HELICAL CURRENTS

1) Different pitch of the helical currents

We considered a deviation from the standard case $\frac{d\Theta}{d\varphi} = 5/2$ according to the formula $\frac{d\Theta}{d\varphi} = 5/2\ (1 - \beta \cos\Theta)$ with $\beta = -0.074$. In this case we obtain regions of positive and negative shear. (Fig.9). A perturbation of the m = 1 type then generates two systems of islands as can be seen in Fig.10.

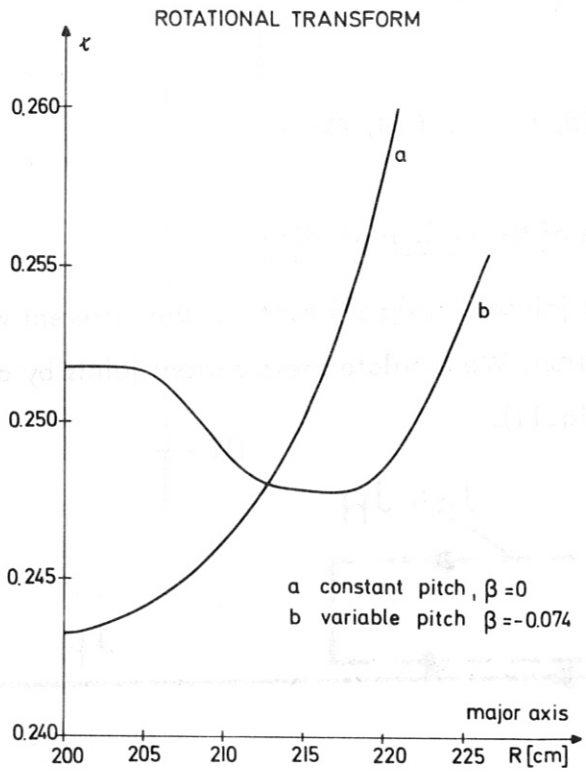

Fig.9. Rotatational transform a:ß = 0; b:ß = -0.074

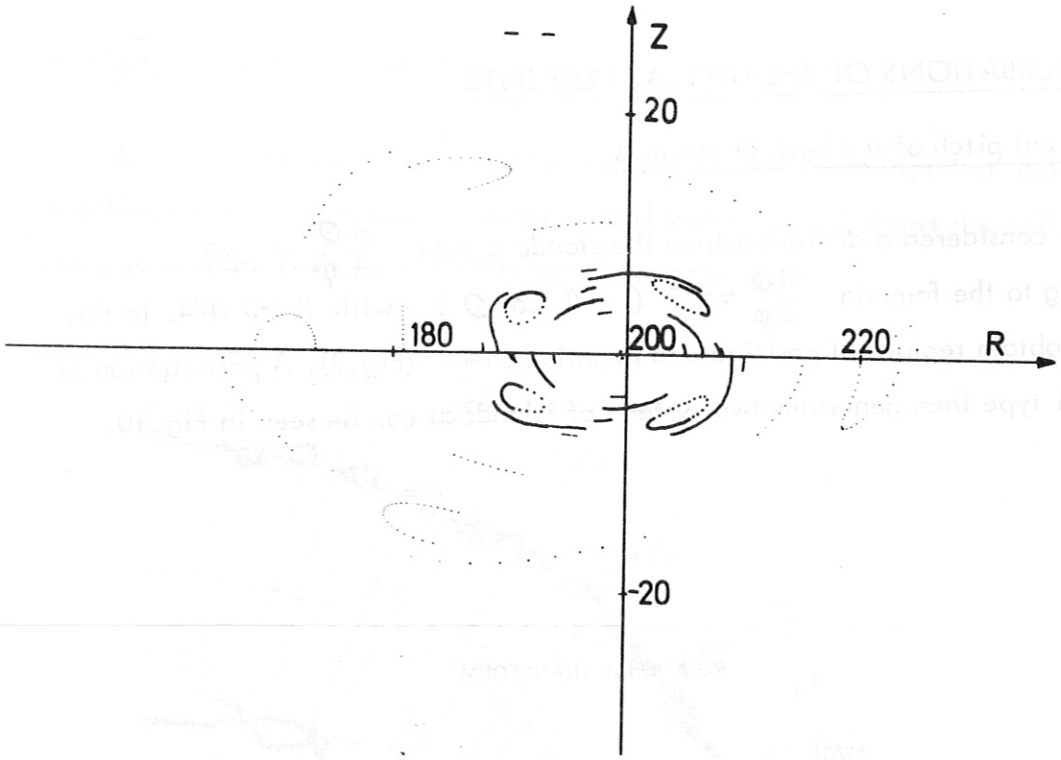

Fig.10. $t = 0.25$, $\beta = -0.074$, $\Delta x = 0.25$ cm

2) Current joints of the helical windings

The current joints ("bridges") between the different wires of the helix introduce a m = 1 perturbation. We simulate these current joints by adding a current loop to the ideal winding (Fig.11).

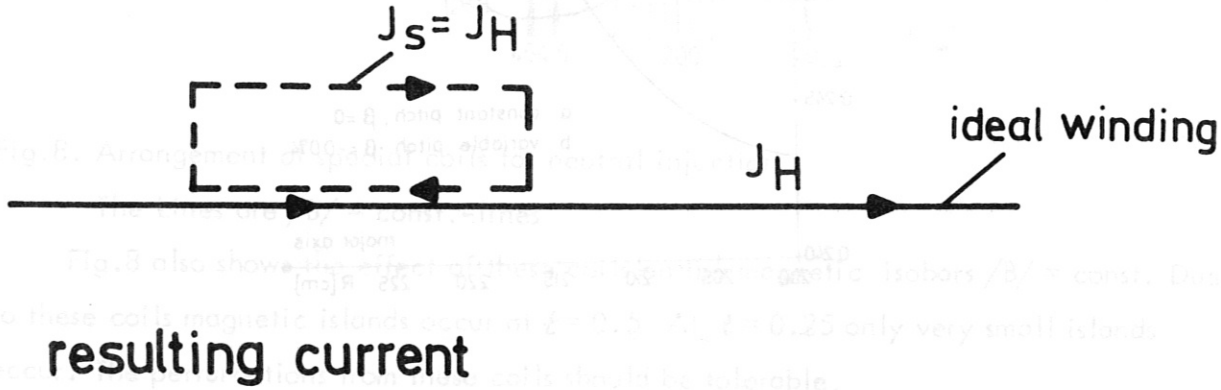

Fig. 11

Over an angle of $\varphi = 9^{\circ}$ the helix is shifted 2 cm outward. Even this small shifting of the helical windings cause rather large islands in the vicinity of $\iota = 0.5$ (Fig.12) and 0.25. On the contrary the current leads to the helical windings do not generate islands.

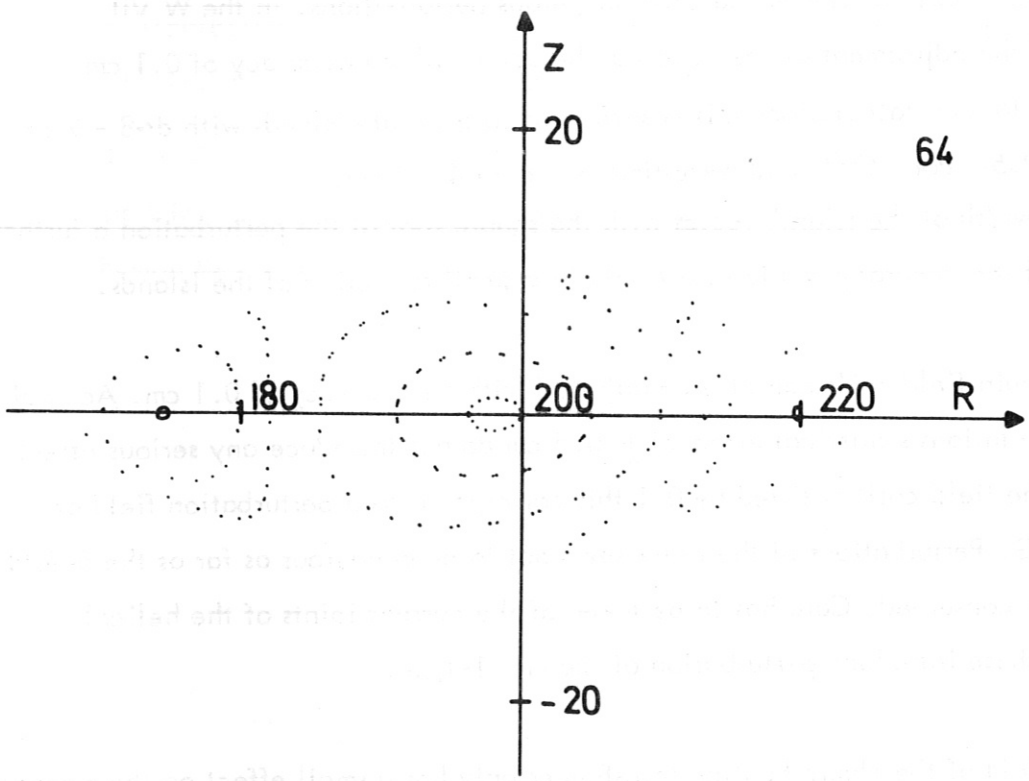

Fig.12. $\iota = 0,5$, effect of helix bridges

V) OHMIC HEATING TRANSFORMER

A tilting of the toroidal circular coils of the ohmic heating air core transformer or vertical field coils will lead to a m = 1 perturbation. This will generate islands if the tilting is large but the effect is small in comparison to the other m = 1 perturbations.

CONCLUSIONS

The numerical calculations show that due to perturbation fields large islands occur in the magnetic field of the W VII-stellarator. A comparison with the unperturbed case shows that natural islands, which are caused by the toroidal curvature, do not occur. As already noticed by Gourdon et al. [5] the displacement and tilting of the torus are one of the most dangerous perturbations. In the W VII stellarator the adjustment of the torus can be done with an accuracy of 0.1 cm. According to our calculations this is sufficient to generate islands with $d \sim 8 - 9$ cm (at $\iota = 0.5$). For $\iota = 0.333$ we estimate $d \sim 4 - 5$ cm.
Since the width of the islands scales with the square root of the perturbation a further increase of the accuracy would result only in a small reduction of the islands.

The main field coils can also be adjusted with an accuracy of 0.1 cm. According to the calculations statistical errors of $\pm$ 0.5 cm do not introduce any serious effect. If one of the field coils is tilted by 0.1 this corresponds to a perturbation field of $B_h \approx 14$ G. Perturbations of the helix seem not to be dangerous as far as the 5-fold symmetry is conserved. Care has to be taken of the current joints of the helical windings, these introduce perturbation of the m = 1-type.

The field of the ohmic heating transformer only has a small effect on the magnetic surfaces. The coils for neutral injection also introduce perturbation of the m = 1-type, but at $\iota = 0.25$ the effect seems not to be serious.

This allows us to extrapolate the calculation to small values of the perturbation. The choice of perturbation investigated by us is by no means complete, but it seems to cover the most important ones.

1) BEREZHETSKII, M.S., GREBENSCHIKOV, S.E., POPRYADUKHIN, A.P., SHPIGEL, I.S., Soviet Physics - Technical Physics 10 (1966) 1662

2) GIBSON, A., Physics Fluids 10 (1967) 1553

3) HAMZEH, F.M., Phys. Rev. Letters 29, 1492 (1972)

4) ROSENBLUTH, M.N, SAGDEEV, R.Z., TAYLOR, J.B., ZASLAVSKI, G.M., Nuclear Fusion 6 (1966) pp 297 - 300

5) GOURDON, C., MARTY, D., MASCHKE, E.K., DUMONT, J.P., pp 847 - 859, Proc. of JAEA Conf. on Plasma Physics and Contr. Nuclear Fusion Research, August 1968

Paper No. 12

TORUS WITH HELIX W VII A

by

H.J.Jäckel, J.Kißlinger, F.Rau, H.Wobig

Max-Planck-Institut für Plasmaphysik,

D-8046 Garching, W.Germany,

EURATOM-Association.

ABSTRACT

The design of the component torus with helix W VII A is made as simple as possible as compared to the torus with helix W VII B, in order to have it available by the end of summer 1974. Thus we reduced the minor radius, the rotational transform, the number of observation ports, and allowed for larger tolerances. The torus W VII A is made from forged stainless steel, major diameter 4 m. Radial and vertical observation ports are at azimuthal distances of 36 degrees. The $l = 2$, $m = 5$ helix is designed to carry a total current up to 160 kA, yielding a rotational transform of $t = 0.2$ (0.4) at a toroidal magnetic field of 4 T (3 T). Radial electromagnetic forces act on the helix up to $2.5 \cdot 10^5$ N/m. The stress due to the thermal expansion of the helix is reduced by the use of flexible copper elements in the helix bridges. The perturbations of the magnetic field structure caused by the helical steps are comparable to those introduced by the imperfections of the adjustment of torus with helix and toroidal field coil system, i.e. a radial offset or tilt of both components against another.

INTRODUCTION

The use of the torus with helix W VII A as a component of the experimental facility WENDELSTEIN VII allows to proceed towards plasma experiments in a large stellarator prior to the delivery of the highly complex torus with helix W VII B which is described in Ref.1 in more detail. According to the present time schedule by the end of summer 1974 those components of the W VII facility will be available which are due in the assembly procedure before the installation of torus with helix. Since the final decision to build W VII A could not be obtained before the end of November 1973 a main criterium in the design of W VII A is a short time of construction. Thus we are aiming at simple technical solutions, which allow to perform most of the construction at the institute and without too much tooling. The discussion of the aspects of the above criteria, and the sometimes conflicting general interest in a versatile plasma physics device leads to the characteristic design data of torus with helix W VII A as given in Table I.

TABLE I

Characteristic design data of W VII A

Torus	major diameter	4 m
	minor inner diameter	0.35 m
	minor outer diameter	0.406 m
	radial and vertical ports	0.1 m dia, every 36 degree
Helix	l = 2, m = 5, no shear	
	average radius of helix conductors	0.23 m
	total helical current	160 kA
	rotational transform (at a toroidal field)	0.2 (4 T), 0.4 (3 T)
	Kruskal current 200 kA, at toroidal field 4 T	

In comparison to torus with helix W VII B in the present design of W VII A we reduce the minor radius, the rotational transform, the number and direction of observation ports, and allow for larger tolerances. A considerable simplification for the design of torus with helix W VII A is the ample radial clearance towards the bore of the toroidal field coils. The design of the helix provides for a stellarator magnetic field having a rotational transform of $\iota = 0.2$, in a series connection of the helix and the toroidal field coils. An increase up to $\iota = 0.4$ can be envisaged by shunting the toroidal field coils to about 75 % of their current.

TORUS W VII A

The torus is made from forged stainless steel. It had been ordered some years ago, at a state of planning when W VII had been aimed to be equipped with superconducting toroidal field coils. At the time of defining W VII A (mid-summer 1973) the inner and outer torus surfaces had been already machined.

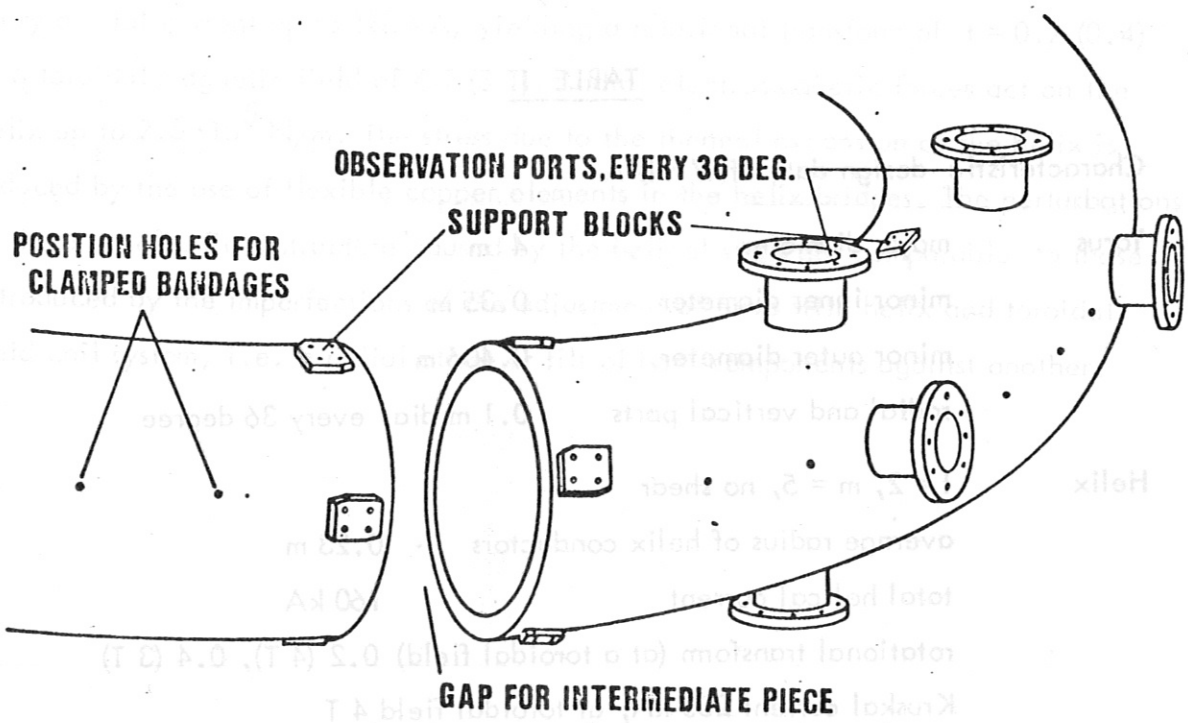

Fig. 1. Torus W VII A
Final Mechanical Jobs

During a period of less than 4 months the final mechanical jobs were performed by Schoeller-Bleckmann, Vienna, at the torus W VII A, see Fig. 1. Small radial holes every 9 deg. azimuthal distance allow to center bandages which define the poloidal position of the helix conductors. Support blocks are welded onto the torus for clamping the intermediate piece and for the crane. A total of 27 observation ports with an aperture of 10 cm provide vertical and radial access. Slanting or tangential port holes are omitted because a considerable additional construction time would have been the consequence. Finally, the gap for the intermediate piece was cut and machined to high vacuum quality.

Due to the manufacturing process the torus acts like a spring, mainly in the azimuthal direction. The corresponding force of about $5 \cdot 10^4$ N assists in closing the vacuum seal of the intermediate piece. The design[+)] of the cylindrical intermadiate piece is well in progress. Some boundary conditions are given by

- the limited radial space available for a device to widen the gap in the torus in order to insert the intermediate piece,
- the limited poloidal space available between the individual helix units to clamp the vacuum seal against the high[++)] magnetic forces, and the resulting distortions of torus and intermediate piece,
- the insulation necessary at the vacuum seal because of the Ohmic Heating and pre-ionization voltages.
- the requirements of the limiter to be built into the intermediate piece.

HELIX W VII A

The helix is of the $\ell = 2$, $m = 5$ type. The helix conductors are arranged at an average radius of .2 m; their angular co-ordinates being described by the relationship

$$d\varphi / d\vartheta = \ell / m \, (1 - \alpha \cdot \cos\vartheta),$$

+) R. Zickert (IPP)
++) as calculated by B. Streibl (IPP)

where ϑ and φ are the poloidal and azimuthal angles, resp. The quantity α, governing mainly the weak shear of the field configuration, is of the order of 1 %. It approximates a path which is perpendicular to a geodetic line.

As helix conductor we use circular copper tubes of 2 cm diam. having a cooling channel of .7 cm diam. No tilt is necessary when mounting these tubes in helical geometry onto the torus. Four copper tubes are connected electrically in one parallel bundle to carry a current up to 40 kA. Four such bundles form a helical unit. At design current a total power of about 6.5 MW yields a temperature increase of about 25 deg. at a pulse length of 3 sec.

Considerable forces act on the helix conductors, mainly caused by the W VII stellarator toroidal field of up to 4 Tesla. They are directed parallel and antiparallel to the minor torus radius in the helix units with positive and negative current direction, resp. These forces tend to distort the minor torus cross section into an elliptical shape. Due to the toroidal curvature their magnitude varies with poloidal angle between $1.8 \cdot 10^5$ and $2.5 \cdot 10^5$ N/m, corresponding to a net radial force of $8 \cdot 10^4$ N/m rotating at $d\vartheta/d\varphi \approx 5$.

To begin with, the helical conductors are bent onto a dummy torus where the helix path had been marked by bolts. The final mounting of the precurved helix conductors is facilitated by a system of stainless steel guide-bolts (Fig.2) which are welded onto stainless steel bandages. These bandages are clamped onto the torus every 9° in azimuthal direction using the small positioning holes mentioned earlier. The guide bolts carry suitable spacers machined from glassfibre-epoxy which position the helix bundles. After mounting the bandages, the torus is insulated on its outer surface by glassfibre-epoxy laminates up to a thickness of 3.5 mm. At the bandages this insulation is slightly reduced in thickness. A layer of .1 mm KAPTON improves the insulation.

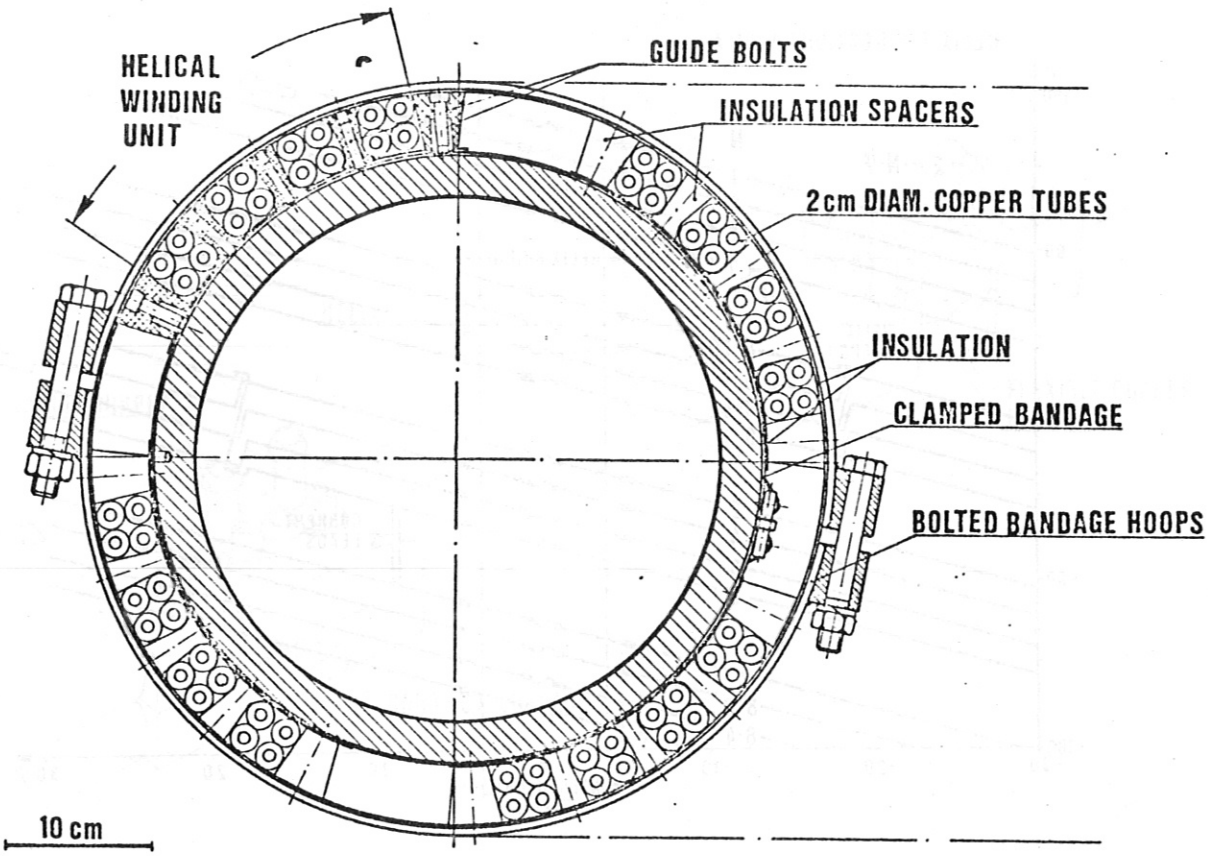

Fig.2 W VII A Torus with Helix Cross Section

Helix connections

Three types of electrical connections are used for the helical conductors of W VII A, as shown schematically in Fig.3:

- the 16 helix bridges connecting the conductor bundles across the gap at the intermediate piece of the torus acting as terminals of the different cooling circuits,
- the two times (3 + 1) helix steps connecting the conductor bundles to two current loops running up to N = 8 times around the torus, $\varphi^* = 2\pi$ N,
- the current leads connecting the two helix loops with opposite current direction to one current path in series to the toroidal field coils.

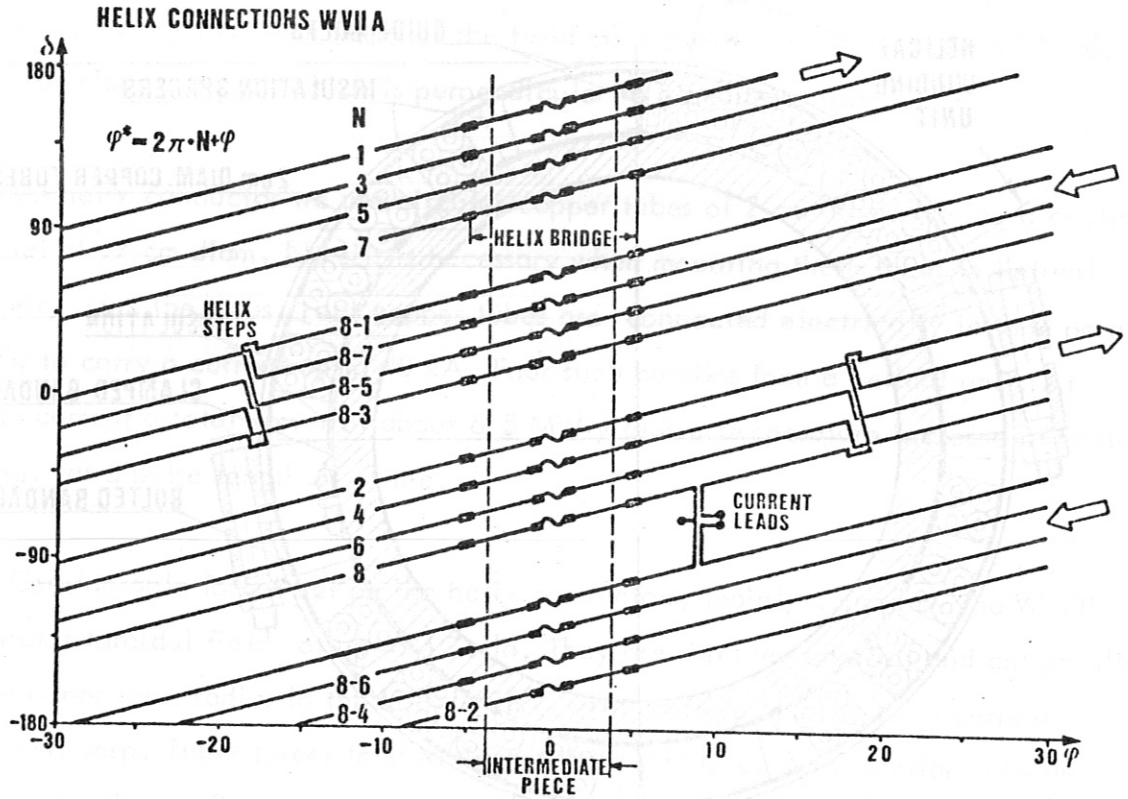

Fig. 3. Wiring Diagram of the Helix W VII A

Fig. 4 shows in more detail the design of a helix bridge. Simple copper blocks with appropriate channels for cooling water supply are equipped with two short pieces of helix conductors. After i) matching the lengths and shaping the bridge to a torus geometry ii) brazing to the helix, and iii) bolting the copper pieces tightly the interlinked current contact surfaces are soldered.

Flexible copper elements in the middle of each bridge provide for fine adjustment and for leeway with respect to the thermal expansion of the helix. Here, over a distance of about 5 cm, the cooling path is interrupted. The flexible elements as well as a prototype of the helix bridge had been tested at a maximum current of about 140 % of the W VII A design value at a pulse length of 2.5 seconds yielding a temperature rise of about 10 K at the contact surface and about 30 K at the flexible elements.

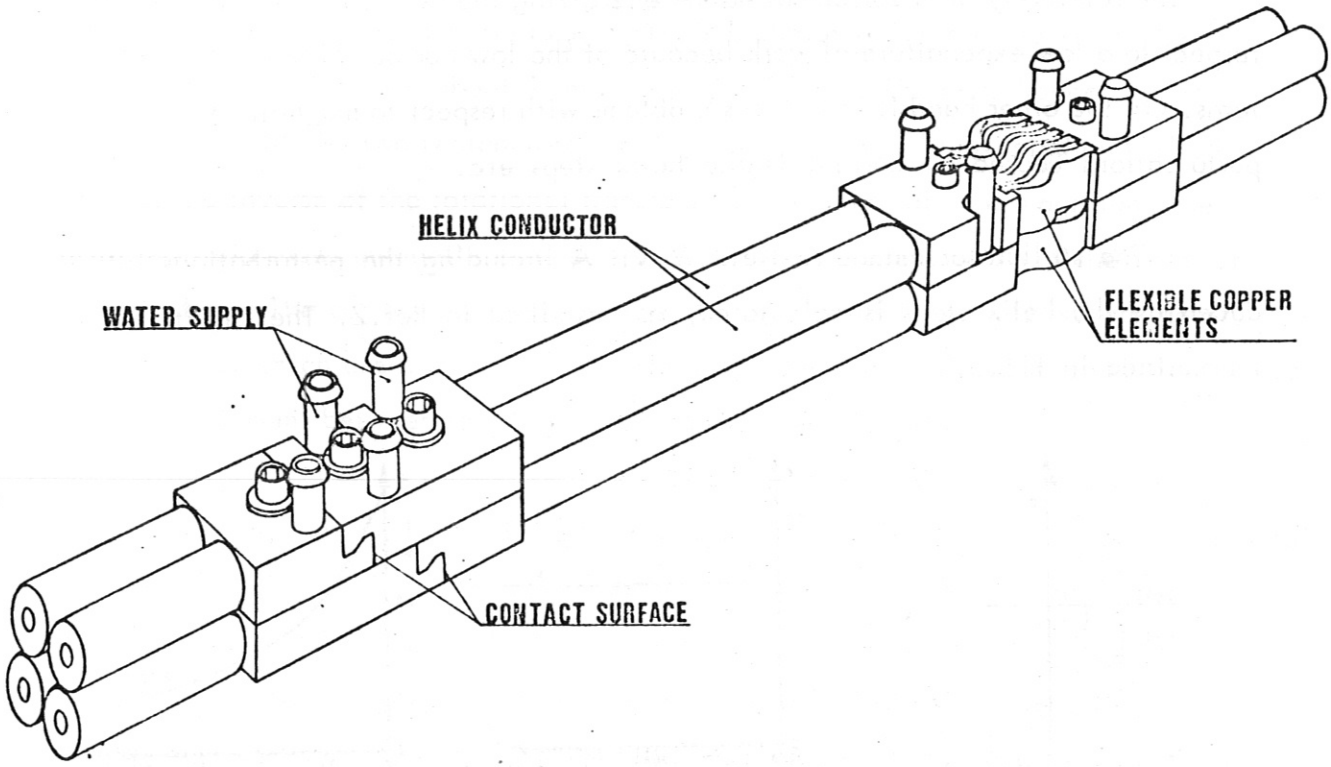

Fig.4. W VII A Helix Bridge

The helix steps are placed at the outside of the torus (ϑ = o), since there the magnetic forces are minimum. Three short steps connect neighbouring conductor bundles and one long step connects the outer bundles of the helix unit, as shown in Fig.3. The long step is placed radially above the helix conductors. The stellarator magnetic field is subject to perturbations induced by the helix steps, as will be described below.

The current leads are curved radially off the torus. They introduce only minor magnetic field perturbations. A third conductor next to the current leads will be connected to an emergency switch. It connects the point of highest transient voltage $V = 8\,V_o$, which will be induced either by the Ohmic heating transformer providing a maximum voltage V_o to the plasma or, worse, by disruptive instabilities of the induced plasma current.

STELLARATOR MAGNETIC FIELD W VII A

The relatively high current of 40 kA energizing the helix is advantageous with respect to a low expenditure of work because of the low number of helical conductor turns. On the other hand it introduces problems with respect to maghetic field perturbations caused by current leads, helix steps etc.

The stellarator magnetic field W VII A including the perturbations introduced by the helix steps is calculated, as described in Ref.2. The results are summarized in Fig.5.

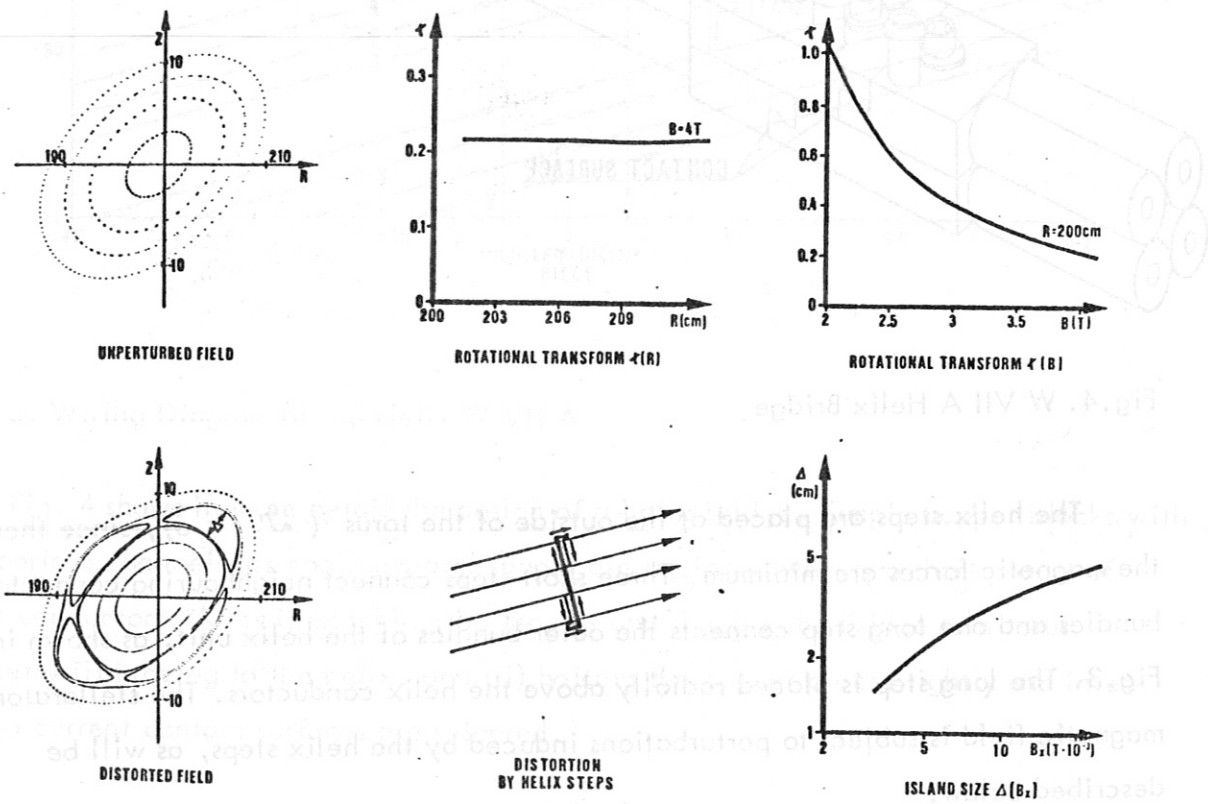

Fig.5. W VII A Magnetic Field

The upper left of Fig.5 shows the unperturbed field with well centered magnetic surfaces, in radial and vertical co-ordinates R and Z, resp. The magnetic field is of negligeable shear. The rotational transform can be increased from 0.2 to about 0.4 by a reduction of the toroidal field B when keeping the helix current constant (upper middle and upper right of Fig.5).

The distortions of the W VII A stellarator field caused by the systems of helix steps are calculated for $\iota = 1/4$ (Fig.5 lower left). In the lower middle of the figure a series of straight filamentary currents is shown which are placed at the average helix radius, and about 3 cm above (bold line). The disturbance can be described roughly by two rectangular current loops, oppositely directed and tilted. Only if the inverse of the rotational transform is an integer of low magnitude the distorted field shows magnetic islands, having a radial extension Δ of the order of $\Delta = 3$ cm. The comparison of the size of islands caused by a different design of helix bridges which are combined with helix steps shows that the present solution seems to be an optimum between simplicity and magnetic field quality.

Similar magnetic islands of the same size are caused by a homogeneous horizontal field $B_x = 6 \cdot 10^{-3}$ T. At higher values of this field one finds Δ proportional to $B_x^{0.5}$, whereas at lower B_x a higher power seems to be more appropriate, $\Delta \sim B_x$ (Fig.5, lower right). In Ref.2, for the case of the W VII B, effects of further disturbances are studied, e.g. a radial offset of torus with helix and toroidal field and the size of the islands is given proportional to $B_x^{0.5}$.

At present, it is not yet clear to which extent a deliberate radial offset of torus with helix W VII A with respect to the toroidal field could compensate for the field distortions caused by our helix steps or whether additional compensating coils, energized separately, would promise better results. These questions will be further pursued.

ACKNOWLEDGEMENTS

The authors would like to thank the other members of the W VII group for many stimulating discussions and useful quantitative information.

REFERENCES

1) BLAUMOSER, M. et al., "On the technical concept of the W VII stellarator"; these proceedings.

2) REHKER, S., and WOBIG, H., "The effects of perturbations on the magnetic field of the W VII stellarator", these proceedings.

Paper No. 26

HIGH-POWER DC NEUTRAL PARTICLE INJECTION FOR W VII

by

J.Bäumler, J.Junker, W.Melkus, F.Probst,
G.Schilling, E.Speth

Max-Planck-Institut für Plasmaphysik,
D-8046 Garching b. München, W.Germany
EURATOM Association

ABSTRACT

The physical requirements for a neutral particle injection system for the stellarator W VII are given together with the present status of their technical realization. Injectors with power levels of 10-20 kW DC have been developed and are being extended.

A. W VII A REQUIREMENTS

The lack of tangential access and the relatively small plasma diameter allow only a small fraction of a vertically injected neutral particle beam to be absorbed in the target plasma. A heating and/or filling experiment would be doubtful. The possibility exists, however, of creating an adequate initial ion density of about 10^{12} cm^{-3} for good preionization for the Ohmic heating current by injecting into the filling gas in the presence of the stellarator's initial rotational transform, which gives stable confinement of the newly created ions. The efficiency may be improved considerably by injecting the beam into a crossed jet of the filling gas.

The resulting requirements on the injector, 8 A ion beam current at 40 kV extracting voltage pulsed for 0.2 sec, can be satisfied by slight extrapolation of existing pulsed DuoPIGatrons and other designs.

Only straight-through vertical injection is possible for technical reasons, the injector will be located below the torus,

a beam dump directly above the torus. The usual magnetic shielding of the extraction region and pumping of the source and neutralizing gas are accomplished in a fashion similar to designs existing at Oak Ridge and Culham.

B. W VII B REQUIREMENTS

The 10 sec magnetic field flat-top makes a quasi-stationary plasma heating and filling injection experiment an attractive possibility. The particle loss rate is estimated to be about 10 A equivalent, the energy loss rate about 200 kW. If no gas recycling from the walls exists, after several containment times the plasma temperature may approach the particle injection energy. Strong gas recycling suggests a lower injected beam current at a higher injection energy.

Tangential injection is possible on the W VII B experiment, which leads to a greater component of particle velocity around the torus as well as a much greater beam absorption path in the target plasma, as compared to transverse injection. As is shown in Fig. 1, a tangential beam line needs to bypass both the toroidal field coils and the helical windings.

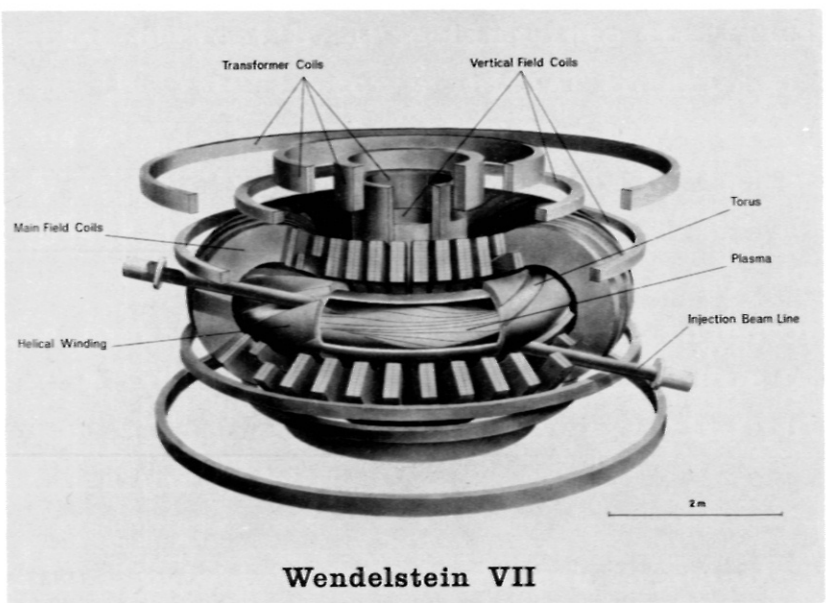

Fig. 1.

The helix, not capable of modification, limits the torus aperture to 160 mm diameter. Two possible modifications to the toroidal field coils exist, both of which are still being optimized. One modification, shown in Fig. 1, involves the reduction in radial dimension of the coil windings to either decrease the outer diameter at normal inner diameter or to increase the inner diameter at normal outer diameter of each of a pair of coils. Another modification involves the construction of "bumpy" coils, with winding height reduction only in the vicinity of the beam line. Both solutions require extra electrical power for the modified coils, leading to a slight reduction in magnetic field strength. Computer calculations of the resulting magnetic field perturbations show these to be tolerable. Force perturbations must be covered by slight modifications to the existing structure. The beam line again is similar to existing designs, differing primarily in the approximately 3 m long flight path, necessary to get out to tolerable magnetic fields which may be shielded without perturbing the stellarator field, and the 10 sec. gas load, meaning greater gas handling capacity. For a 10 A beam we expect a gas load of about 1.5 Torr ls^{-1}, the desired beam line pressure of 10^{-4} Torr gives a needed pumping speed of up to 10^{4} ls^{-1}. The volume getter pumps used for the W VII B vacuum system will also be installed here. Retractable calorimeters will allow measurement of beam power into and through the target plasma.

The injector requirements are given by the particle loss rate, energy loss rate, and injection duration. We expect 0.25 - 0.5 of the extracted ion current to go into plasma heating. A particle loss rate of 10 A then requires a total extracted ion current of 40 A, to be supplied by 4 injectors of 10 A at an extraction voltage of 20 - 40 kV each, operating in opposed pairs. Existing pulsed injector designs are capable of supplying this beam power, but not for the required 10 sec. A test stand, shown in Fig. 2, was constructed to allow injector

development under conditions similar to the expected W VII B geometry to be made.

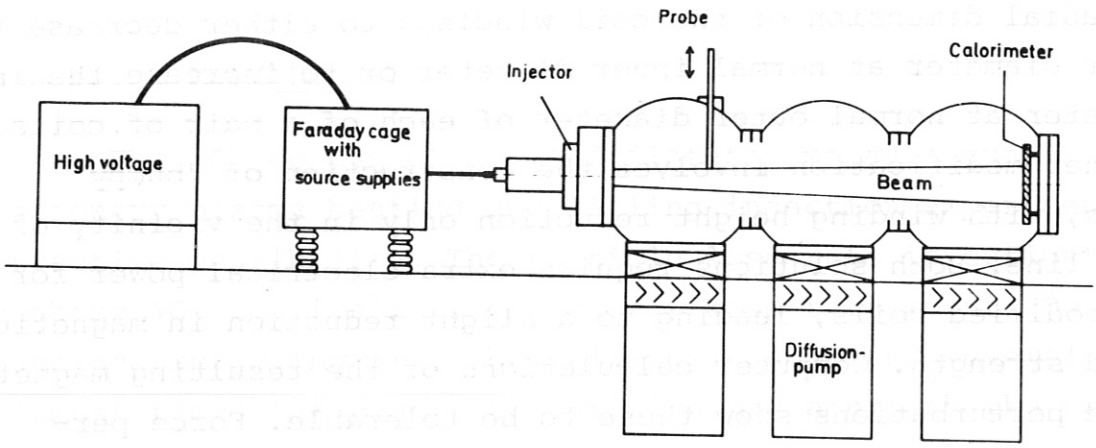

Fig. 2. Test stand.

The basic dimensions are: beam flight path 3 meters, vacuum pumping speed 10^5 ls^{-1}, DC beam power handling capability 1 MW.

A block diagram of the injector is shown in Fig. 3.

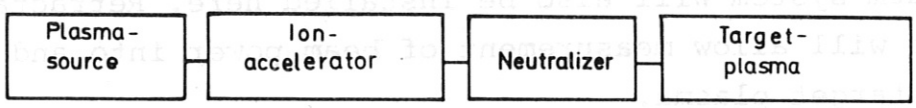

Fig. 3. Injector block diagram.

For DC operation it was primarily necessary to increase the DC power handling capability of the plasma source and especially the grid structure. The Duo PIGatron plasma source we have been working with, shown in Fig. 4, was improved by increasing the anode cooling.

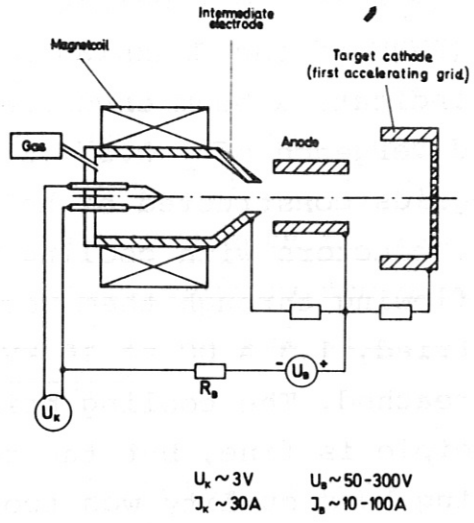

Fig. 4. DuoPIGatron plasma source.

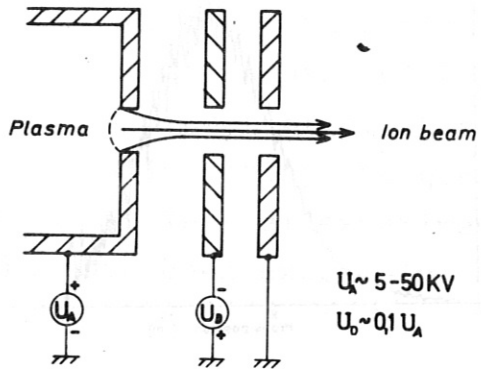

Fig. 5. Accelerating grid structure.

The accelerating grid structure, shown schematically in Fig. 5, is power limited by warpage or melting due to heating by spray primary beam and secondary electrons.

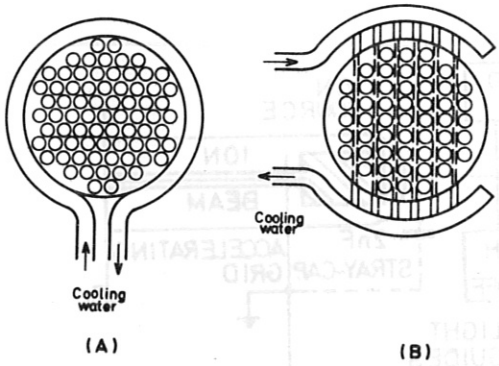

Initial investigations of the DC power limit of the standard edge-cooled multi-aperture OFHC Cu grids used in pulsed injectors, shown in Fig. 6 (A), allowed power levels of about 10 kW DC with good beam divergence to be reached.

Fig. 6. Grid designs.

A beam profile taken at a 5 kW DC power level, 0.4 A at 12 kV, 50 mm extraction surface diameter, is shown in Fig. 7.

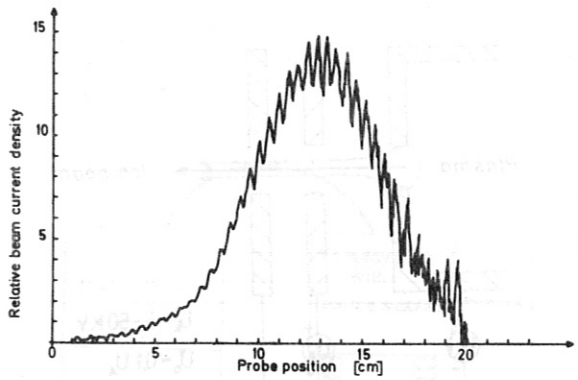

Fig. 7. Beam profile.

The half-power points (FWHM of the Gaussian profile) indicate a beam envelope divergence of $\pm$ 0.5°. Slotted grids constructed of hollow conductors with cooling water flowing through them were tried, 1.3 A DC at 16 kV was reached. The cooling principle is fine, but the resulting beam quality was too poor to allow use here. An arrangement of circular apertures in rows, with cooling water between rows, as shown in Fig. 6 (B), is now under construction, and this principle should allow the design goals to be achieved.

Protection of the accelerating grid structure in case of high-voltage breakdown is a necessity at high power levels. We have developed a fast interrupt switch between the high voltage supply and the injector, as shown in Fig. 8. We use a fast

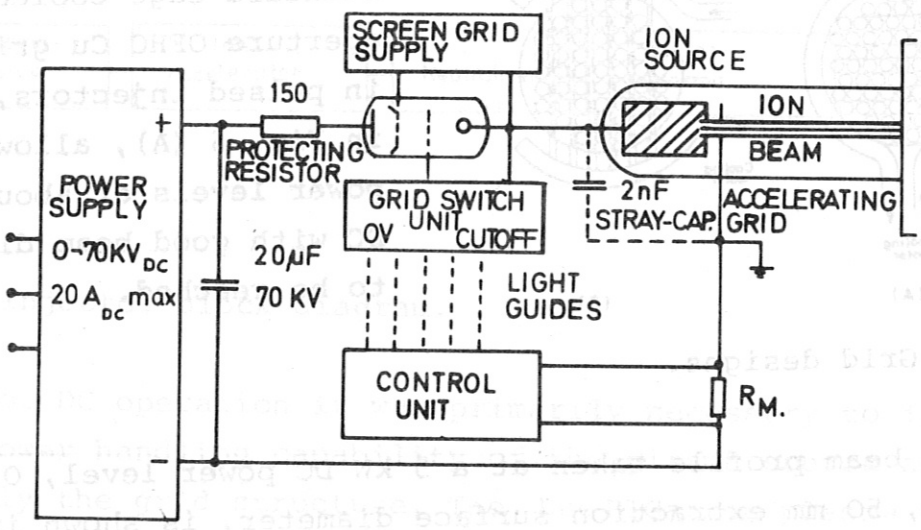

Fig. 8. HV switch.

overcurrent sensor to cut off a series transmitting tetrode within 3 μsec; after a preset delay interval the tube is switched into the conducting mode again with a turnon time of 10 μsec. A continuing short causes cutoff again, with the cycle repeatable up to 10 times within a preset time. This procedure protects the grid structure while saving the greater portion of each 10 sec experimental shot. Initial experiments at the 10 kW level with a 25 kV tube have been extremely successful.

A useful byproduct of our DC beam development work is the capability of using the beam for wall erosion studies. At the present time we are experimenting with a mass-analyzed H^+ beam of 1 mA cm^{-2} at 10 kV.